ECRC

Environmental Change Research Centre

Research Report No. 104

Temporal trends of toxic trace metals across the UK using ^{210}Pb-dated sediment cores:

Final report to the Department for Environment, Food and Rural Affairs

H. Yang and N.L. Rose

June 2005

ISSN: 1366-7300

Environmental Change Research Centre
University College London
26 Bedford Way
London, WC1H 0AP

Temporal trends of toxic trace metals across the UK using ^{210}Pb-dated sediment cores

Final report to the Department for the Environment, Food and Rural Affairs
(Extension to Contract No. EPG 1/3/160)

Handong Yang & Neil L. Rose

ECRC / ENSIS Ltd
University College London
26 Bedford Way
London WC1H 0AP

June 2005

Cover photograph: Powdermill Lake, East Sussex
(Photo: Neil Rose)

Executive Summary

A suite of toxic trace metals (Hg, Pb, Cd, Ni, Cu, Zn) were analysed from ^{210}Pb-dated sediment cores taken from ten lakes across southern and eastern UK.

These data revealed that contamination over background levels occurred as early as the late-18th century suggesting that setting a mid-19th century level as a restoration target for trace metals, under the Water Framework Directive, will not restore sites to reference conditions at many UK sites.

Despite considerable reductions in UK trace metal emissions, surface sediment concentrations in many of these lakes are not declining. This can only be due to increased inputs from catchment sources derived from historical atmospheric deposition. It is thought this is primarily due to catchment disturbance but climate enhanced erosion will also play a role and could significantly increase in the future.

Sediment accumulation rates have also increased over the last 100 years, at some sites by a considerable degree. Apart from accelerating lake-infilling, this also results in steady or increasing trace metal fluxes (input rates) to the sediments at many of the sites. Catchment inputs therefore already form an important trace metal source.

Probable Effect Levels (PEL) for trace metals, at which detrimental biological effects are frequently seen, were exceeded for at least one metal at 9 out of the 10 sites. PEL exceedence occurred for Cd, Ni, Pb and Zn at Llyn Fach, for Pb, Hg and Zn at Diss Mere and for Pb, Zn and Ni at Turton and Entwistle Reservoir. The PEL for Pb was exceeded at 6 of the sites, Ni at 5 and Zn at 4, whilst that of Cd was exceeded twice and Cu only once. Where the Hg PEL was exceeded, it also exceeded the Apparent Effects Level, the sediment concentration of Hg at which biological effects are always seen. This occurred at Diss Mere and Gull Pond the most easterly sites in the dataset. PEL exceedence of trace metals is therefore widespread across the UK and, in places, greatly exceeded, with several metals exceeding the PEL by factors of 5-6.

These data are in agreement with previous work which showed evidence for toxicity to benthic invertebrates at a number of UK sites mainly to the north and west of the UK. Our study confirms the widespread nature of exceedence over this biological threshold level across southern Scotland, England and Wales. However, the full extent of these exceedences is unknown, both spatially and by degree of exceedence.

Despite emissions reductions there is increasing evidence for biological impact from trace metals in freshwaters in the UK and the likelihood of continued and possibly increasing trace metal inputs from catchment sources. Therefore, there is now an urgent need to fully assess the distribution and extent of trace metal concentrations in waters, sediments and biota, and trace metal exceedence across the whole of the UK. There is also a need to determine impacts across the freshwater food chain. Furthermore, given the potential for increased inputs there is a need to establish a UK-wide trace metals monitoring network for freshwaters, to include a range of lake and stream types, to identify future rates and directions of change.

Contents

Background

Despite a recent increase in interest in trace metal contamination in the UK as a result of the forthcoming Daughter Air Quality Directives, UNECE protocols and the development of critical loads for trace metals, there remains a considerable lack of data on both the spatial and long-term temporal scales. Only the Rural Monitoring Network has measured metals deposition for more than 20 years (Baker, 2001) and, in the absence of long-term monitoring, lake sediments remain one of the few means by which the record of metal deposition can be determined over periods of decades or centuries, placing contemporary depositional status into its correct historical context. Further, using the sediment record, rates and directions of change can be clearly and retrospectively identified for a whole suite of contaminants. For Hg the situation is far worse than for other trace metals. There are very few data available for the UK (Lee et al., 2000) and most of these are from sites in the north and west of the UK. For the south and east of the UK, temporal data for Hg exists for a single site (DETR contract EPG 1/3/159; Yang et al., 2001).

As part of another project 18 sediment cores were taken from across the UK in 2000 by the ECRC. These cores have been ^{210}Pb-dated, freeze-dried and archived. They have therefore been stored in a way compatible with the analysis of trace metals, including Hg. The aim of this project was to select ten of these cores from areas where temporal trace metals data are absent (i.e. particularly in the south and east of the UK) and analyse these for Hg, Cd, Pb, Ni, Cu and Zn. This will provide:

- the full post-industrial record of metal deposition for areas of the UK where such data are absent;
- an indication as to the rates of change in inputs to freshwaters and an assessment as to whether freshwater inputs across the UK are responding to emission reduction policies;
- data for critical loads modellers;
- an assessment of any risk posed to freshwater organisms by linking these data with toxicological studies.

Sites

The ten sites selected for study are shown in Figure 1. The sites were selected primarily for their geographical location (i.e. to provide a good coverage of the UK where data were not available) but also where previous studies had indicated that a reliable sediment record existed. Additional information is provided in Table 1.

***Figure 1**: Location map of the ten selected sites.*

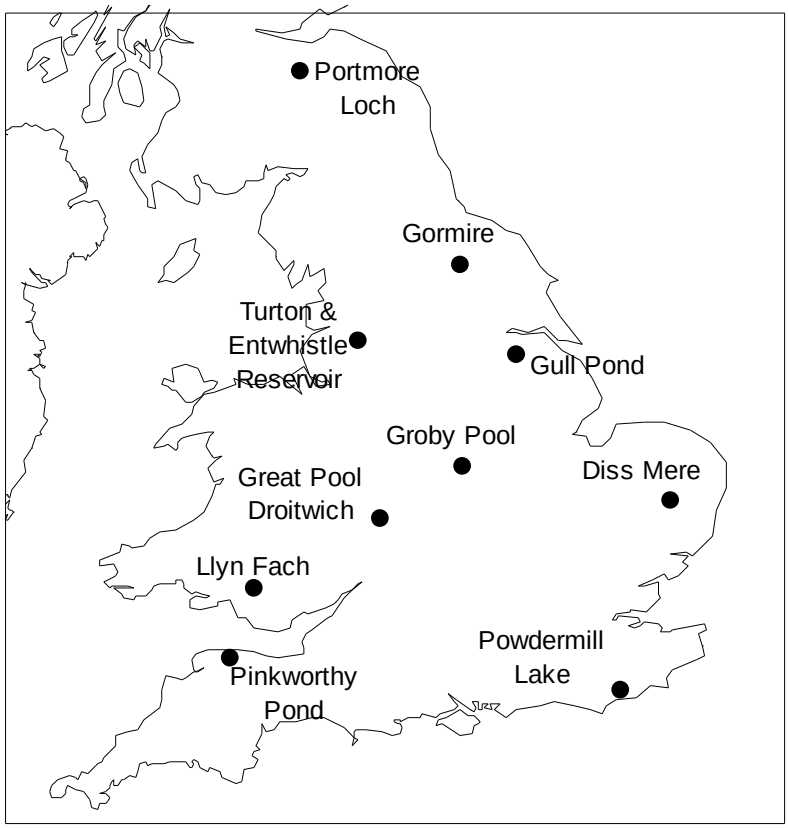

***Table 1**. Selected site data*

Site	Grid Reference	Max. Depth (m)	Use
Diss Mere	TM 115 798	6.5	Recreation
Llyn Fach	SN 905 037	5.7	Fishing
Gormire	SE 503 833	4.6	Fishing
Great Pool Droitwich	SQ 880 634	3.7	Recreation
Groby Pool	SK 521 083	1.8	Ornamental / wildfowl
Gull Pond	SE 939 060	1.0	Recreational / wildfowl
Pinkworthy Pond	SS 722 423	7.6	Recreation
Portmore Loch	NT 260 504	14.5	Fishing
Powdermill Lake	TQ 741 147	1.5	Ornamental
Turton & Entwistle Res.	SD 720 175	22.0	Reservoir

Methods

Lithostratigraphy
Samples from every level of each core were analysed for water content and loss-on-ignition (550°C). Wet density measurements were undertaken on every fifth sample from each core. Standard methods were employed for these analyses (e.g. Dean, 1974; Stevenson et al., 1987).

Radiometric dating
Sediment samples from each core were analysed for ^{210}Pb, ^{226}Ra, ^{137}Cs and ^{241}Am by direct gamma assay using Ortec HPGe GWL series well-type coaxial low background intrinsic germanium detectors (Appleby et al. 1986). ^{210}Pb was determined via its gamma emissions at 46.5keV, and ^{226}Ra by the 295keV and 352keV γ-rays emitted by its daughter isotope ^{214}Pb following 3 weeks storage in sealed containers to allow radioactive equilibration. ^{137}Cs and ^{241}Am were measured by their emissions at 662keV and 59.5keV. The absolute efficiencies of the detectors were determined using calibrated sources and sediment samples of known activity. Corrections were made for the effect of self absorption of low energy γ-rays within the sample (Appleby *et al.* 1992).

Supported ^{210}Pb activity was assumed to be equal to the measured ^{226}Ra activity and unsupported ^{210}Pb activity was calculated by subtracting supported ^{210}Pb from the measured total ^{210}Pb activity. ^{210}Pb radiometric dates were calculated using the CRS (constant rate of supply) and CIC (constant initial concentration) dating models (Appleby & Oldfield, 1978) where appropriate, and validated where possible against the 1986 and 1963 depths determined from the ^{137}Cs and ^{241}Am stratigraphic records. Definitive chronologies were based on an assessment of all the data using the methods described in Appleby & Oldfield (1983) and Appleby (2001).

Trace metals
All sediment samples were freeze-dried prior to analysis. Precisely weighed 0.3g sediment samples were heated with 10 ml Aristar HNO_3 in 50 ml Teflon beakers at 100 °C on a hotplate for 1 hour. The resulting solutions were then made up to 30 ml using deionised water (18.2 MΩ). The final solutions were homogenised and 10 ml used for Pb, Zn, Cu, Cd and Ni analyses, whilst the remaining 20 ml was retained for Hg. Mercury in the digested sediment solutions was measured by cold vapour atomic adsorption spectrometry (CV-AAS), following reduction of Hg in the solution to its elemental state by 2 ml fresh $SnCl_2$ (10% in 20% v/v HCl; Engstrom & Swain, 1997). The other metals were measured using normal AAS. Certified standard reference materials (Buffalo River sediment SRM2704, Stream sediment GBW07305) were digested and analysed along with the sample analyses. Standard solutions and quality control blank digestions were measured every five samples to monitor measurement stability. Calibrations were made using these standard solutions. Measurement accuracy and analytical detection limits are given in Tables 2 and 3 respectively.

Trace metal toxicity
Previous studies on toxic compounds in UK lake sediments (Rose et al., 2003) have shown that trace metals contribute more of the sediment toxicity to benthic organisms than persistent organic pollutants (e.g. PAHs, PCBs, other organochlorines). In order to predict sediment trace metal toxicity alone, numerical sediment quality guidelines

for freshwater ecosystems have been developed using a variety of approaches. Based on these, MacDonald et al (2000) developed a threshold effect level (TEL) and a probable effect level (PEL). The definitions and trace metal concentrations for these are shown in Table 4. More detailed toxicity data are available for Hg and five effects levels for freshwater sediments have been identified (Table 5) (Avocet Consulting, 2003). In this project, the guideline levels shown in Tables 4 and 5 are used to assess the potential toxicity of trace metal sediment concentrations.

Table 2: *Measurement accuracy of standard reference materials (SRM2704). The values in parentheses are standard deviations (n = 10). Hg and As are measured using GBW07305. Hg data are given in ng g^{-1}, the remainder in $\mu g\ g^{-1}$.*

	Hg	Pb	Zn	Cu	Cd	Ni
Certified value	100	161	438	98.6	3.45	44.1
Measured value	93 (8.6)	158 (6)	318 (32)	84 (7)	3.72 (0.12)	37 (2.5)
Recovery	93%	98%	73%	85%	108%	84%

Table 3: *Detection limits for metal analyses. Hg in ng g^{-1}, the remainder in $\mu g\ g^{-1}$.*

	Hg	Pb	Zn	Cu	Cd	Ni
LOD	6.3	2.9	1.9	1.1	0.33	2.0

Table 4*. Threshold Effect Level (TEL) and Probable Effect Level (PEL) of trace metals for freshwater sediments. Hg is in ng g^{-1}, the remainder in $\mu g\ g^{-1}$.*

	Ni	Cu	Zn	Cd	Hg	Pb
TEL	18	35	123	0.596	174	35
PEL	36	197	315	3.54	486	91.3

Table 5*. Freshwater sediment quality values for total Hg*

Freshwater sediment quality value	Hg (ng g^{-1})	Effects level
Apparent effects threshold	560	Level above which biological effects have always been observed
Floating percentile method	500	Proposed level which optimises reliability and sensitivity in predicting adverse biological effects
Probable effects level	490	Level at which adverse biological effects are frequently seen
Lowest effects level	200	Level at which adverse biological effects are seen in 5% of benthic species
Threshold effects level	170	Level below which adverse biological effects rarely occur

Results

Lithostratigraphy

Figure 2 shows the lithostratigraphic data for the ten sediment cores. These data provide useful background and interpretative data to the trace metals results. Dry weight provides information on sediment water content, loss-on-ignition (LOI) gives an estimate of organic content and wet density is used in the calculation of inventories such as those used in chronologies. Dry weight and LOI data often show inverse correlations, and whilst dry weight tends to increase down-core as a result of sediment compaction, coincident peaks in dry weight and wet density data can give an indication of changes in sediment source (for example from in-washes of inorganic material from the catchment).

Figure 2. *Dry weight, loss-on-ignition and wet density data.*

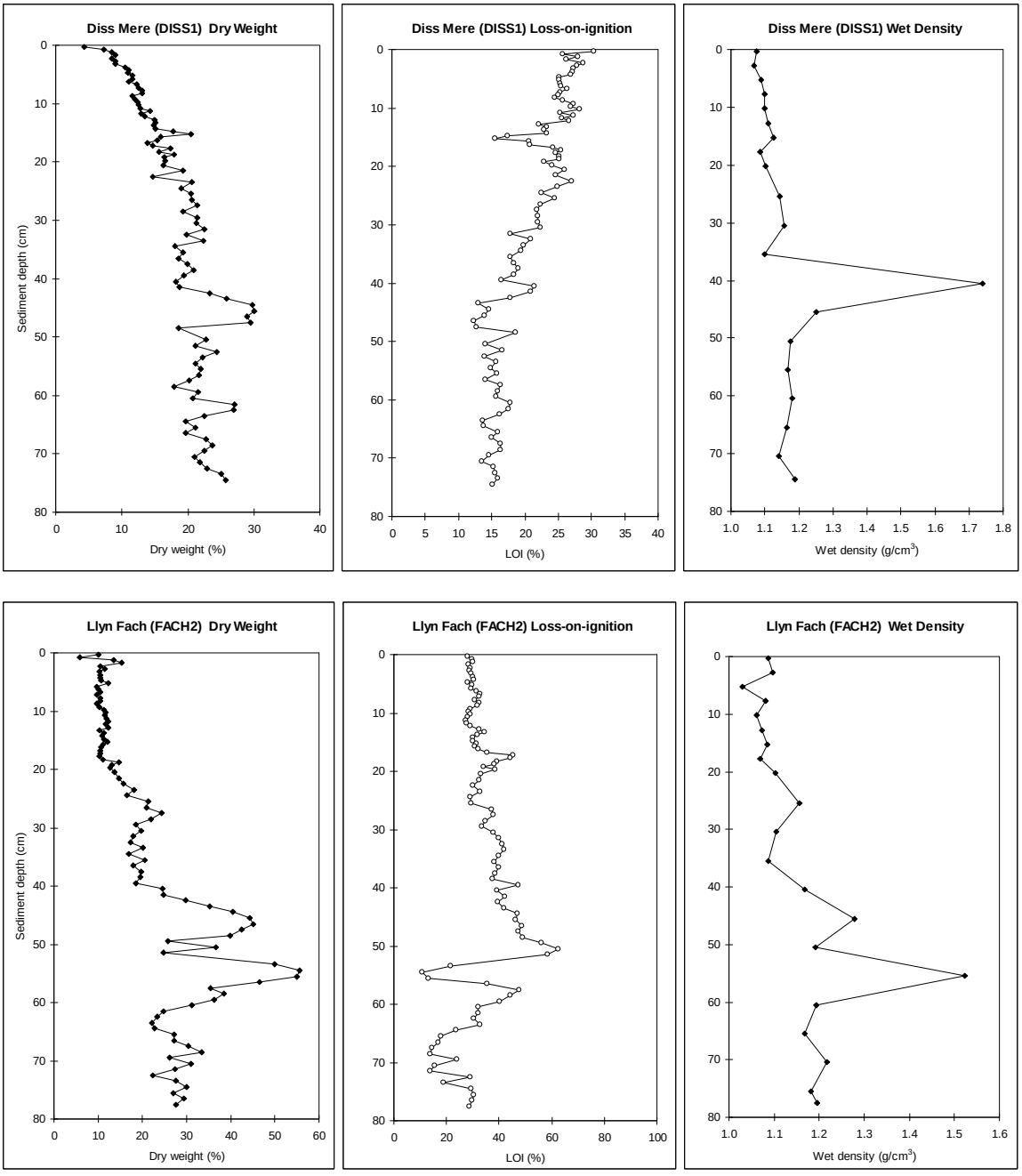

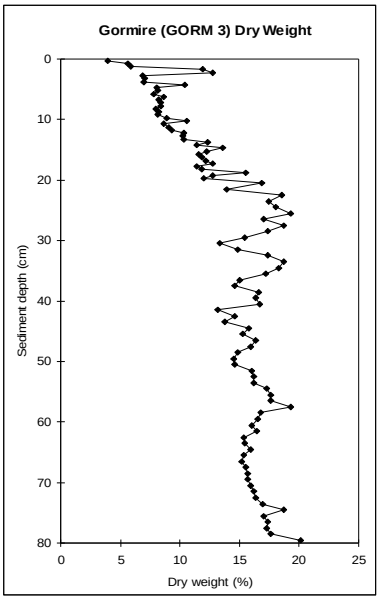
Gormire (GORM 3) Dry Weight
Sediment depth (cm)
Dry weight (%)

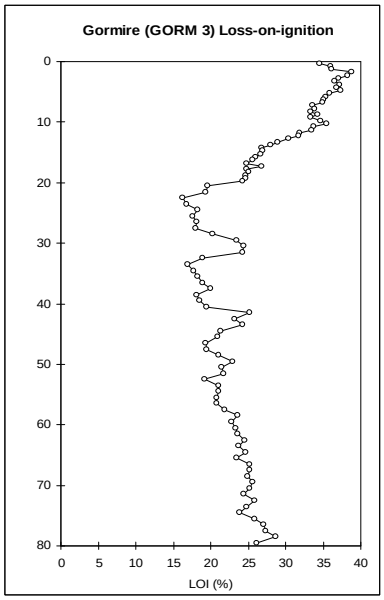
Gormire (GORM 3) Loss-on-ignition
LOI (%)

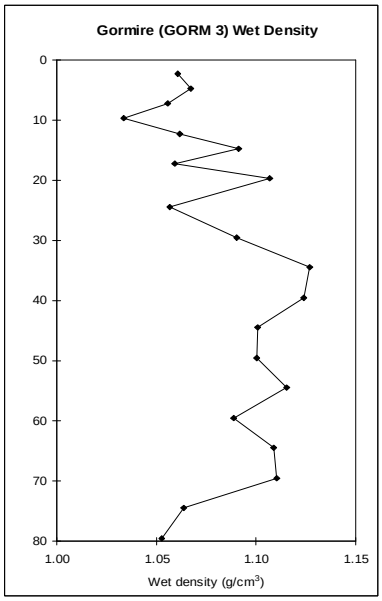
Gormire (GORM 3) Wet Density
Wet density (g/cm3)

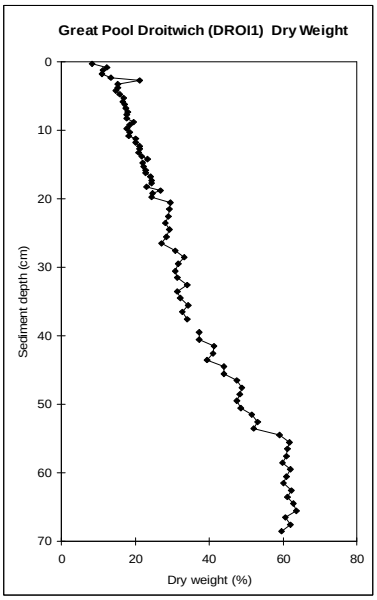
Great Pool Droitwich (DROI1) Dry Weight
Sediment depth (cm)
Dry weight (%)

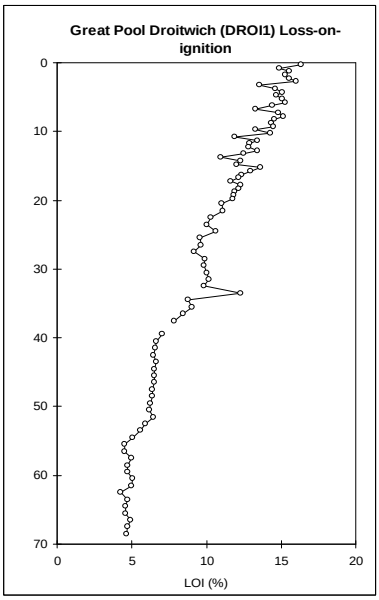
Great Pool Droitwich (DROI1) Loss-on-ignition
LOI (%)

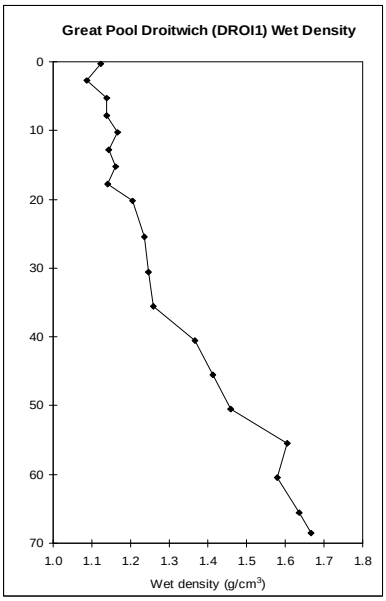
Great Pool Droitwich (DROI1) Wet Density
Wet density (g/cm3)

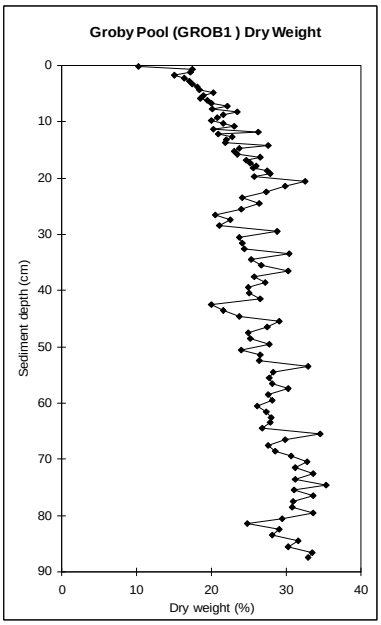
Groby Pool (GROB1) Dry Weight
Sediment depth (cm)
Dry weight (%)

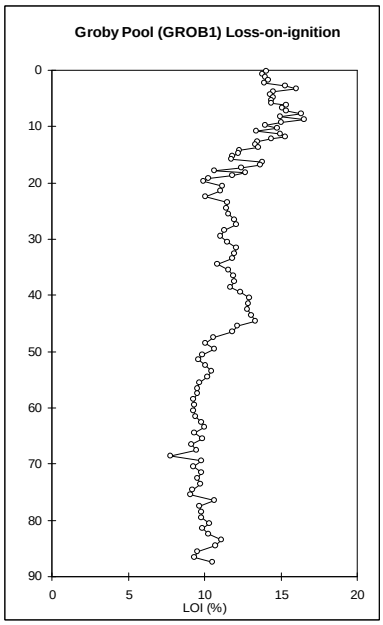
Groby Pool (GROB1) Loss-on-ignition
LOI (%)

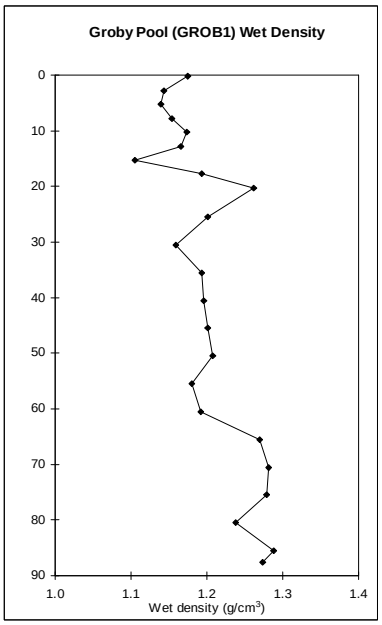
Groby Pool (GROB1) Wet Density
Wet density (g/cm3)

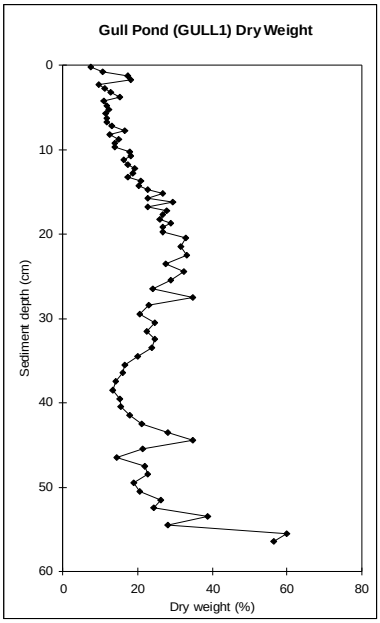
Gull Pond (GULL1) Dry Weight
Sediment depth (cm)
Dry weight (%)

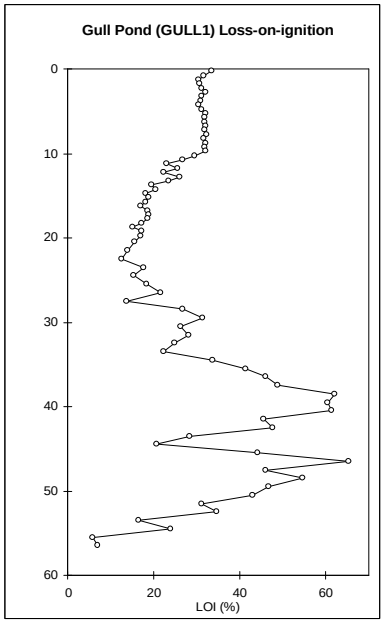
Gull Pond (GULL1) Loss-on-ignition
LOI (%)

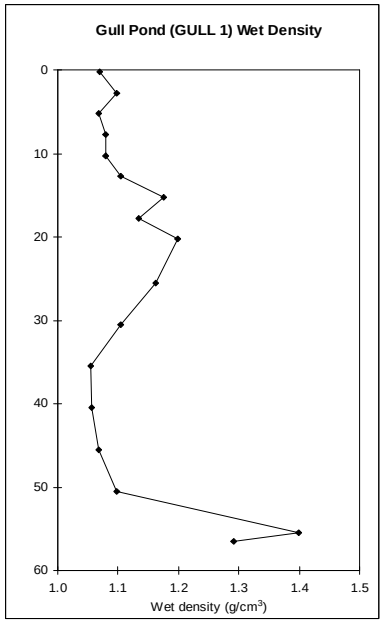
Gull Pond (GULL 1) Wet Density
Wet density (g/cm3)

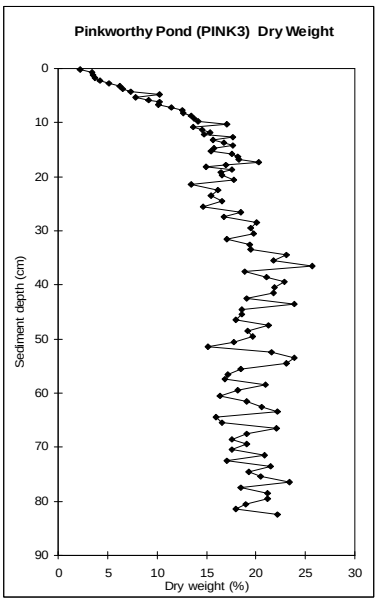
Pinkworthy Pond (PINK3) Dry Weight
Sediment depth (cm)
Dry weight (%)

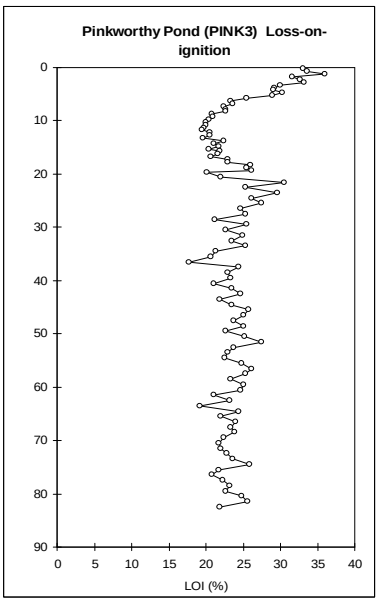
Pinkworthy Pond (PINK3) Loss-on-ignition
LOI (%)

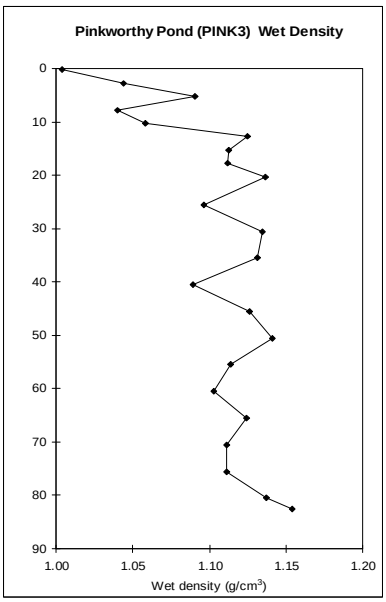
Pinkworthy Pond (PINK3) Wet Density
Wet density (g/cm3)

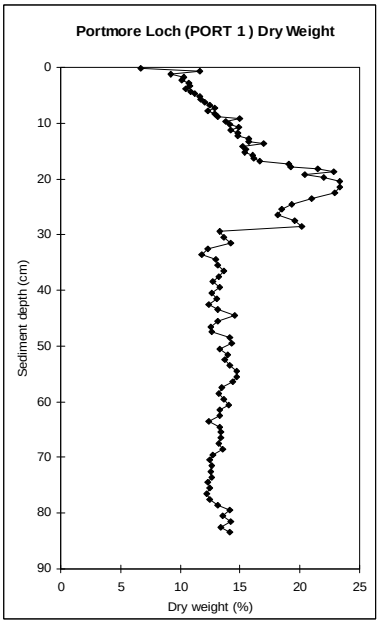
Portmore Loch (PORT 1) Dry Weight
Sediment depth (cm)
Dry weight (%)

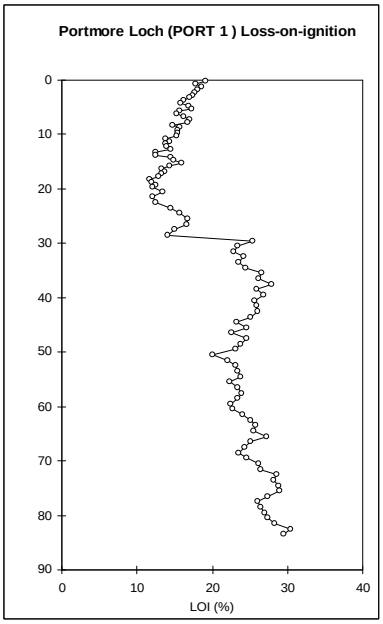
Portmore Loch (PORT 1) Loss-on-ignition
LOI (%)

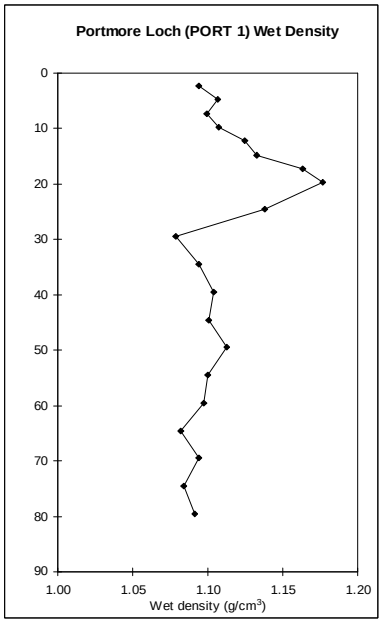
Portmore Loch (PORT 1) Wet Density
Wet density (g/cm3)

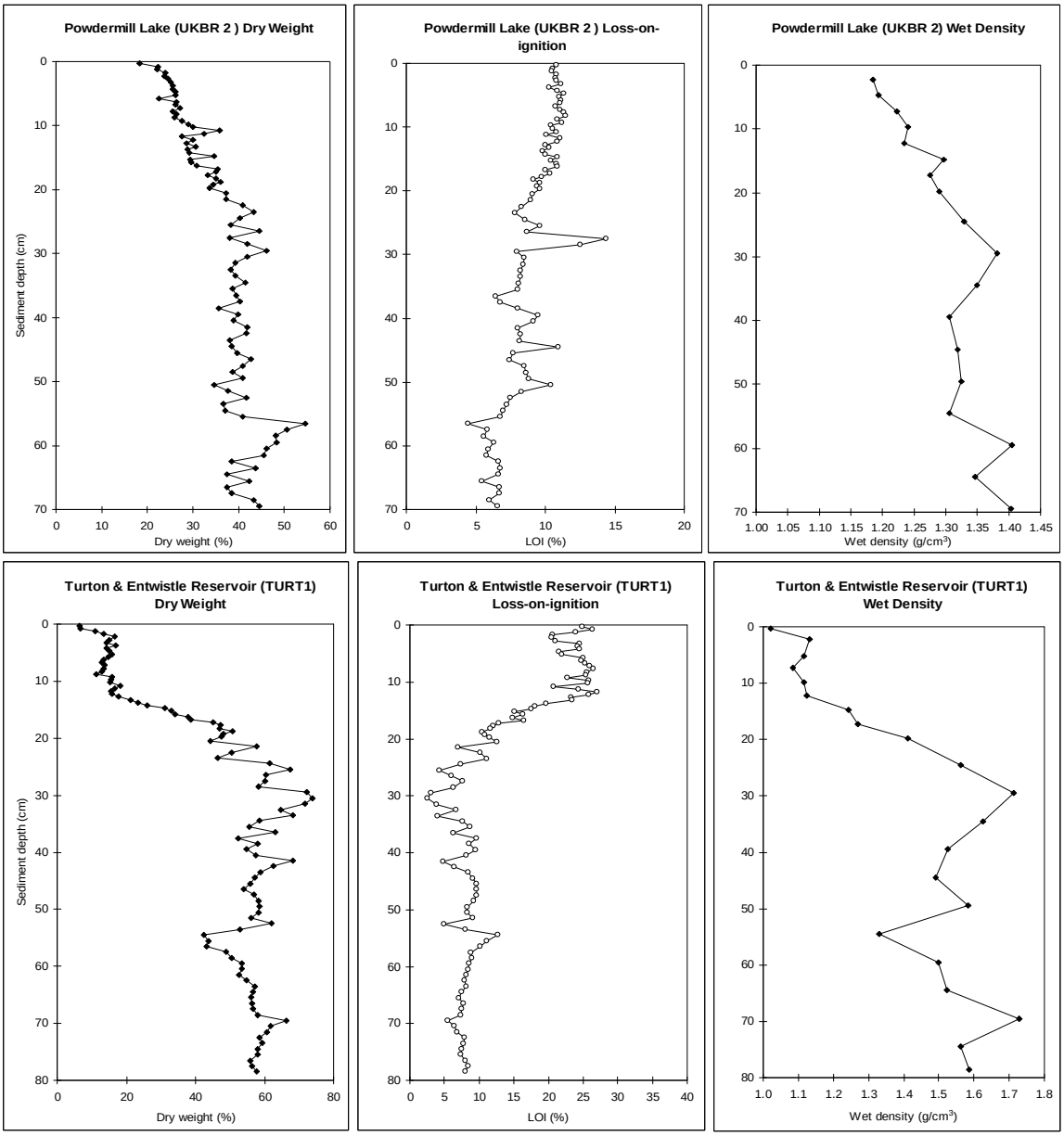

Diss Mere

Chronology

This core has an erratic ^{210}Pb record. Concentrations are significantly above that of the supporting ^{226}Ra only in the surficial sample, and in a small section between 20-30 cm (Figure 3a). The unsupported ^{210}Pb inventory (Table 6) is estimated to be just 30% of the estimated atmospheric flux. The ^{137}Cs record (Figure 3c) appears to be more reliable, though an abrupt decline between 25-29 cm points to the possibility of a hiatus in the sediment record. It is however reasonable to suppose that the high concentrations between 16-25 cm record the high fallout levels in the 1960s from the atmospheric testing of nuclear weapons. Because of the very poor ^{210}Pb record it was not possible to calculate ^{210}Pb dates for this core. From the ^{137}Cs record, the mean post-1960 sedimentation rate is estimated to be 0.09 ± 0.02 g cm^{-2} y^{-1} (0.61 ± 0.11 cm y^{-1}). Table 7 gives a tentative chronology for the past 60 years assuming a constant

sedimentation rate of this value. Supporting evidence from spheroidal carbonaceous particle (SCP) dating suggests that this chronology is reasonable (Rose & Appleby, in press).

Figure 3. *Fallout radionuclides in Diss Mere core DISS1 showing (a) total and supported ^{210}Pb, (b) unsupported ^{210}Pb, (c) ^{137}Cs concentrations versus depth.*

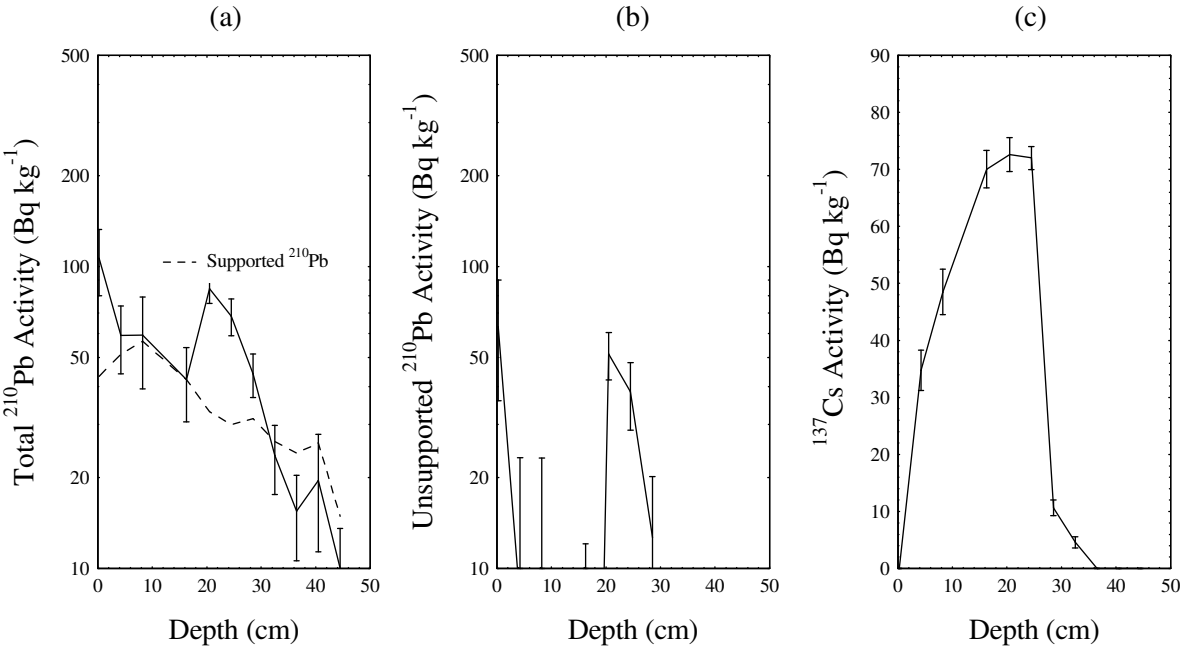

Table 6. *Fallout radionuclide concentrations in Diss Mere core DISS1*

Depth		^{210}Pb Total		^{210}Pb Unsupported		^{210}Pb Supported		^{137}Cs	
cm	g cm^{-2}	Bq kg^{-1}	±	Bq kg^{-1}	±	Bq kg^{-1}	±	Bq kg^{-1}	±
0.25	0.01	106.3	26.2	63.1	27.1	43.2	7.1	0.0	0.0
4.25	0.38	59.1	14.9	7.8	15.5	51.3	4.0	34.8	3.5
8.25	0.89	59.3	19.9	2.7	20.6	56.6	5.2	48.5	4.0
16.25	2.16	42.2	11.6	0.0	12.1	42.2	3.2	70.0	3.3
20.50	2.92	84.4	8.9	51.3	9.2	33.1	2.3	72.6	3.0
24.50	3.73	68.4	9.5	38.4	9.7	30.0	1.8	72.0	2.0
28.50	4.66	44.1	7.2	12.7	7.4	31.4	1.9	10.6	1.4
32.50	5.64	23.7	6.1	-2.6	6.2	26.3	1.3	4.6	1.0
36.50	6.53	15.5	4.9	-8.6	5.1	24.1	1.4	0.0	0.0
40.50	7.43	19.6	8.2	-6.4	8.4	26.0	1.6	0.0	0.0
44.50	8.50	10.0	3.5	-4.9	3.7	14.9	0.9	0.0	0.0

Table 7. *^{210}Pb chronology of Diss Mere core DISS1*

Depth		Chronology			Sedimentation Rate		
		Date	Age				
cm	g cm^{-1}	AD	y	±	g cm^{-2} y^{-1}	cm y^{-1}	± (%)
0.25	0.01	2000	0	0			
4.25	0.38	1996	4	1	0.09	0.67	20
8.25	0.89	1990	10	2	0.09	0.62	20
16.25	2.16	1976	24	5	0.09	0.54	20
20.50	2.92	1968	32	6	0.09	0.48	20
24.50	3.73	1958	42	8	0.09	0.42	20
28.50	4.66	1948	52	10	0.09	0.40	20
32.50	5.64	1937	63	13	0.09	0.38	20
36.50	6.53	1927	73	15	0.09	0.38	20

Trace metals

The trace metal profiles (Figure 4) show that Ni and Pb concentrations increase only slightly, whilst Zn and Cd concentrations increase more significantly from around 55 cm and 35 cm, respectively, to the surface. Copper and Hg are unusually high at the base of the core, especially Hg, which reaches almost 19000 ng g^{-1}. The core can thus be divided into two phases. First, from the base to about 55 cm, and second from 55cm to the surface. Mercury and Cu concentrations decrease when Zn and Cd increase between these phases. This suggests a change in pollution source and the high trace metal concentrations of Cu, Hg and Zn indicate an anthropogenic influence. The high Hg concentrations in the base of DISS1 have not been observed in other UK lake sediments before and are more than 30 times higher than the apparent effects threshold level for freshwater sediments. Although Hg concentrations in the upper part of the core are much lower, they are still four times higher than the apparent effects threshold level. Zinc and Pb concentrations are also much higher than their probable effect levels. The results show that this site has been severely contaminated by Hg, Zn, Pb and Cu, in the past.

Trace metal concentrations may be affected by other sedimenting matter deposited at the same time. Conversion of concentrations to fluxes takes this into account and provides an indication of the rate of trace metal deposition over time. The trace metal flux profiles of DISS1 are shown in Figure 5 and were calculated using the chronology data. However, this limits direct interpretation to post-1927 (above 35.5cm) (Table 7). The fluxes of Ni, Cu and Zn increase only slightly from 1927 to 2000 while the Hg flux decreases from 1927 to the 1940s and then increases again from the 1970s to the surface (2000). Fluxes of Hg, Zn, Cu and Pb are extremely high when compared with many other sites and this is due to the high sediment concentrations. If the basal sedimentation rate of 0.38 cm y^{-1} is extrapolated we calculate that the bottom sediments were deposited c. 1830. The fluxes of Hg and Cu could be as high as 1.71 and 16.1 μg cm^{-2} y^{-1} at this time.

Figure 4. *The trace metal concentration profiles in DISS1*

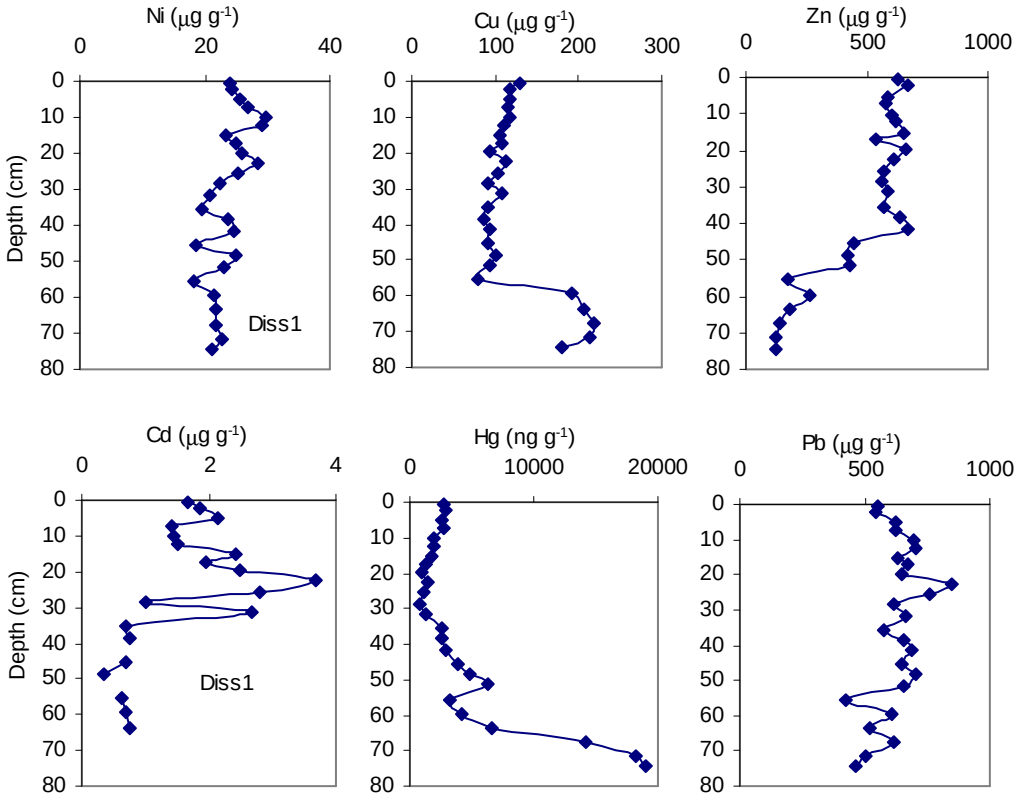

Figure 5. *The trace metal flux profiles in DISS1*

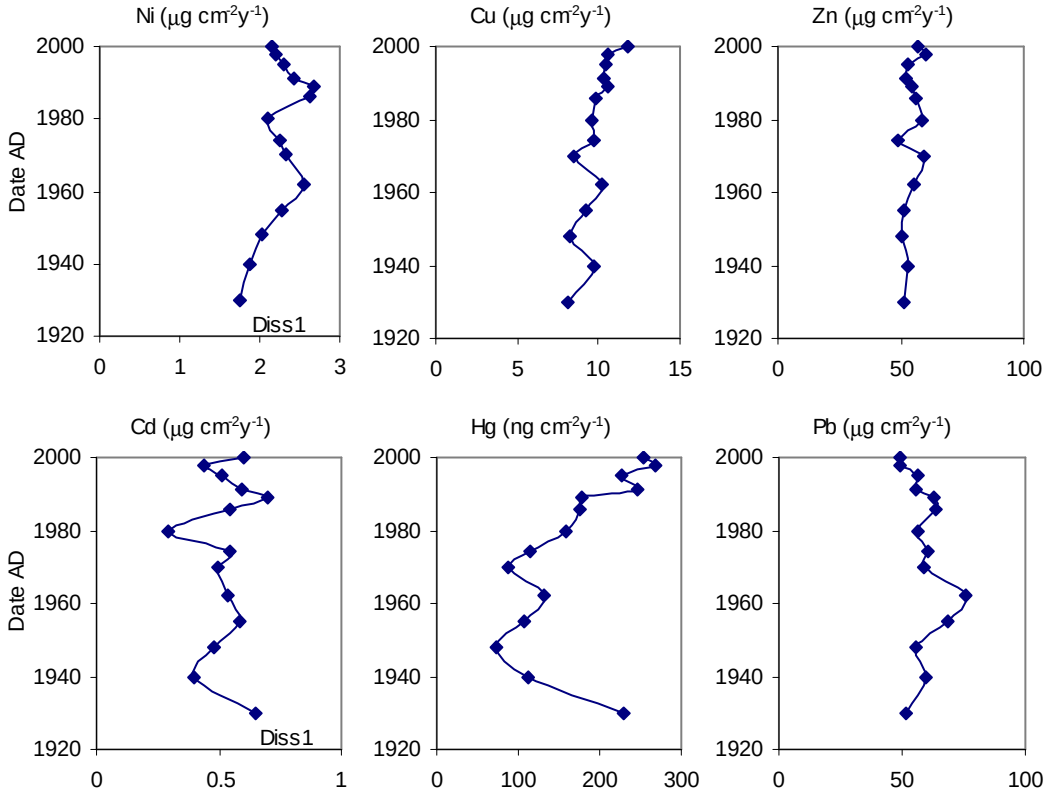

Llyn Fach

Chronology

This core appears to have a good fallout record with a ^{210}Pb supply rate (Table 8) that is comparable to the estimated atmospheric flux. Total ^{210}Pb activity reaches equilibrium with the supporting ^{226}Ra at a depth of c.25 cm (Figure 6a). The gradient of the unsupported ^{210}Pb profile varies significantly with depth with two sections of steeply declining concentrations (<4 cm and >13 cm) separated by a zone of almost uniform activity (Figure 6b). The ^{137}Cs activity versus depth profile has a well-resolved peak at 12.25 cm (Figure 6c). A small but significant ^{241}Am peak at the same depth shows that this feature records the 1963 fallout maximum from the atmospheric testing of nuclear weapons. The irregular ^{210}Pb record precluded use of the CIC model and Figure 7 plots ^{210}Pb dates calculated using the CRS model, together with the 1963 date suggested by the ^{137}Cs and ^{241}Am records. The ^{210}Pb dates place 1963 at a depth of 11 cm, in reasonably good agreement with the ^{137}Cs and ^{241}Am. Corrected ^{210}Pb dates and sedimentation rates have however been calculated using the ^{137}Cs and ^{241}Am 1963 date as a reference point. The results are shown in Figure 7 and given in detail in Table 9. These indicate a relatively uniform sedimentation rate of 0.022 ± 0.03 g cm^{-2} y^{-1} (0.15 cm y^{-1}) from the later part of the 19th century through to the mid-1960s, but that since then there has been a significant acceleration in accumulation rates. The mean value for the post-1970 period is calculated to be 0.041 g cm^{-2} y^{-1} (0.36 cm y^{-1}).

Table 8. *Fallout Radionuclide Concentrations in Llyn Fach core FACH1*

Depth		^{210}Pb Total		^{210}Pb Unsupported		^{210}Pb Supported		^{137}Cs		^{241}Am	
cm	g cm^{-2}	Bq kg^{-1}	±	Bq kg^{-1}	±	Bq kg^{-1}	±	Bq kg^{-1}	±	Bq kg^{-1}	±
0.25	0.03	431.8	48.5	378.3	49.2	53.5	7.9	293.3	10.5	0.0	0.0
2.25	0.27	309.4	25.7	222.0	26.6	87.3	7.0	301.8	9.2	0.0	0.0
4.25	0.50	261.5	21.0	192.5	21.6	69.0	5.4	350.0	8.5	0.0	0.0
6.25	0.73	259.1	19.4	183.0	20.1	76.1	5.3	359.5	7.9	0.0	0.0
8.25	0.94	243.7	25.4	186.6	26.3	57.0	6.8	358.3	10.0	0.0	0.0
10.25	1.17	240.2	27.2	166.4	28.3	73.9	7.5	414.9	10.3	0.0	0.0
12.25	1.42	244.0	13.7	192.9	14.3	51.0	4.1	430.4	8.4	6.6	1.8
14.25	1.66	149.2	17.2	86.8	17.9	62.4	5.0	310.4	7.3	6.0	2.1
16.25	1.91	118.7	14.9	62.2	15.4	56.5	4.1	127.3	4.9	0.0	0.0
18.25	2.14	77.7	12.1	38.5	12.5	39.2	3.4	62.3	4.4	0.0	0.0
20.50	2.46	103.0	16.7	56.7	17.0	46.3	3.2	72.0	3.4	0.0	0.0
22.50	2.79	71.6	10.1	13.2	10.6	58.4	3.1	50.9	2.7	0.0	0.0
24.50	3.18	86.6	9.2	32.0	9.6	54.6	2.8	42.8	2.0	0.0	0.0
26.50	3.64	30.8	8.6	-4.9	8.7	35.7	1.8	8.5	1.4	0.0	0.0
28.50	4.16	36.7	8.7	-10.9	8.9	47.6	1.9	6.7	1.4	0.0	0.0
32.50	5.00	34.3	5.7	-6.7	5.9	41.0	1.7	1.4	1.3	0.0	0.0

Table 9. *^{210}Pb chronology of Llyn Fach core FACH1*

Depth		Chronology			Sedimentation Rate		
		Date	Age				
cm	g cm^{-1}	AD	y	±	g cm^{-2} y^{-1}	cm y^{-1}	± (%)
0.00	0.00	2000	0	0			
0.25	0.03	1999	1	1	0.035	0.39	13.9
2.25	0.27	1993	7	2	0.049	0.39	13.3
4.25	0.50	1989	11	2	0.049	0.38	13.0
6.25	0.73	1984	16	3	0.045	0.37	13.2
8.25	0.94	1978	22	4	0.037	0.31	16.3
10.25	1.17	1972	28	5	0.034	0.25	14.8
12.25	1.42	1963	37	6	0.023	0.22	14.8
14.25	1.66	1952	48	6	0.022	0.20	13.0
16.25	1.91	1941	59	7	0.022	0.18	13.0
18.25	2.14	1931	69	9	0.022	0.16	13.0
20.50	2.46	1916	84	13	0.022	0.14	13.0
22.50	2.79	1901	99	18	0.022	0.13	13.0
24.50	3.18	1883	117	23	0.022	0.12	13.0

Figure 6. *Fallout radionuclide concentrations in Llyn Fach core FACH1 showing (a) total and supported ^{210}Pb, (b) unsupported ^{210}Pb, (c) ^{137}Cs and ^{241}Am.*

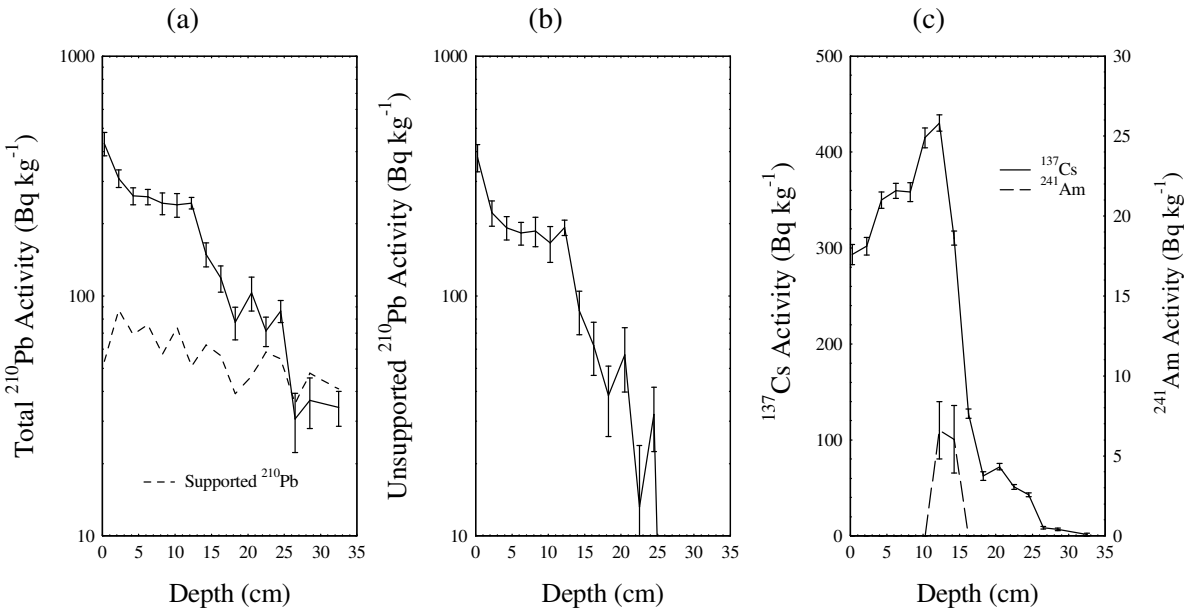

Figure 7. *Radiometric chronology of Llyn Fach core FACH1 showing CRS model ^{210}Pb dates (raw and corrected) together with dates determined from the ^{137}Cs/^{241}Am stratigraphy. Also shown are sedimentation rates calculated using the corrected CRS model.*

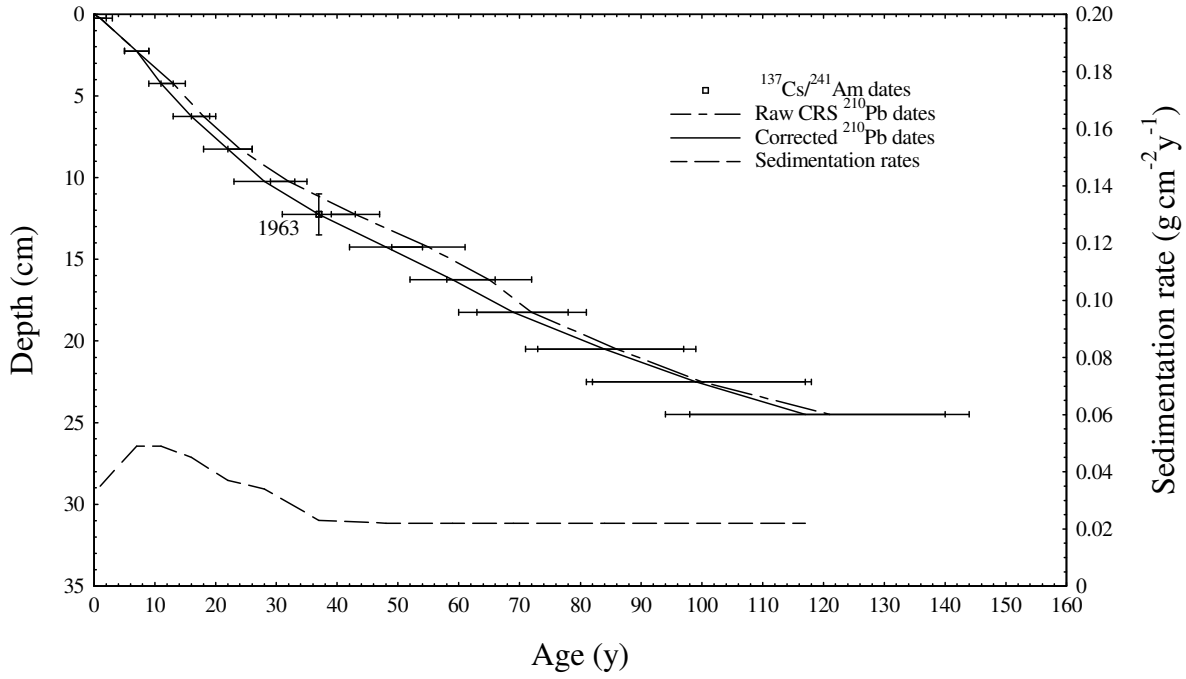

Trace metals

In FACH1, the trace metal profiles (Figure 8) show that the concentrations of Cu, Zn, Cd and Pb fluctuate from the base of the core up to c. 45 cm. Above this they generally increase, although Pb and Cd concentrations decline in the surface sediments. Ni and Hg concentrations show an overall increase from the bottom to the surface. The chronology places 24.5cm at around 1883 ± 23 but the declining LOI profile from 50cm to the surface (Figure 2) and the increasing sedimentation rate above 24.5 cm implies that the sediment accumulation rate could be increasing from 50 cm. Therefore, the sediments in the upper 50cm of the core could cover at least 230 years. This suggests that Llyn Fach has been contaminated by some trace metals since the late 18th century. The increases in contamination since this time have resulted in Ni, Zn, Cd and Pb concentrations in the surface sediments being above their probable effect levels.

Trace metal fluxes were calculated for the period covered by the reliable chronology (post-1880) and are shown in Figure 9. This indicates that between the 1880s and the 1940s, the input of these metals to the lake sediments was relatively stable, although all the metals excluding Cu show a slight increase while Cu shows a decline. From the 1940s onwards metal inputs increased significantly although Pb, Cd and Ni show a decrease over the last decade. However, since distribution of Cd and Ni in sediments can be affected by factors such as acidification, the reason for the decline of these elements in the surface sediments remains uncertain.

Figure 8. *The trace metal concentration profiles of FACH1*

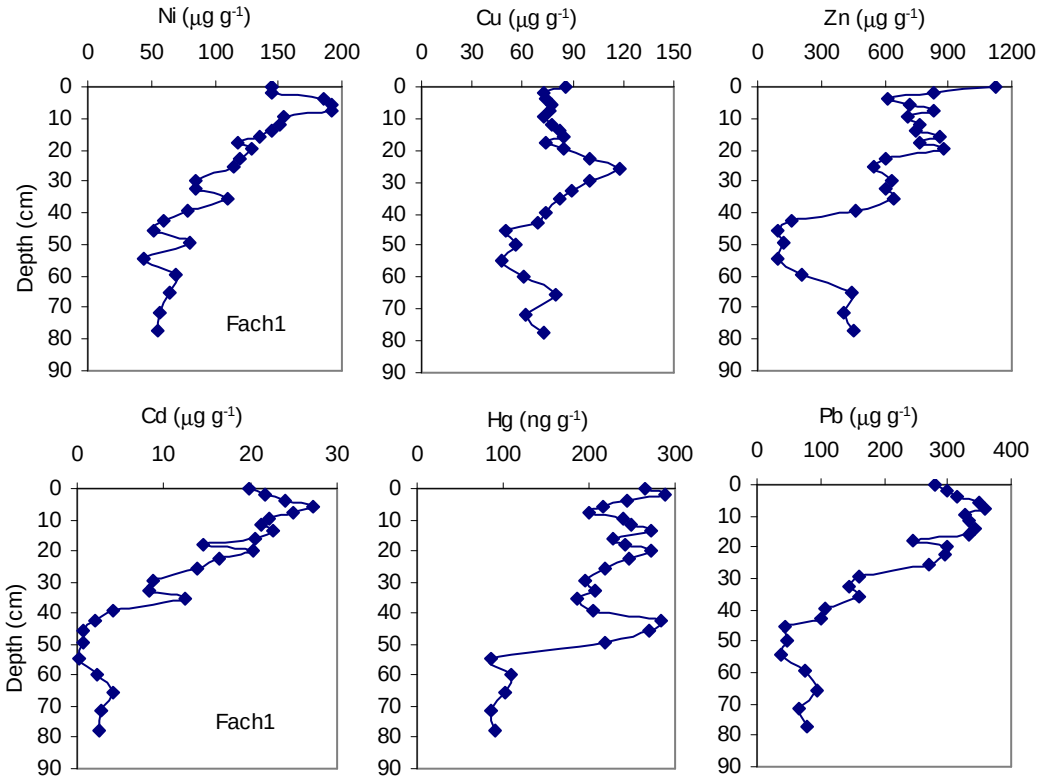

Figure 9. *The trace metal flux profiles of FACH1.*

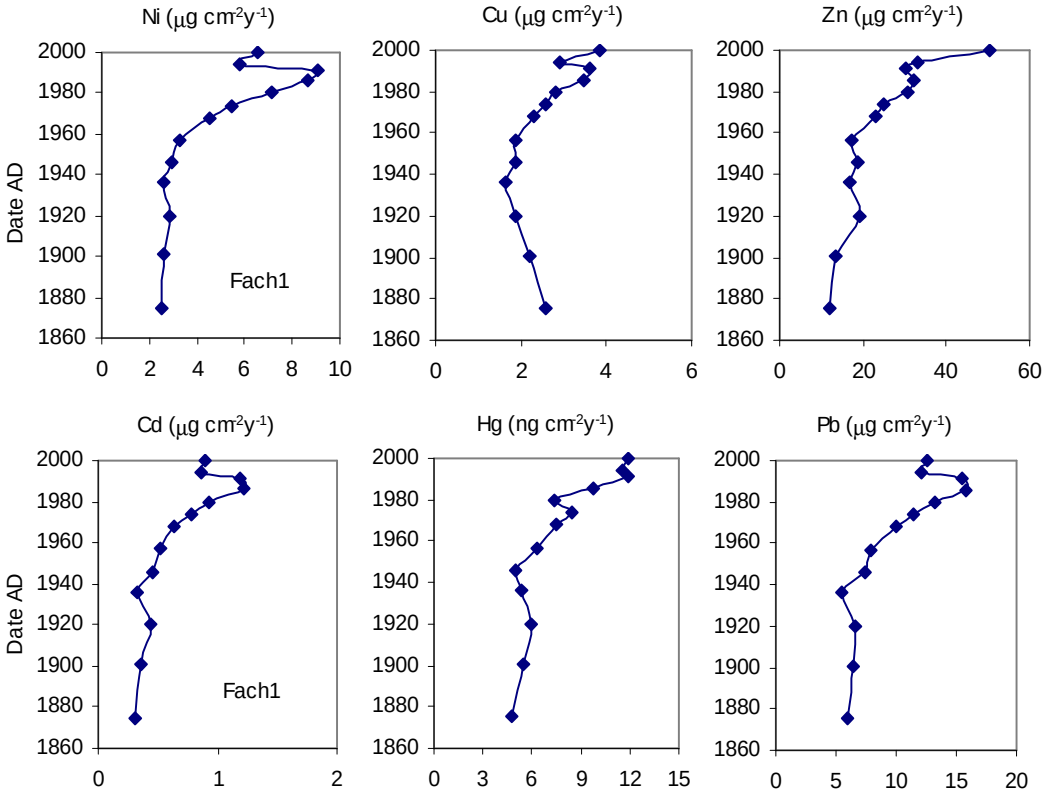

Gormire

Chronology

Total ^{210}Pb activity in this core reaches equilibrium with the supporting ^{226}Ra at a depth of c.19 cm (Figure 10a), though an abrupt drop in concentrations between 11.5-14.5 cm points to the possibility of a hiatus in the sediment record. Unsupported concentrations vary irregularly with depth (Figure 10b), the maximum concentration occurring in the 11-11.5 cm section. The ^{137}Cs activity versus depth profile has a relatively well defined peak between 8-11.5 cm that almost certainly records the 1963 fallout maximum from the atmospheric testing of nuclear weapons. Figure 11 shows ^{210}Pb dates calculated using the CRS model, together with the 1963 depth determined from the ^{137}Cs record. Use of the CIC model was precluded by the non-monotonic nature of the ^{210}Pb profile. The ^{210}Pb dates place 1963 at a depth of 9.7 cm, in reasonably good agreement with the ^{137}Cs date. They suggest very low accumulation rates (c.0.0048 g cm^{-2} y^{-1}) up to c.1950 and an increase since then. The mean post-1963 sedimentation rate of 0.023 g cm^{-2} y^{-1} is nearly 5 times higher than the pre-1950 value (c.0.0048 g cm^{-2} y^{-1}). The pre-1950 rate is significantly lower than that recorded in other Gormire cores (0.01-0.02 g cm^{-2} y^{-1}) and could be due to a hiatus in the sediment record. In view of this the earlier dates given in Table 11 should be regarded with some caution.

Table 10. *Fallout radionuclide concentrations in Gormire core GORM3*

Depth		^{210}Pb						^{137}Cs	
		Total		Unsupported		Supported			
cm	g cm^{-2}	Bq kg^{-1}	±	Bq kg^{-1}	±	Bq kg^{-1}	±	Bq kg^{-1}	±
0.25	0.01	184.9	55.9	108.9	57.6	76.0	13.8	229.9	18.4
2.25	0.18	246.7	29.7	157.7	30.8	89.0	8.3	185.5	10.5
4.25	0.35	198.6	36.7	135.3	37.6	63.3	8.4	197.9	10.8
6.25	0.53	248.1	25.5	185.9	26.4	62.2	6.8	229.0	8.0
8.25	0.70	210.9	21.1	164.4	21.6	46.5	5.0	262.8	7.6
9.25	0.79	214.1	23.7	139.9	24.6	74.2	6.3	251.7	8.0
10.25	0.88	206.9	35.1	133.7	35.8	73.2	6.9	228.8	8.2
11.25	0.98	301.0	37.2	235.4	37.8	65.6	6.6	270.6	8.4
12.25	1.08	156.4	18.8	103.3	19.4	53.0	4.7	218.4	7.6
14.25	1.31	70.3	13.0	11.4	13.6	58.9	3.8	114.1	4.6
16.25	1.58	77.4	17.2	15.4	17.9	61.9	4.8	72.3	4.4
18.25	1.84	62.8	13.1	9.0	13.6	53.8	3.5	31.6	3.6
20.50	2.18	34.6	5.9	-5.8	6.1	40.4	1.6	22.5	1.4
22.50	2.52	26.2	5.5	-16.0	5.9	42.2	2.0	10.1	1.1
24.50	2.90	35.7	5.8	-4.0	6.1	39.7	1.6	6.0	1.0

Table 11. *^{210}Pb chronology of Gormire core GORM3*

Depth		Chronology			Sedimentation Rate		
		Date	Age				
cm	g cm^{-1}	AD	y	±	g cm^{-2} y^{-1}	cm y^{-1}	± (%)
0.00	0.00	2000	0	0			
0.25	0.01	2001	0	1	0.052	0.56	54.1
1.25	0.09	1999	2	2	0.042	0.48	39.0
2.25	0.18	1997	4	2	0.032	0.40	23.8
3.25	0.26	1994	7	3	0.031	0.35	27.8
4.25	0.35	1991	10	3	0.031	0.31	31.7
5.25	0.44	1988	14	4	0.025	0.26	27.8
6.25	0.53	1984	17	5	0.018	0.22	23.8
7.25	0.62	1979	23	6	0.016	0.20	26.7
8.25	0.70	1973	28	7	0.015	0.18	29.5
9.25	0.79	1967	34	9	0.014	0.15	36.1
10.25	0.88	1960	41	11	0.012	0.10	47.3
11.25	0.98	1946	55	17	0.0044	0.06	60.6
12.25	1.08	1925	76	21	0.0052	0.05	72.1

Figure 10. *Fallout radionuclides in Gormire core GORM3 showing (a) total and supported ^{210}Pb, (b) unsupported ^{210}Pb, (c) ^{137}Cs concentrations versus depth.*

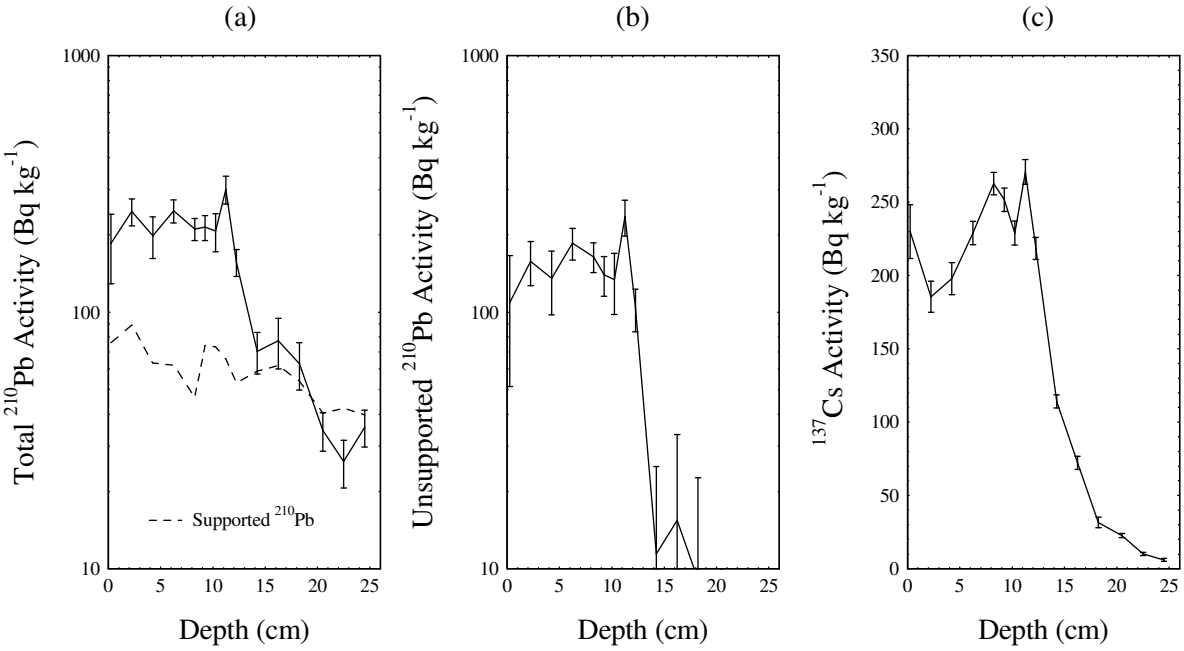

Figure 11. *Radiometric chronology of Gormire core GORM3 showing CRS model ^{210}Pb dates together with 1963 depth determined from the ^{137}Cs record. Also shown are sedimentation rates calculated using the CRS model.*

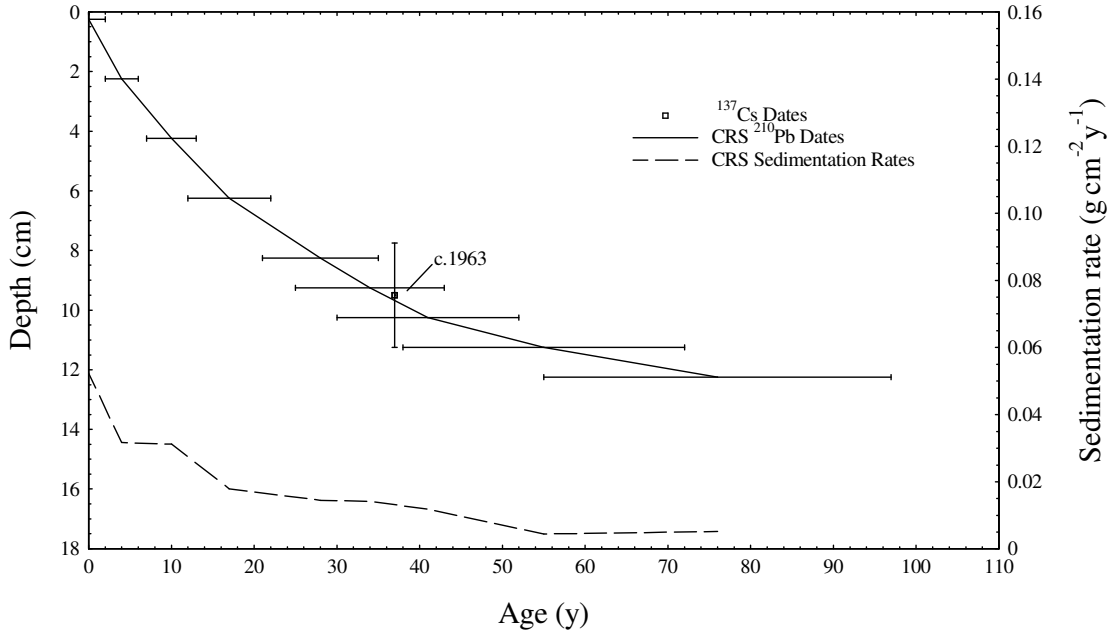

Trace metals

Mercury, Pb, Cu and Zn concentration profiles (Figure 12) show a slow increase from the base of the core to about 22 cm. Below 45 cm, Cd concentrations are below the limit of detection, but above this depth most Cd concentrations are above the limit of detection and show an increase in concentration to the surface. The rapid increase in Cu, Zn, Hg, Pb and Cd concentrations occur from 22 cm. This dates to the mid-19th century and is therefore probably due to contamination from atmospherically deposited pollutants during the industrial period. Nickel concentrations fluctuate throughout the core and remain relatively stable suggesting that human influence has not greatly affected Ni in the sediments at this site. All surface sediment trace metal concentrations exceed their Threshold Effect Levels (Table 4) in this core, while the concentration of Pb also exceeds the Probable Effect Level.

Conversion of trace metal concentration data to fluxes (Figure 13) show that the inputs of trace metals to the lake sediment at Gormire have increased since 1925 (12.25cm). The Pb concentration profile of GORM3 shows a decline in Pb concentration in the surface sediments, but the Pb flux profile does not show this trend. It is likely that Pb concentrations in the surface sediments were diluted by other sediment material deposited at the same time.

Figure 12. *The trace metal concentration profiles in GORM3.*

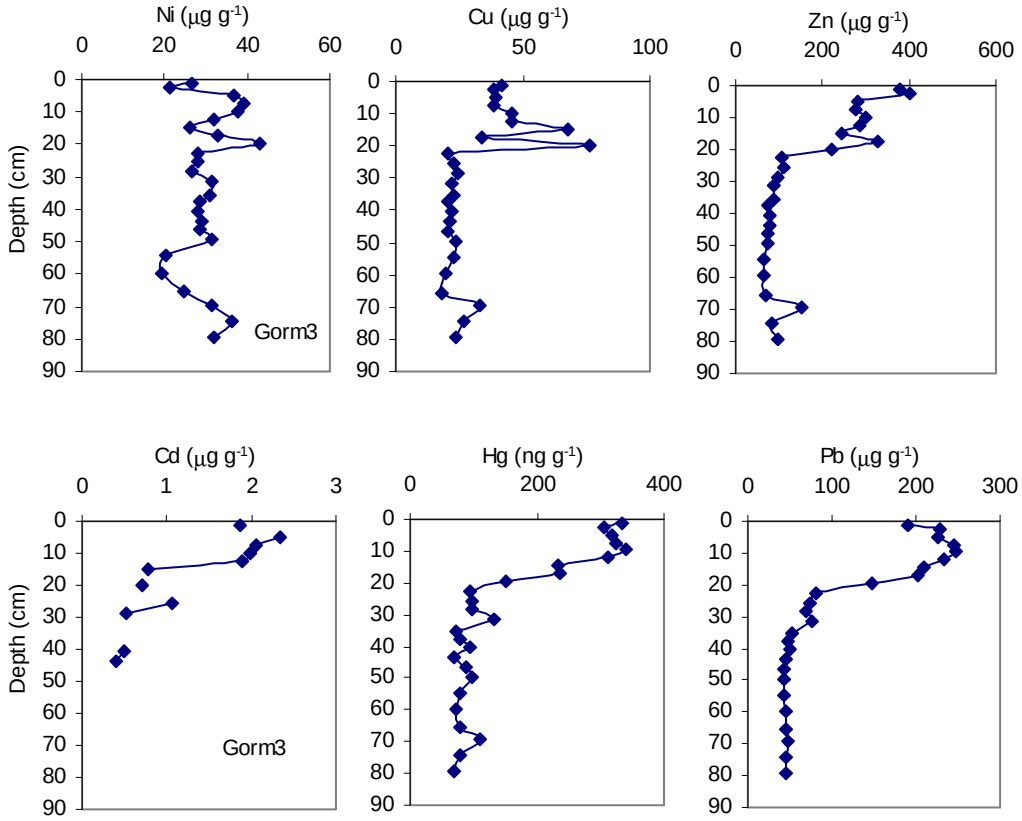

Figure 13*. The trace metal flux profiles in GORM3.*

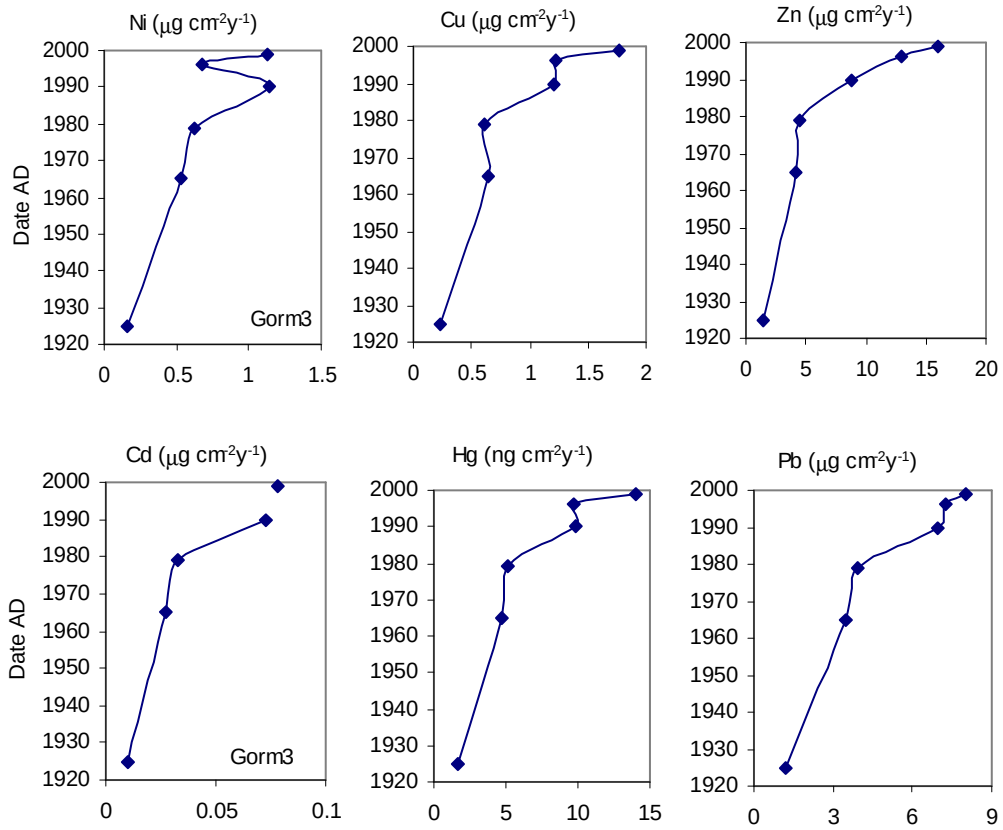

Great Pool Droitwich

Chronology

This core has a poor ^{210}Pb record. Concentrations are scarcely above that of the supporting ^{226}Ra in all sections analysed (Figure 14a). The unsupported ^{210}Pb inventory (Table 12) is estimated to be less than 15% of the estimated atmospheric flux. However, there appears to be quite a good record of ^{137}Cs fallout, in contrast to that of ^{210}Pb. The inventory is a little low, but there is a reasonably well defined peak at 16.25 cm that probably records the high fallout levels in the 1960s from the atmospheric testing of nuclear weapons (Figure 14c). Because of the poor ^{210}Pb record it was not possible to calculate ^{210}Pb dates for this core. From the ^{137}Cs record, the mean post-1963 sedimentation rate is estimated to be 0.09 ± 0.02 g cm^{-2} y^{-1} (0.44 ± 0.10 cm y^{-1}). Table 13 gives a tentative chronology for the past 60 years assuming a constant sedimentation rate of this value. Spheroidal carbonaceous particle (SCP) dating (Rose & Appleby, 2005) suggests that this chronology is reasonable.

Table 12. *Fallout radionuclide concentrations in Great Pool Droitwich core DROI1*

Depth		^{210}Pb Total		^{210}Pb Unsupported		^{210}Pb Supported		^{137}Cs	
cm	g cm^{-2}	Bq kg^{-1}	±	Bq kg^{-1}	±	Bq kg^{-1}	±	Bq kg^{-1}	±
0.25	0.02	70.5	11.1	16.4	11.6	54.1	3.4	31.3	3.1
4.25	0.64	51.9	19.9	-22.3	20.8	74.2	6.2	47.6	4.9
8.25	1.41	63.8	24.4	9.0	24.9	54.8	4.8	28.2	4.2
16.25	3.30	53.4	10.1	7.7	10.4	45.7	2.7	38.5	2.9
20.50	4.54	63.3	5.5	21.3	5.7	42.0	1.5	30.2	1.5
24.50	5.95	35.7	10.4	-12.2	10.6	47.9	2.2	6.0	1.5
28.50	7.41	43.0	7.1	-4.1	7.3	47.1	1.7	2.1	1.0

Table 13. *^{210}Pb chronology of Great Pool Droitwich core DROI1*

Depth		Chronology Date	Age		Sedimentation Rate		
cm	g cm^{-1}	AD	y	±	g cm^{-2} y^{-1}	cm y^{-1}	± (%)
0.25	0.02	2000	0	0			
4.25	0.64	1993	7	2	0.09	0.43	21
8.25	1.41	1984	16	3	0.09	0.40	21
16.25	3.30	1963	37	8	0.09	0.34	21
20.50	4.54	1949	51	11	0.09	0.32	21
24.50	5.95	1933	67	14	0.09	0.32	21

Figure 14. *Fallout radionuclides in Great Pool Droitwich core DROI1 showing (a) total and supported ^{210}Pb, (b) unsupported ^{210}Pb, (c) ^{137}Cs concentrations versus depth.*

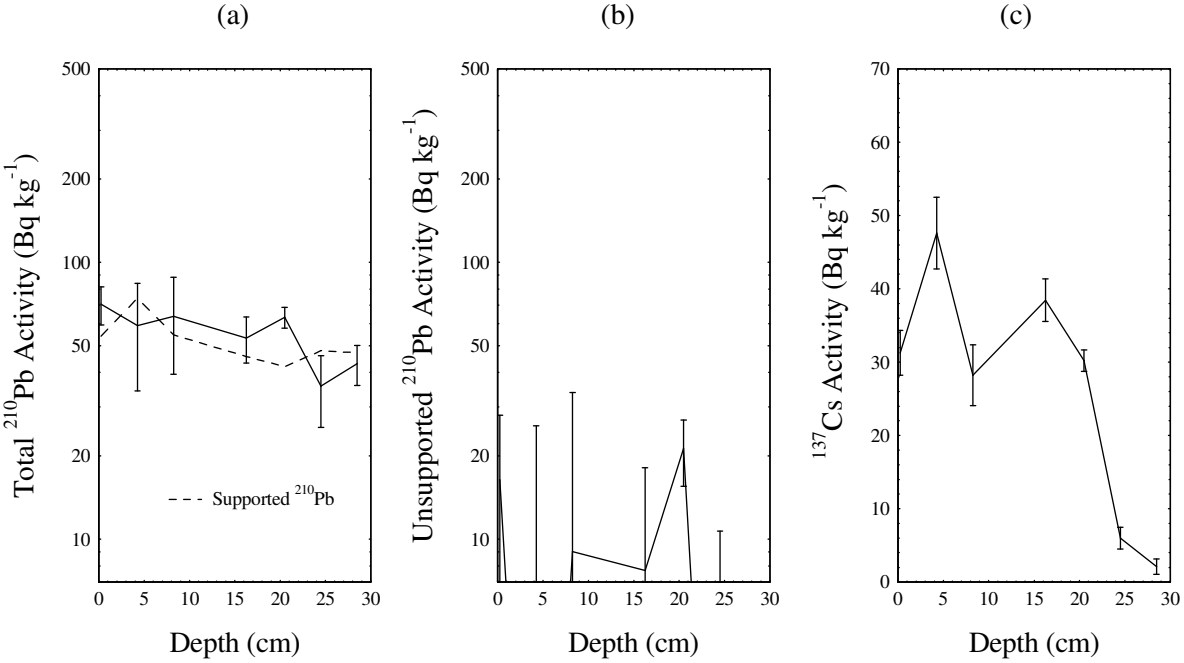

Trace metals

The trace metal concentration and flux profiles for core DROI1 taken from the Great Pool Droitwich are shown in Figures 15 and 16 respectively. All concentration profiles show an increase from the bottom of the core to the surface except Cd for which concentrations in the sediments below 35 cm are below the limit of detection. Above 35cm, Cd concentrations are relatively stable until an increase in the uppermost 5 cm. The LOI profile (Figure 2) shows a steady increase in organic content from the bottom to the surface suggesting a gradual change in sediment source and / or an increase in productivity. Ratios of Cu/LOI and Zn/LOI are relatively stable implying that the increase in Cu and Zn may be linked to this organic input. The increase of Hg/LOI and Pb/LOI ratios suggest an increase in Hg and Pb contamination. The reason for the Pb peak at 4.75 cm is currently unclear but the relatively high Cu, Zn and Cd concentrations in the surface sediments may be due to redox or pH changes at the sediment-water interface.

Conversion of concentrations to flux data is limited by the short chronology (post-1930), but show little change in Ni flux while Cd and Cu increase slightly to the 1990s. High fluxes of Cu, Zn and Cd in the surface sediments may simply be an artefact of the high concentrations and may not reflect true increases in trace metal input. Inputs of Pb and Zn increase from 1933 to the present. Neither the concentration nor the flux profile for Pb shows any decline in the surface sediments thereby failing to identify the huge reduction in UK Pb emissions. However, this could be masked by contributions from the catchment, or increased scavenging from the water column by algae as a result of elevated productivity at the site. Surface sediment concentrations of Pb, Cu, and Zn exceed their Threshold Effect Levels, while Ni and Cd exceed the Probable Effect Level. Hg surface sediment concentrations do not exceed any guideline value.

Figure 15 *The trace metal concentration profiles in sediment core DROI1.*

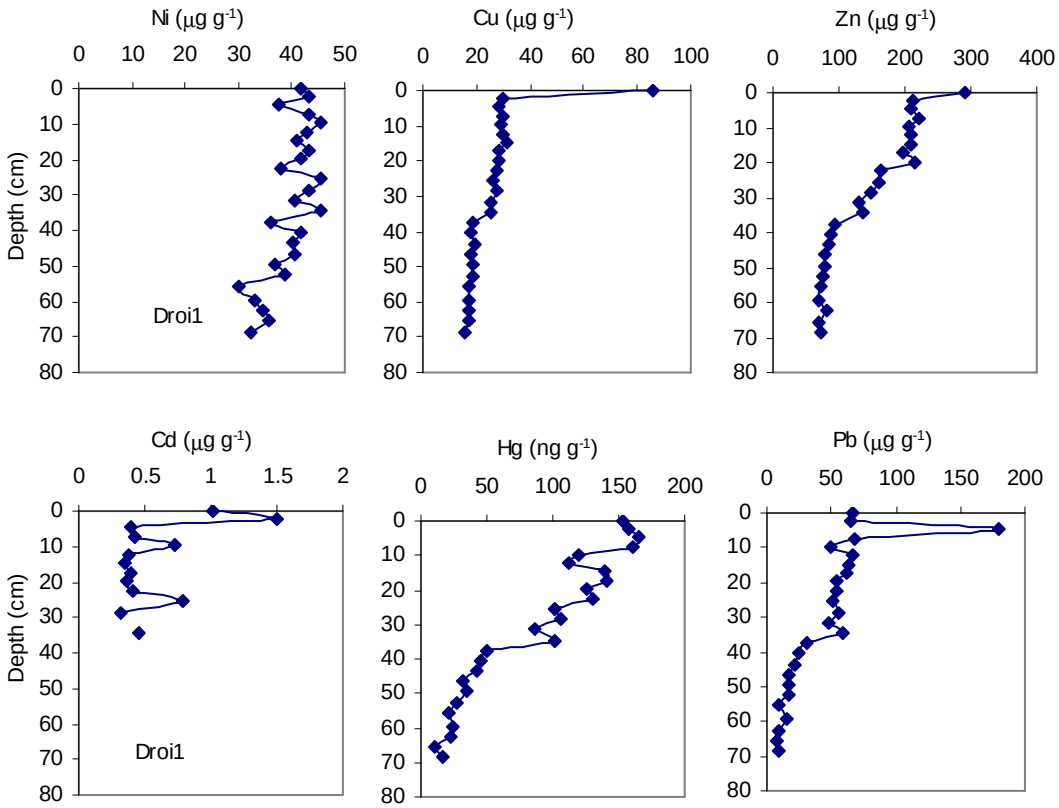

Figure 16. *The trace metal flux profiles in core DROI1.*

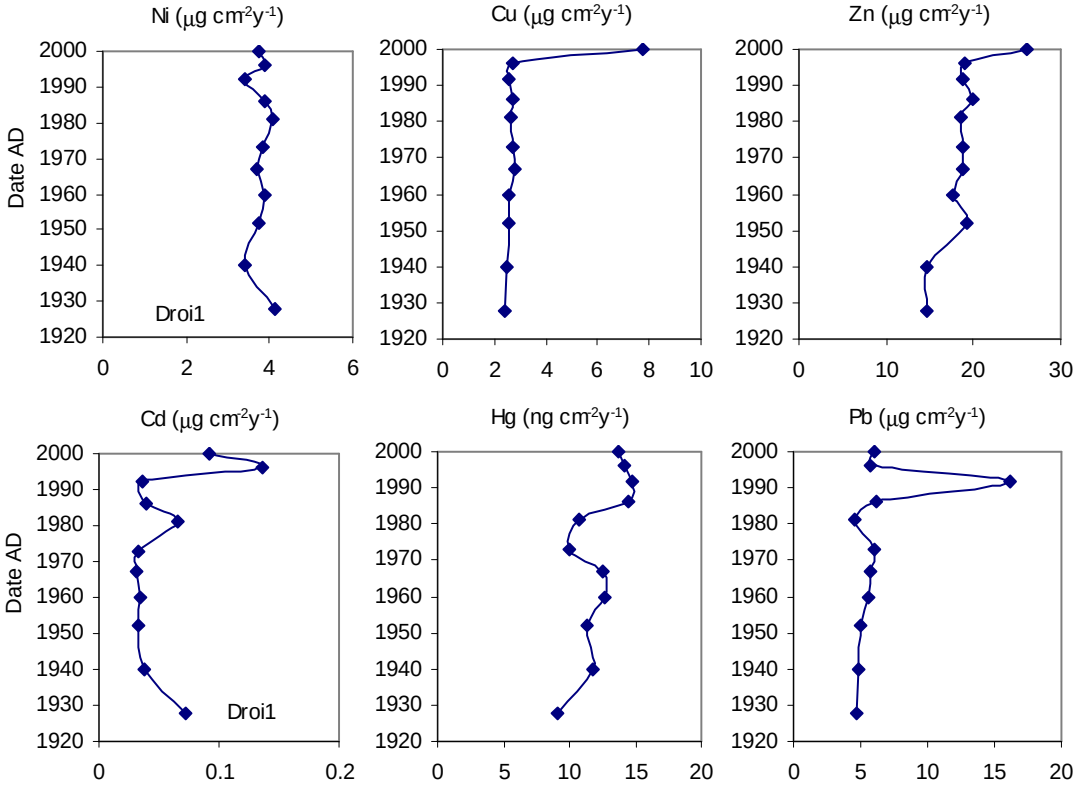

Groby Pool

Chronology

The GROB1 core has a poor ^{210}Pb record. Concentrations are very low and scarcely above that of the supporting ^{226}Ra even in the surficial sediments (Figure 17a). The unsupported ^{210}Pb inventory (Table 14) is less than 25% of the estimated atmospheric flux. In contrast to ^{210}Pb, there appears to be quite a good record of ^{137}Cs fallout with a relatively well defined peak at 20.5 cm that probably records the 1963 fallout maximum from the atmospheric testing of nuclear weapons (Figure 17c). Because of the very poor ^{210}Pb record it was not possible to calculate ^{210}Pb dates for this core. From the ^{137}Cs record, the mean post-1963 sedimentation rate is estimated to be 0.14 ± 0.03 g cm^{-2} y^{-1} (0.55 ± 0.11 cm y^{-1}). Table 15 gives a tentative chronology for the past 60 years assuming a constant sedimentation rate of this value.

Table 14. *Fallout radionuclide concentrations in Groby Pool core GROB1.*

Depth		^{210}Pb Total		^{210}Pb Unsupported		^{210}Pb Supported		^{137}Cs	
cm	g cm^{-2}	Bq kg^{-1}	±	Bq kg^{-1}	±	Bq kg^{-1}	±	Bq kg^{-1}	±
0.25	0.03	64.9	16.4	17.5	18.6	47.4	8.8	1.0	6.7
4.25	0.80	55.5	9.9	13.7	10.3	41.8	2.7	32.8	2.3
8.25	1.72	69.4	19.4	8.0	20.0	61.4	4.8	17.2	4.0
12.25	2.74	57.5	12.3	14.0	12.6	43.5	2.9	34.6	3.1
16.25	3.81	50.4	9.7	7.4	10.1	43.0	2.8	37.2	2.6
20.50	5.18	42.9	8.3	9.2	8.6	33.7	2.0	45.8	2.1
24.50	6.55	29.0	9.6	-1.6	9.8	30.6	2.0	39.7	2.5
28.50	7.64	31.5	7.2	-6.6	7.5	38.1	2.0	26.0	2.0
32.50	8.80	39.8	5.7	3.3	5.9	36.5	1.5	12.8	1.2
36.50	10.10	27.4	6.0	-11.0	6.3	38.4	1.9	4.8	1.1

Table 15 *^{210}Pb chronology of Groby Pool core GROB1*

Depth		Chronology Date	Age		Sedimentation Rate		
cm	g cm^{-1}	AD	y	±	g cm^{-2} y^{-1}	cm y^{-1}	± (%)
0.00	0.00	2000	0	0			
0.25	0.03	2000	0	0	0.14	0.67	21
4.25	0.80	1994	6	1	0.14	0.63	21
8.25	1.72	1988	12	3	0.14	0.59	21
12.25	2.74	1980	20	4	0.14	0.52	21
16.25	3.81	1973	27	6	0.14	0.47	21
20.50	5.18	1963	37	8	0.14	0.46	21
24.50	6.55	1953	47	10	0.14	0.46	21
28.50	7.64	1945	55	12	0.14	0.46	21
32.50	8.80	1937	63	13	0.14	0.46	21

Figure 17*. Fallout radionuclides in Groby Pool core GROB1 showing (a) total and supported ^{210}Pb, (b) unsupported ^{210}Pb, (c) ^{137}Cs concentrations versus depth.*

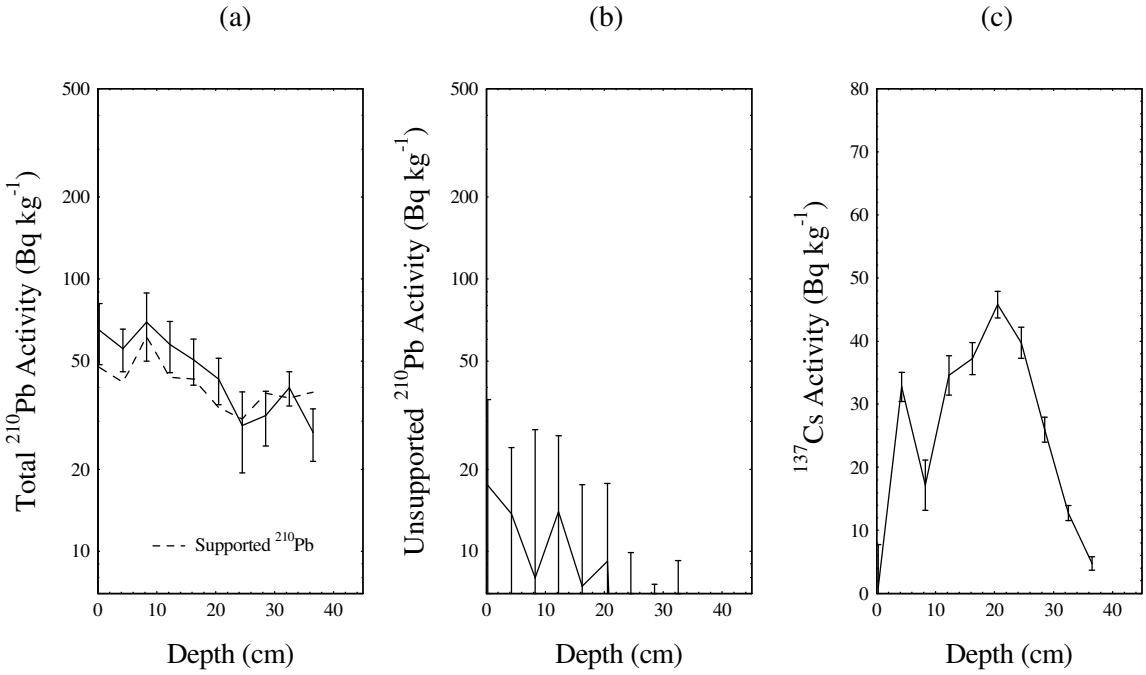

Trace metals

In GROB1 from Groby Pool, all trace metals except Ni show similar trends. From the base of the core to c. 70cm concentrations are relatively stable and increase only slowly. Concentrations then increase more rapidly up to 20cm, above which, Zn, Pb and Cu once again show little change whilst Hg and Cd continue to increase. By contrast, Ni concentrations decrease from the base of the core to the surface (Figure 18). ^{137}Cs dates 20.5 cm to 1963, suggesting that Zn, Pb and Cu concentrations have not changed much since this time. Extrapolation of the chronology places 70 cm in the mid-19th century indicating that this was the period when trace metal concentrations started to increase.

Surface sediment concentrations for GROB1 exceed the Threshold Effect Level for all metals. Pb surface sediment concentrations exceed the Probable Effect Level.

The trace metal flux profiles are presented in Figure 19 and show increases in Cu and Pb flux from the 190s to the 1970s and an increase in Cd from 1950s to 2000. Although this core shows some decline in Pb input to the lake sediments since the 1970s, the reduction is not significant. For the other trace metals, no decrease is apparent over the last 30 years.

***Figure 18 The** trace metal concentration profiles in core GROB1.*

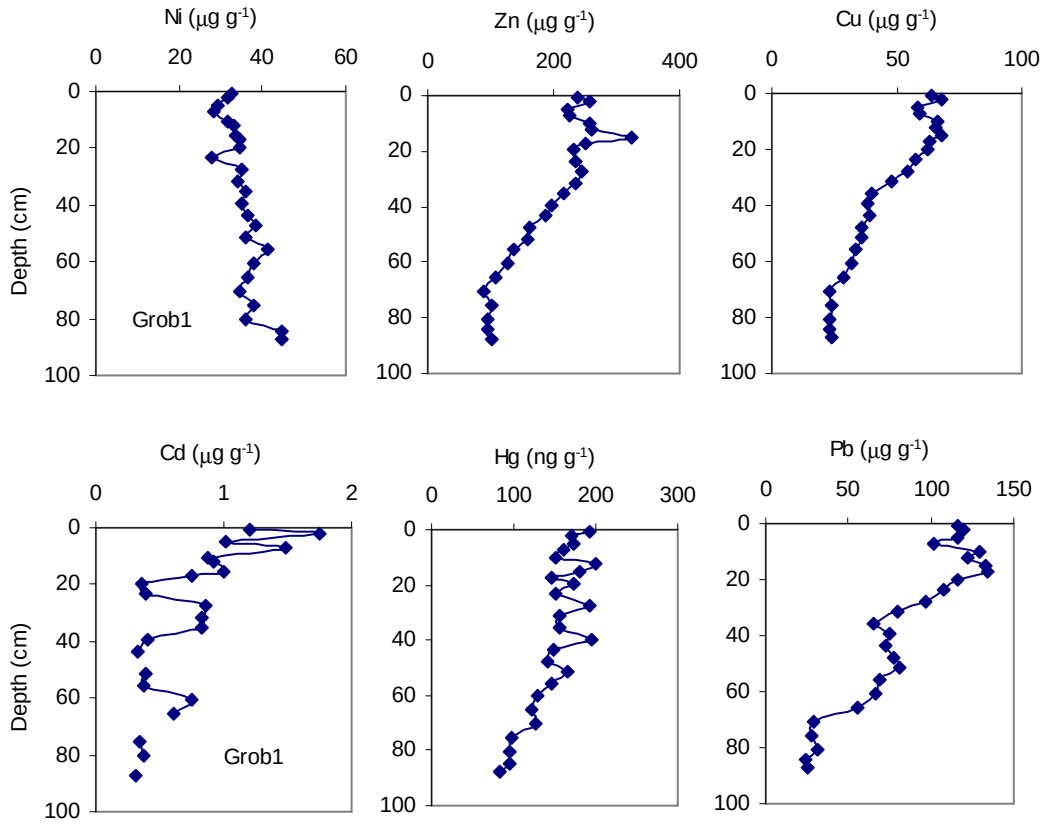

***Figure 19.** The trace metal flux profiles in the core GROB1.*

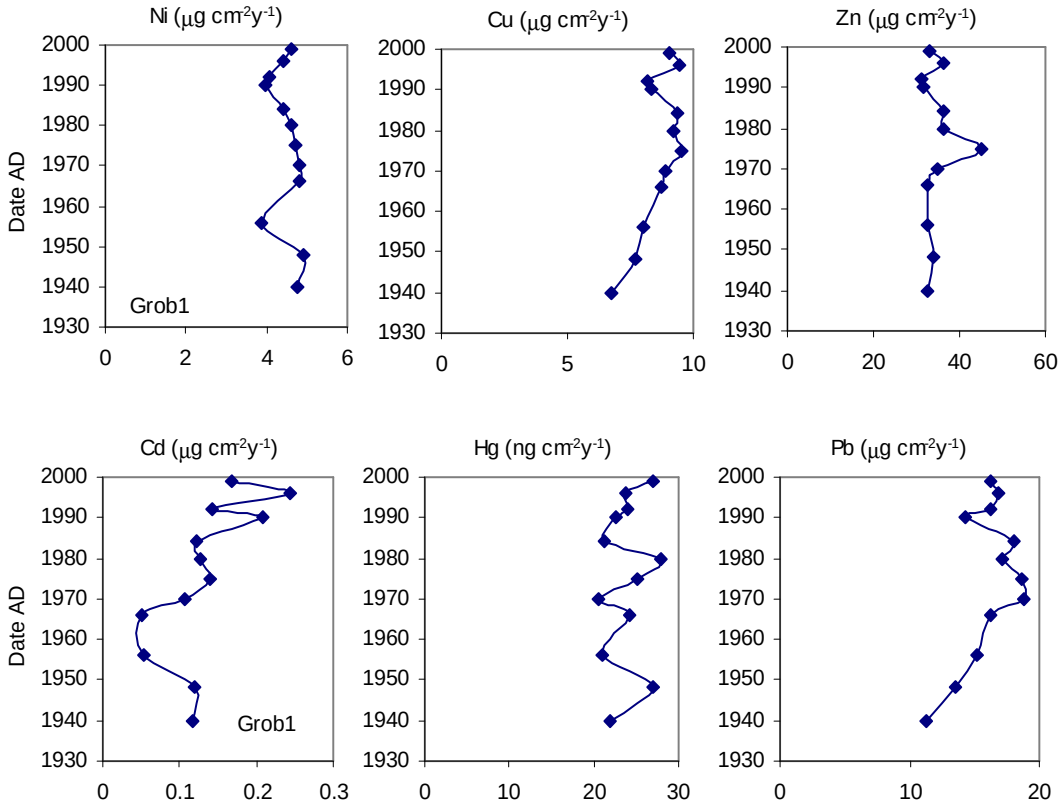

Gull Pond

Chronology

Total ^{210}Pb activity in this core reaches equilibrium with the supporting ^{226}Ra at a depth of c.20 cm (Figure 20a). Unsupported ^{210}Pb concentrations are low and decline a little irregularly with depth (Figure 20b) though the overall trend suggests relatively uniform accumulation. The ^{137}Cs record is a little irregular though there is a fairly well defined peak at 6.25 cm (Figure 20c) that probably records the 1963 fallout maximum from the atmospheric testing of nuclear weapons. Figure 21 plots ^{210}Pb dates calculated using the CRS model, together with the 1963 date suggested by the ^{137}Cs record. CIC model dates have not been plotted due to large uncertainties arising from the irregular variations in ^{210}Pb activity in the top few sections. The ^{210}Pb dates place 1963 at a depth of 10.5cm, significantly below the depth suggested by the ^{137}Cs peak. This could be due to a loss of sediment from the top of the core before or during coring. Alternatively, since ^{137}Cs concentrations are relatively constant in all sections above 10.5 cm, it is possible that these sediments all date from the post-1960 period and that the ^{137}Cs peak at 6.25 cm is due to sedimentological factors that have affected the detailed shape of the ^{137}Cs profile. This is supported by the fact that the ^{137}Cs/^{210}Pb ratio in sediments at c.10.5 cm is higher that at 6.25 cm. It is not possible to resolve these questions from the radiometric data alone. Since the CRS model dates are intermediate between the ^{137}Cs dates and those determined by the CIC model, they have been used to provide the detailed results given in Table 16. In view of the above uncertainties they should be regarded with some caution. However, data from the SCP record in Gull Pond suggest that this chronology is reasonable.

Table 16. *^{210}Pb chronology of Gull Pond core GULL1*

Depth		Chronology			Sedimentation Rate		
		Date	Age				
cm	g cm^{-1}	AD	y	±	g cm^{-2} y^{-1}	cm y^{-1}	± (%)
0.00	0.00	2001	0	0			
0.25	0.02	2001	0	1	0.048	0.38	21.1
2.25	0.32	1995	6	2	0.051	0.31	28.9
4.25	0.59	1988	13	3	0.036	0.31	30.2
6.25	0.84	1982	19	5	0.048	0.31	43.8
8.25	1.13	1975	26	6	0.033	0.25	37.2
10.25	1.44	1966	35	9	0.037	0.20	48.0
12.25	1.83	1955	46	13	0.032	0.17	54.2
14.25	2.25	1942	59	19	0.039	0.11	71.6
16.25	2.82	1920	81	25	0.015	0.09	88.1

Figure 20. *Fallout radionuclides in Gull Pond core GULL1 showing (a) total and supported ^{210}Pb, (b) unsupported ^{210}Pb, (c) ^{137}Cs concentrations versus depth.*

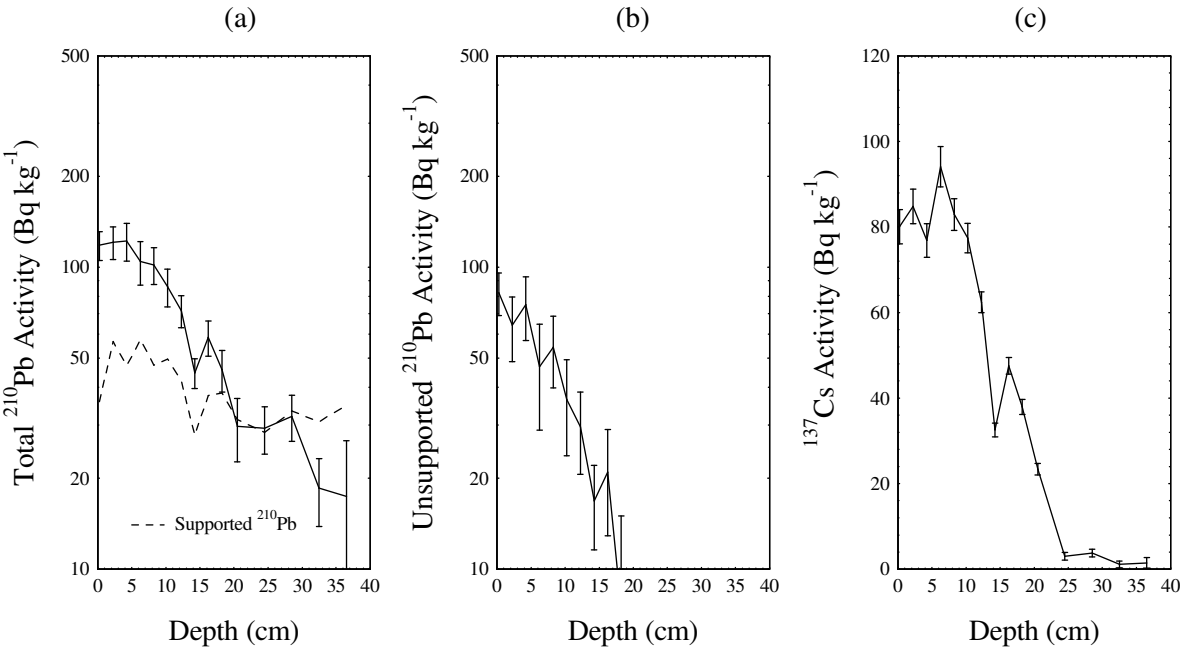

Figure 21. *Radiometric chronology of Gull Pond core GULL1 showing CRS model ^{210}Pb dates together with the approximate 1986 and 1963 depths estimated from ^{137}Cs and ^{241}Am records. Also shown are corrected ^{210}Pb dates and sedimentation rates.*

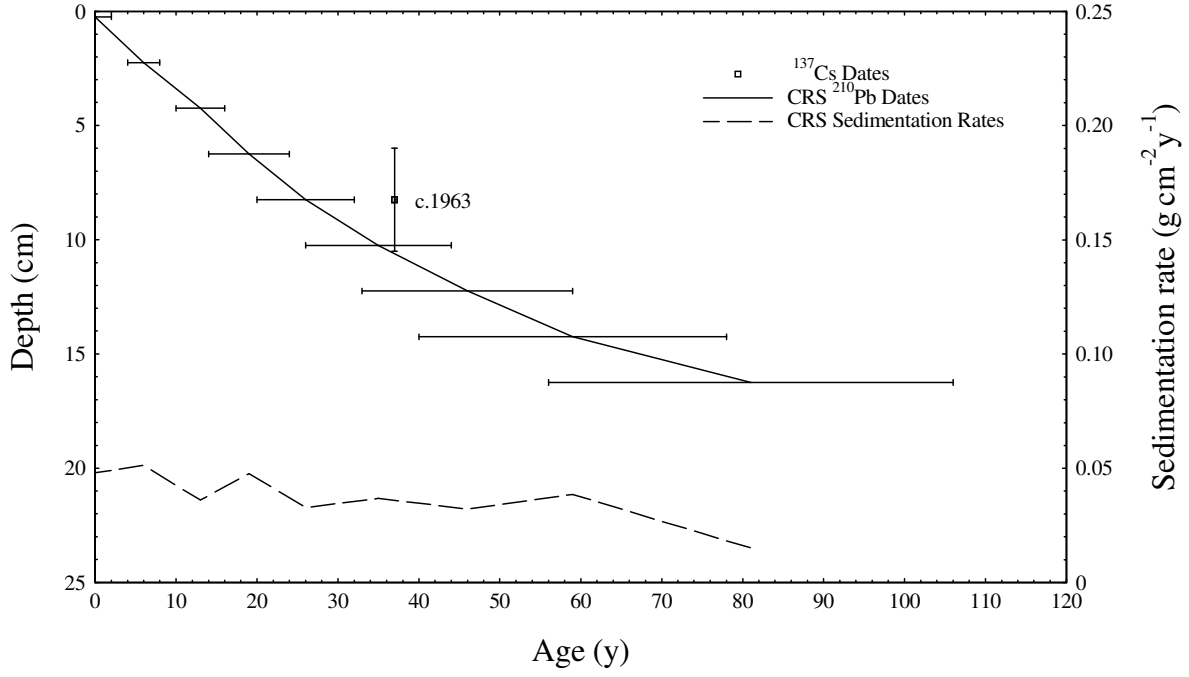

Trace metals

All the trace metal concentration profiles for GULL1 taken from Gull Pond (Figure 22) show a rapid increase from the base of the core with broad peaks between 30 and 15cm for Zn and Cd. Sedimentary trends in organic content (Figure 2) may have contributed to the increases observed in Hg and Pb concentrations between 50 and 35 cm. Although the site is shallow and frequented by wildfowl the metal concentration profiles imply that the sediments have not been disturbed. Concentrations of Hg, Pb, Zn and Cu in the basal sediments are very low (27 ng g^{-1}, 2, 2 and 2.4 µg g^{-1} respectively) suggesting very low background concentrations. However, this implies that the high concentrations in the surface sediments are indicative of significant anthropogenic impact. For Hg, surface concentrations are possibly more than 200 times higher than the background.

Mercury concentrations in the surface sediments are higher the "apparent effects threshold" level, whilst Pb concentrations exceed the Probable Effect Level and all other metals exceed the Threshold Effect Level. The high Zn concentrations between 15 – 30 cm depth also exceed the PEL for this metal.

Extrapolation of the chronology suggests that this core covers more than 270 years suggesting that Gull Pond has been contaminated with trace metals since the second half of the 18th century. The Cu, Ni, Hg and Pb fluxes increase from the base of the core to the surface (Figure 23) while high Zn fluxes in the 1920s are due to the high concentrations in the sediments formed during that period. Hg and Pb concentrations and fluxes reveal no reduction despite emissions reductions.

Figure 22. *The trace metal concentration profiles in core GULL1.*

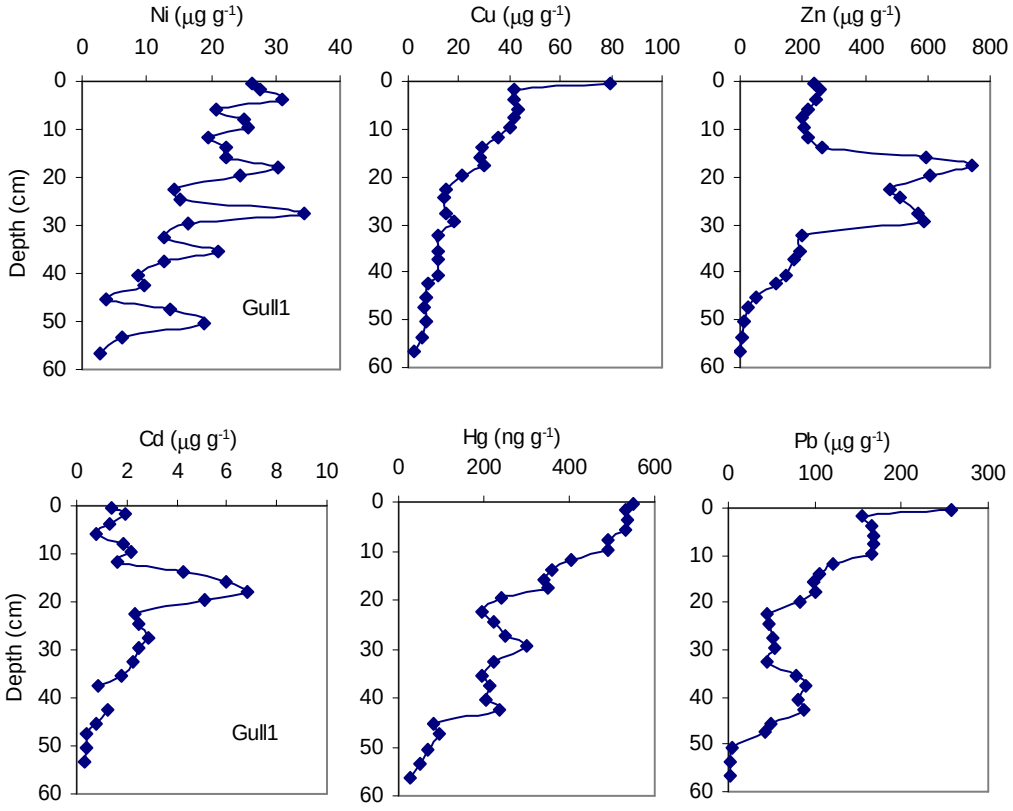

Figure 23. *The trace metal flux profiles in core GULL1.*

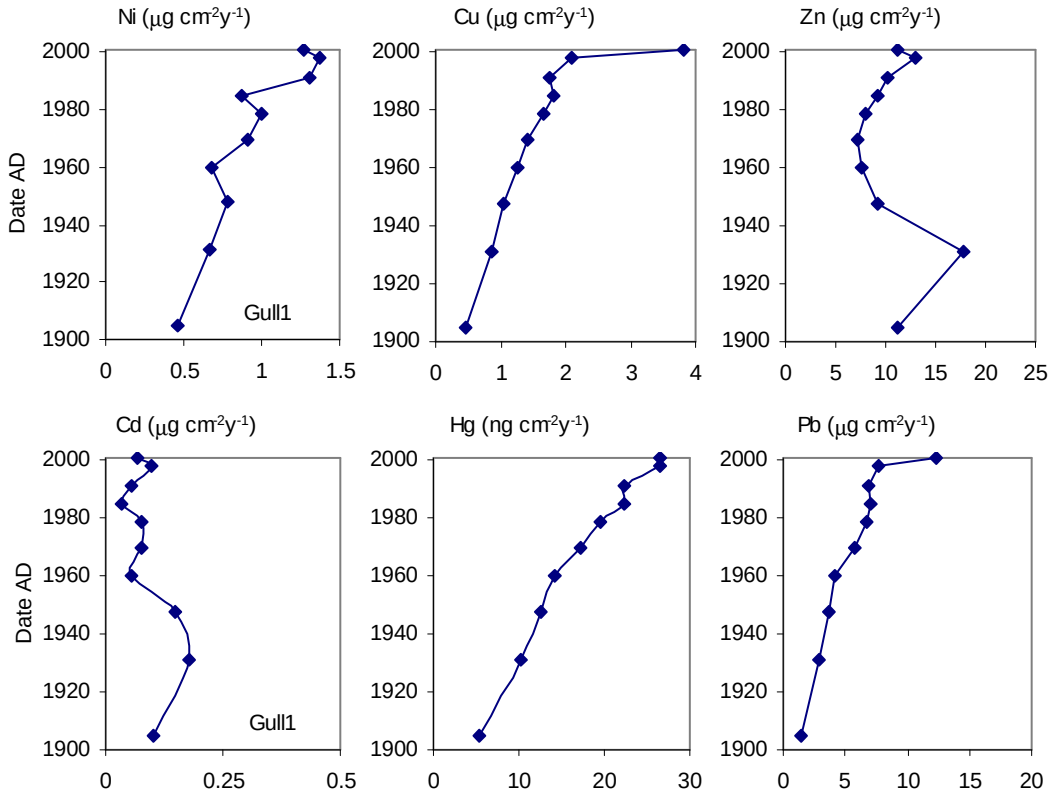

Pinkworthy Pond

Chronology

This core appears to have a good fallout record with a ^{210}Pb supply rate (Table 17) that is comparable to the estimated atmospheric flux. Total ^{210}Pb activity reaches equilibrium with the supporting ^{226}Ra at a depth of c.35 cm (Figure 24a). The unsupported ^{210}Pb profile is however quite irregular with several non-monotonic features suggesting non-uniform sedimentation rates (Figure 24b). The ^{137}Cs activity versus depth profile has a reasonably well-resolved peak at 12.25 cm (Figure 24c). The small feature at 16.25 cm appears to be caused by dilution of the ^{137}Cs concentration due to the onset of a period of higher sedimentation rate. At the same depth there is a similar decline in ^{210}Pb activity. Figure 25 plots ^{210}Pb dates calculated using the CRS model, together with the 1963 date suggested by the ^{137}Cs record. The irregular ^{210}Pb record precluded use of the CIC model. The ^{210}Pb dates place 1963 at a depth of c.18.5 cm, significantly below the depth indicated by the ^{137}Cs record. The discrepancy could be due to loss of part of the record during an episode of rapid sedimentation diluting the ^{210}Pb record between 5-20 cm. This is supported by the fact that the mean post-1963 sedimentation rate (apparently a period of rapid sedimentation) is no higher than the value calculated for the preceding 50 years. From the distribution of the ^{137}Cs inventory a more appropriate depth for the 1963 level could be 14.5 cm. Figure 25 plots a corrected chronology and the results are given in detail in Table 18. In view of these uncertainties the post-1963 chronology must however be regarded with caution.

Table 17. *Fallout Radionuclide Concentrations in Pinkworthy Pond core PINK3*

Depth		^{210}Pb						^{137}Cs	
		Total		Unsupported		Supported			
cm	g cm^{-2}	Bq kg^{-1}	±	Bq kg^{-1}	±	Bq kg^{-1}	±	Bq kg^{-1}	±
0.25	0.01	175.50	40.10	89.94	40.43	85.60	4.92	35.03	2.80
2.25	0.08	366.60	57.70	282.85	58.13	83.78	7.41	69.61	9.27
4.25	0.20	331.50	41.50	249.00	42.30	82.50	8.00	100.81	7.55
6.25	0.40	167.00	19.90	88.50	20.60	78.40	5.20	136.45	5.66
8.25	0.63	146.90	17.30	57.60	18.00	89.20	5.00	183.16	5.93
12.25	1.25	160.30	18.00	71.30	18.80	89.00	5.30	270.61	6.65
16.25	1.99	131.20	17.50	42.30	18.10	88.90	4.50	146.40	4.59
20.50	2.82	155.90	13.20	82.50	13.50	73.40	2.50	152.36	3.15
24.50	3.52	125.40	9.10	42.90	9.40	82.60	2.50	31.20	1.94
28.50	4.27	78.80	10.80	14.60	11.00	64.10	2.40	12.46	1.64
32.50	5.13	67.40	6.10	19.20	6.30	48.10	1.70	10.93	1.42
36.50	6.11	58.90	6.90	-11.20	7.30	70.10	2.20	8.55	1.26
41.50	7.31	66.80	9.00	-0.70	9.40	67.60	2.70	8.17	1.50

Table 18. *^{210}Pb chronology of Pinkworthy Pond core PINK3*

Depth		Chronology			Sedimentation Rate		
		Date	Age				
cm	g cm^{-1}	AD	y	±	g cm^{-2} y^{-1}	cm y^{-1}	± (%)
0.00	0.00	1984	17	0			
0.25	0.01	1984	17	1	0.110	0.85	
2.25	0.08	1983	18	2	0.034	0.80	
4.25	0.20	1979	22	2	0.034	0.50	
6.25	0.40	1975	26	2	0.085	0.67	
8.25	0.63	1973	28	2	0.122	0.75	
10.25	0.94	1970	31	3	0.101	0.66	
12.25	1.25	1967	34	3	0.081	0.57	
14.25	1.62	1963	38	4	0.094	0.47	
16.25	1.99	1959	42	4	0.106	0.38	
18.25	2.38	1952	48	5	0.077	0.33	
20.50	2.82	1945	56	6	0.045	0.28	
22.50	3.17	1937	63	8	0.045	0.26	
24.50	3.52	1929	71	10	0.045	0.25	
26.50	3.90	1920	80	12	0.045	0.23	
28.50	4.27	1912	88	14	0.045	0.22	
30.50	4.70	1902	98	19	0.045	0.21	
32.50	5.13	1893	107	23	0.045	0.21	

Figure 24. *Fallout radionuclides in Pinkworthy Pond core PINK3 showing (a) total and supported ^{210}Pb, (b) unsupported ^{210}Pb, (c) ^{137}Cs concentrations versus depth.*

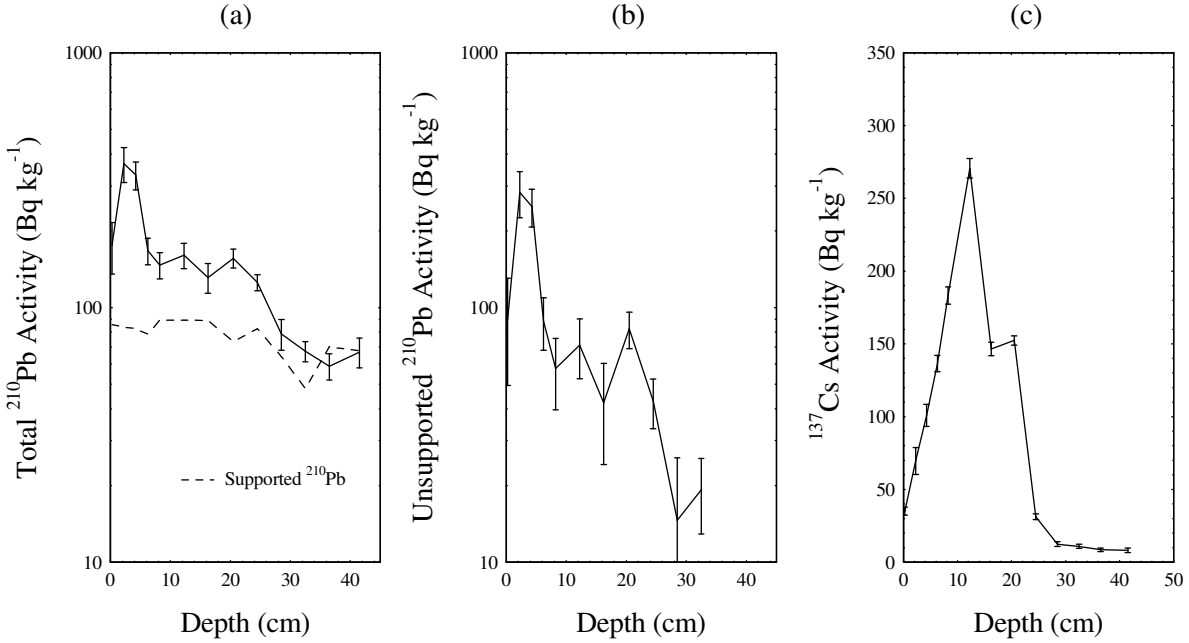

Figure 25. *Radiometric chronology of Pinkworthy Pond core PINK3 showing CRS model ^{210}Pb dates (raw and corrected) together with dates determined from the ^{137}Cs stratigraphy. Also shown are sedimentation rates calculated using the corrected model.*

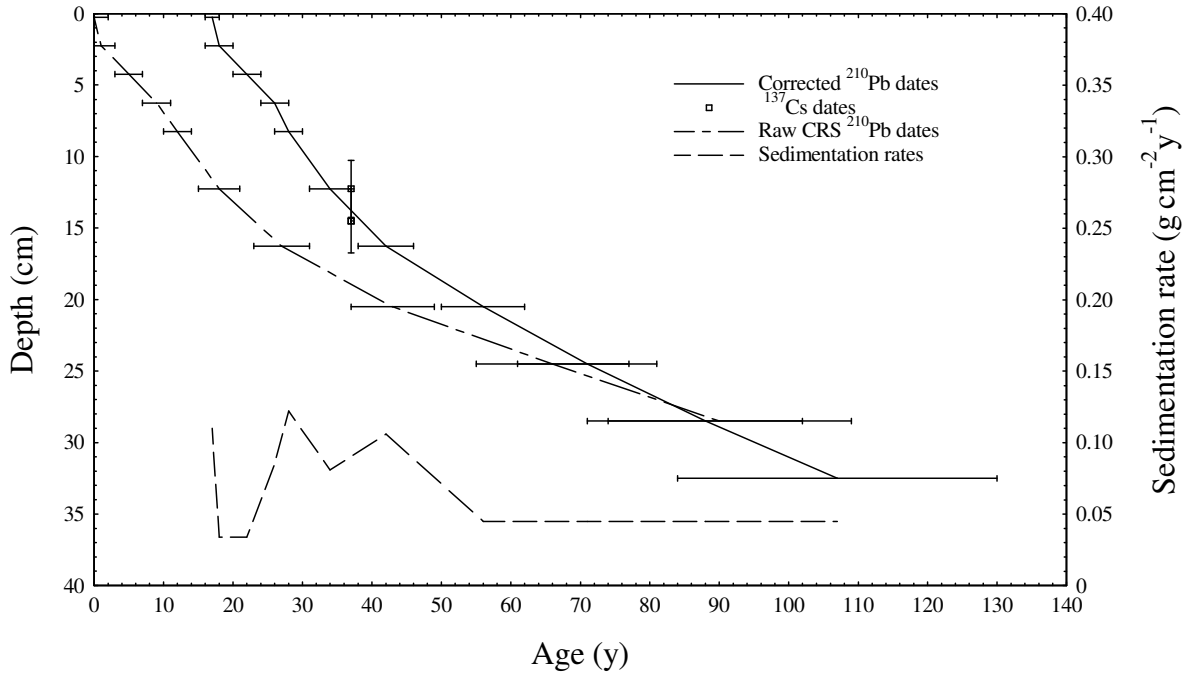

Trace metals

The trace metal concentration profiles of PINK3 taken from Pinkworthy Pond are shown in Figure 26. Hg alone shows an increase in concentration throughout the core whilst the other metals appear to increase from the base of the core to peaks at c. 25cm before declining to the surface. These peaks could indicate a peak in contamination. However, there are considerable variations throughout each of these profiles and this could be due to changes in sediment source.

The features of trace metal flux profiles are quite different from those of their respective concentration profiles (Figure 27). Peak fluxes vary for the different metals and may therefore be derived mainly from changing sedimentation rates rather than a pollution signal.

Threshold Effect Levels for Zn, Hg and Pb are exceeded in surface sediments of Pinkworthy Pond. The peak concentrations of Cd at c. 25cm exceed the Probable Effect Level.

Figure 26. *The trace metal concentration profiles in core Pink3.*

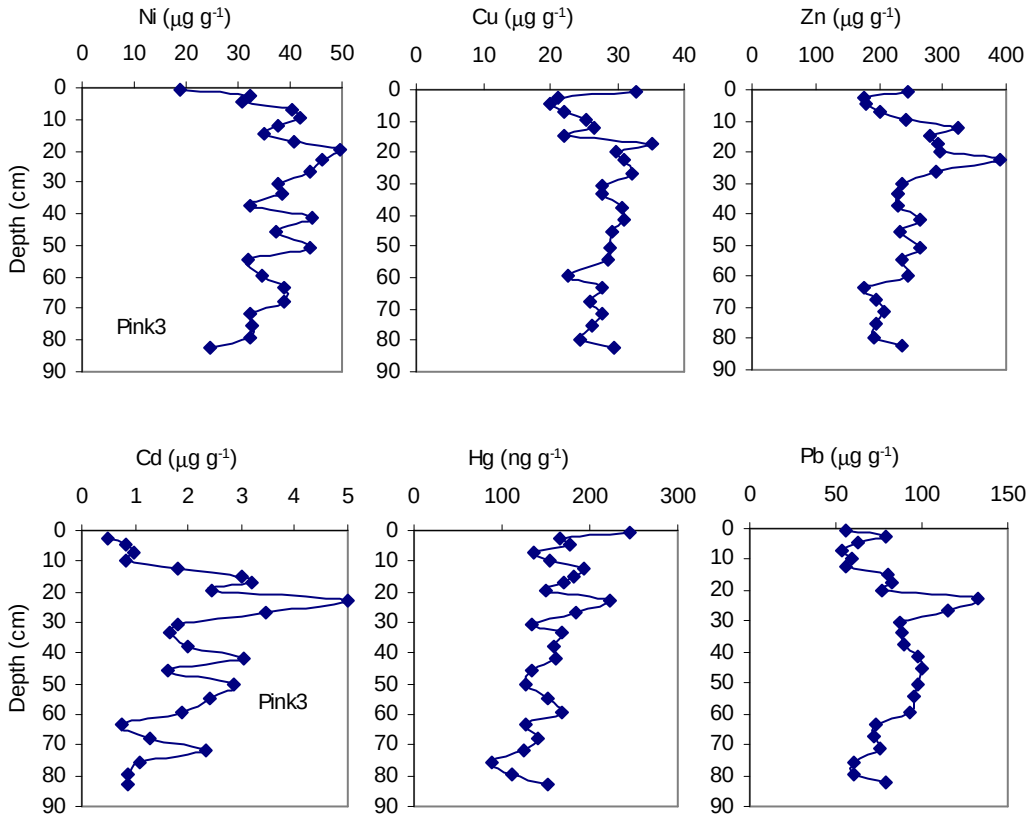

Figure 27. *The trace metal flux profiles in core PINK3.*

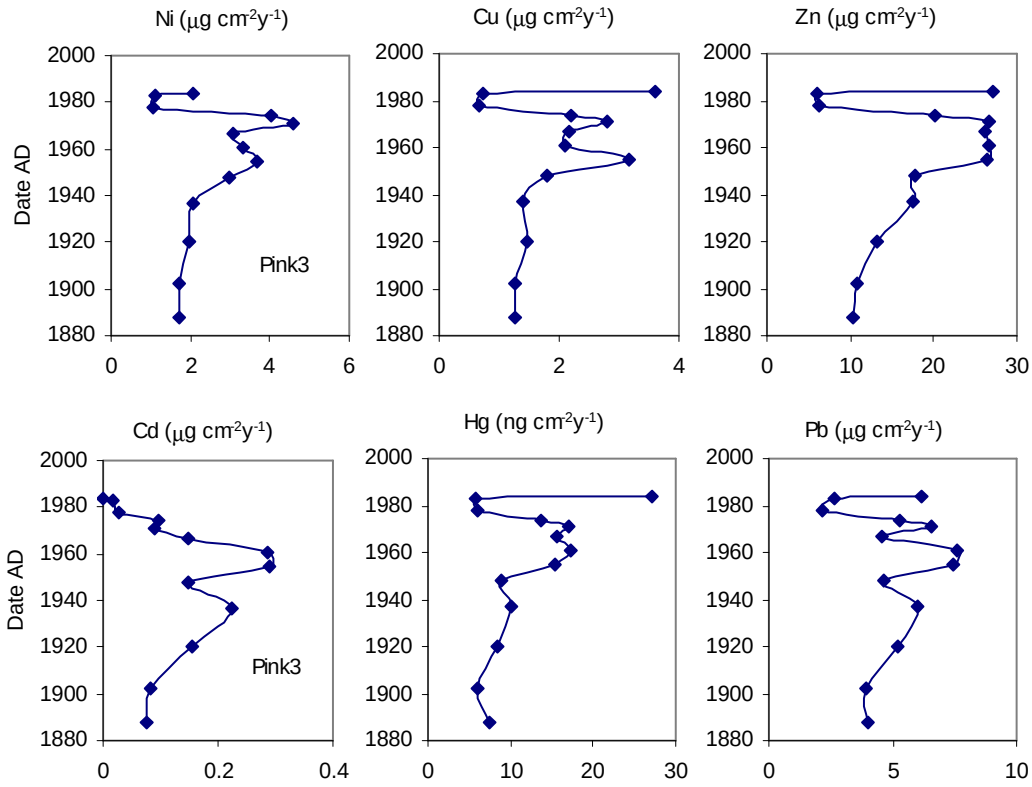

Portmore Loch

Chronology

The fallout parameters for this core suggest that it has a reasonably good record of fallout radionuclides. Total ^{210}Pb reaches equilibrium with the supporting ^{226}Ra at a depth of about 18 cm (Figure 28a). The unsupported ^{210}Pb activity declines fairly regularly with depth (Figure 28b) though the significantly lower gradient of the profile above c.12 cm suggests more rapid accumulation in recent decades. The ^{137}Cs record in this core (Figure 28c) is a little irregular, with a poorly resolved peak between 8-12.5 cm, and a secondary peak at 4.25 cm. Traces of ^{241}Am at 10.25 cm are not sufficient to resolve the origin of these features, though it seems likely that the main peak records the high levels of fallout in the early 1960s from the atmospheric testing of nuclear weapons. Figure 29 shows ^{210}Pb dates calculated using the CRS and CIC models, together with the 1963 and depth suggested by the ^{137}Cs and ^{241}Am records. Both models suggest accelerating sedimentation rates in recent decades, though the CIC model suggests a later and more rapid change. The CRS dates however, are in better agreement with the ^{137}Cs and ^{241}Am records and form the basis of the chronology given in Table 20. In assessing the reliability of these dates it should be noted that there is a layer of dense sediment between 17-29 cm (see wet density data in Figure 2) that may have had a significant influence on fallout records in the deeper parts of this core. If the date and origin of this feature is known they could be used to improve the accuracy of the radiometric dates, particular in the older sections.

Table 19 *Fallout radionuclide concentrations in Portmore Loch core PORT1*

Depth		^{210}Pb Total		^{210}Pb Unsupported		^{210}Pb Supported		^{137}Cs		^{241}Am	
cm	g cm^{-2}	Bq kg^{-1}	±	Bq kg^{-1}	±	Bq kg^{-1}	±	Bq kg^{-1}	±	Bq kg^{-1}	±
0.25	0.02	242.5	17.4	200.1	17.7	42.4	3.1	86.3	3.3	0.0	0.0
2.25	0.23	177.0	32.8	134.5	33.3	42.5	5.8	87.8	6.2	0.0	0.0
4.25	0.46	157.8	17.4	130.4	18.2	27.4	5.3	128.2	4.6	0.0	0.0
6.25	0.72	153.4	18.3	109.6	18.9	43.8	4.7	105.7	6.0	0.0	0.0
8.25	0.99	161.8	12.3	115.9	12.7	45.9	2.9	143.4	3.7	0.0	0.0
10.25	1.30	132.9	11.1	86.8	11.5	46.1	3.1	131.8	3.7	2.1	1.2
12.25	1.62	115.4	11.8	78.0	12.2	37.4	3.0	126.9	3.7	0.0	0.0
14.25	1.98	101.5	18.6	51.8	19.3	49.7	5.1	101.3	4.7	0.0	0.0
16.25	2.34	72.3	12.1	28.5	12.4	43.9	2.8	44.5	2.5	0.0	0.0
18.25	2.77	43.7	6.8	9.2	7.1	34.6	1.9	19.1	1.3	0.0	0.0
20.50	3.35	31.2	6.1	-9.0	6.3	40.2	1.7	8.3	1.1	0.0	0.0
24.50	4.37	15.0	13.2	-15.7	13.4	30.7	2.3	2.2	1.6	0.0	0.0
28.50	5.21	23.4	8.3	-8.8	8.5	32.2	2.0	0.0	0.0	0.0	0.0
32.50	5.84	17.8	10.7	-5.9	10.9	23.8	2.0	0.1	1.3	0.0	0.0

Figure 28. *Fallout radionuclides in Portmore Loch core PORT1 showing (a) total and supported ^{210}Pb, (b) unsupported ^{210}Pb, (c) ^{137}Cs and ^{241}Am concentrations.*

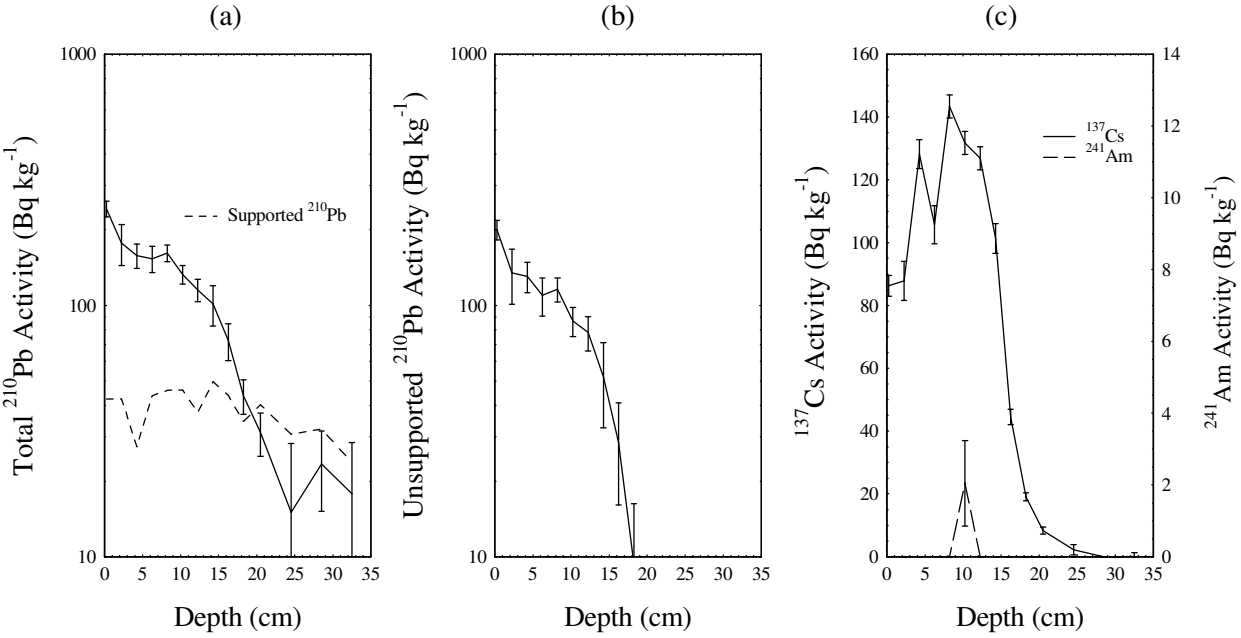

Table 20. *^{210}Pb chronology of Portmore Loch core PORT1*

Depth		Chronology			Sedimentation Rate		
		Date	Age				
cm	g cm^{-1}	AD	y	±	g cm^{-2} y^{-1}	cm y^{-1}	± (%)
0.00	0.00	2000	0	0			
0.25	0.02	2000	0	2	0.036	0.38	11.1
2.25	0.23	1994	6	2	0.046	0.36	25.6
4.25	0.46	1989	11	2	0.040	0.33	15.9
6.25	0.72	1982	18	2	0.039	0.27	19.1
8.25	0.99	1974	26	3	0.029	0.21	15.1
10.25	1.30	1963	37	4	0.027	0.16	19.1
12.25	1.62	1949	51	6	0.019	0.11	25.0
14.25	1.98	1928	72	9	0.015	0.09	45.5
16.25	2.34	1903	97	13	0.013	0.07	57.7

Figure 29*. Radiometric chronology of Portmore Loch core PORT1 showing CRS and CIC model ^{210}Pb dates together with approximate 1963 depth determined from the ^{137}Cs record. Also shown are sedimentation rates calculated using the CRS model.*

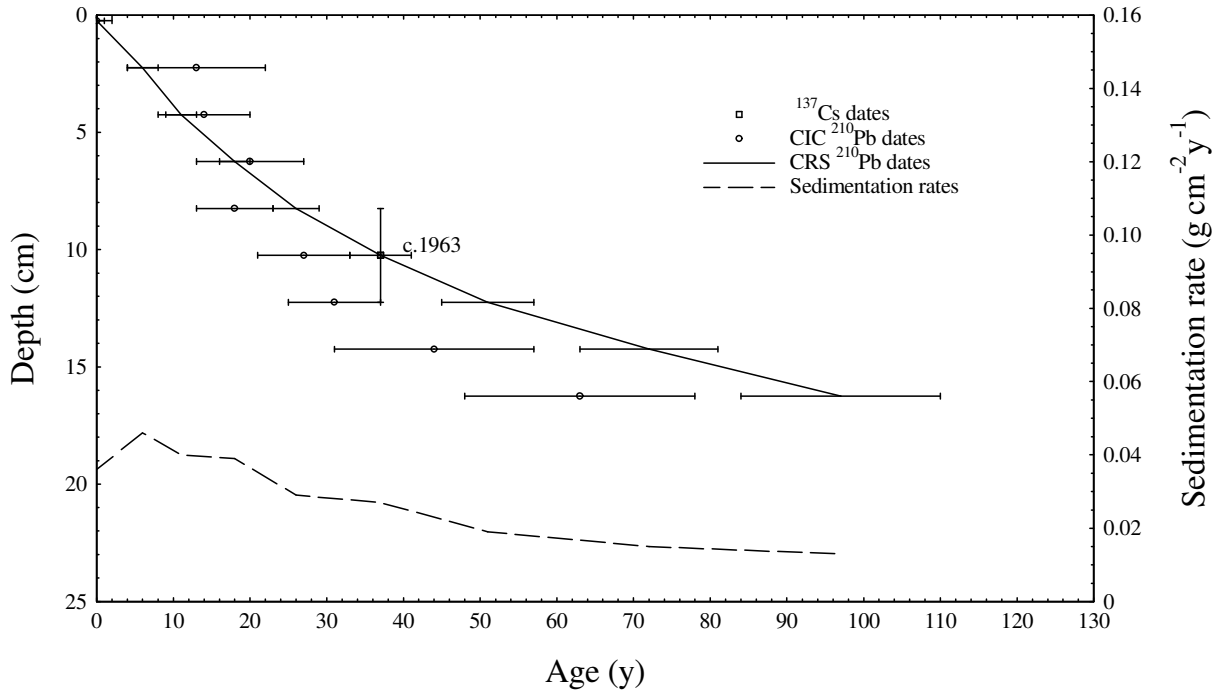

Trace metals

In core PORT1 taken from Portmore Loch, concentrations of Ni, Zn and Pb increase rapidly from 29 cm (Figure 30) while Cu and Hg concentrations increase slowly from this depth before rapidly increasing between 19 and 15cm. Above 15cm Hg, Pb and Zn concentrations are relatively constant. Cu and Ni concentrations decline from 13 cm to the surface. Below 29 cm Cd concentrations are below the limit of detection, but once this limit is exceeded, Cd concentrations increase to the surface. As 16.25 cm is dated to 1903 ± 13, extrapolating this chronology places 29 cm in the mid-19th century. Thus the start of trace metal pollution at Portmore Loch began at around this time. The low concentration levels and the trends in the profiles of Cu, Zn, Pb and Hg suggest that levels below 29 cm could be at, or close to, background. If this is the case, it is also reasonable to assume that Ni concentrations below 30 cm are also close to background. If this is true, the background concentration of Ni in this area is relatively high when compared to other areas of Scotland (Yang and Rose, 2005).

The surface sediment concentrations of Ni and Cu in Portmore Loch exceed the Probable Effect Level, whilst the concentrations of the other trace metals exceed their Threshold Effect Levels.

The trace metal flux profiles are shown in Figure 31 using the reliable chronology post-1903. Mercury, Pb, Cu and Zn fluxes increase from the 1900s to the 1990s, followed by a decline to 2000 for Hg, Cu and Zn. Ni fluxes increase from the 1960s to the 1990s and decline in the surface sample, while Cd increases from 1980. The increase in the Zn signal in the surface sediments may be due to post-depositional movement and therefore may not be a true signal.

Figure 30*. The trace metal concentration profiles in core PORT1.*

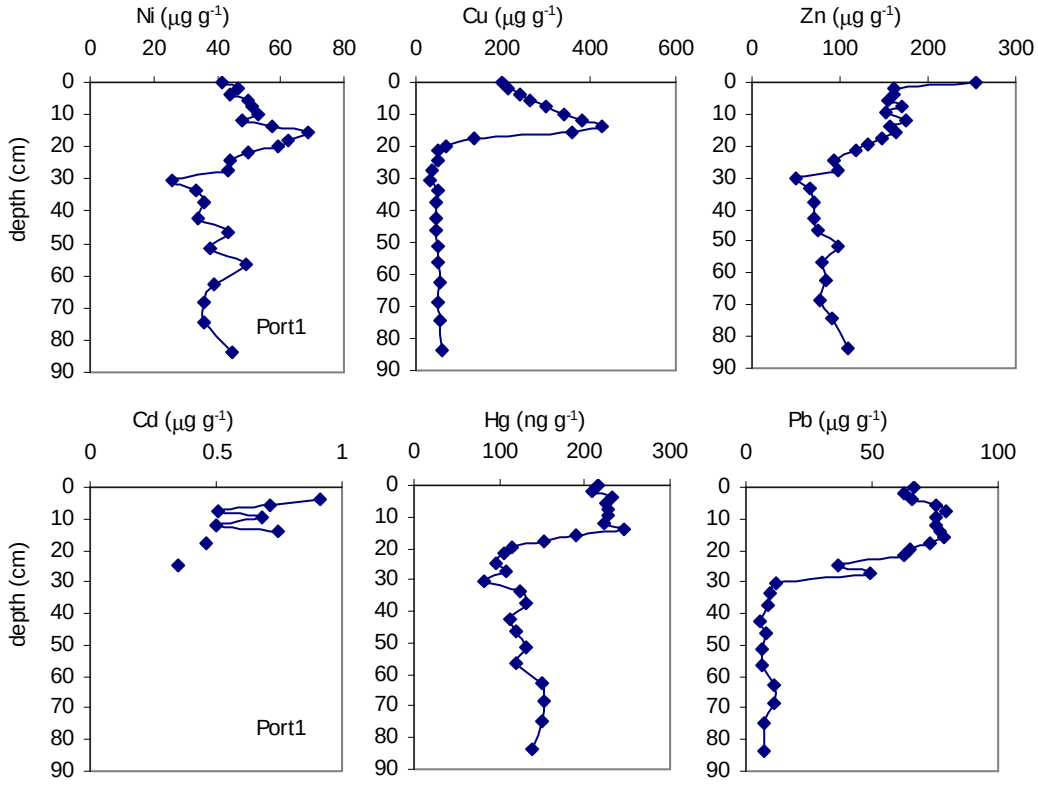

***Figure 31**. The trace metal flux profiles in core PORT1*

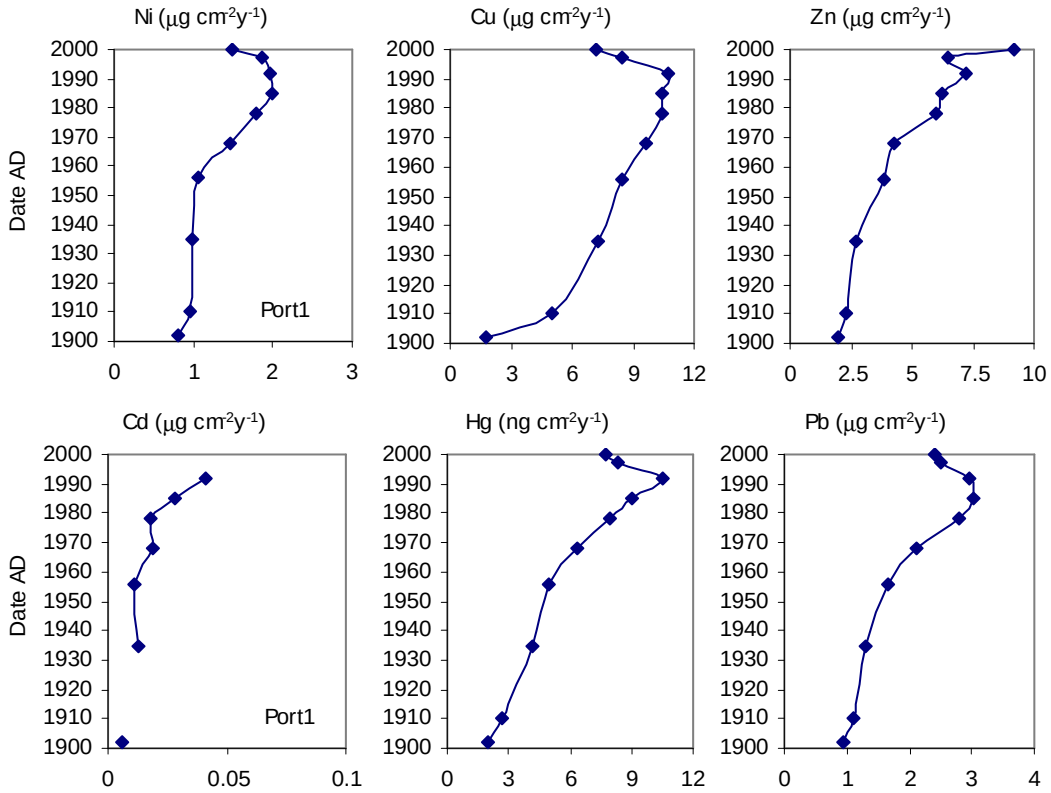

Powdermill Lake

Chronology

^{210}Pb concentrations are significantly in excess of the supporting ^{226}Ra in the top 16 cm of the core (Figure 32a). The unsupported ^{210}Pb concentrations are extremely low (Figure 32b), though since the ^{210}Pb inventory (Table 21) is c.50% of the estimated atmospheric flux these may be due to dilution of the atmospheric signal by rapid sedimentation. The ^{137}Cs record has a double peak between 24-33 cm (Figure 32c), that probably records the 1963 fallout maximum from the atmospheric testing of nuclear weapons. The low ^{137}Cs concentration in the 28.5 cm sample may be related to events giving rise to small increase in dry bulk density and LOI values in sediments immediately above this depth. Because of the very poor ^{210}Pb record it was not possible to calculate ^{210}Pb dates for this core. From the ^{137}Cs record, the mean post-1960 sedimentation rate is estimated to be 0.31 ± 0.05 g cm^{-2} y^{-1} (0.77 ± 0.12 cm y^{-1}). Table 22 gives a tentative chronology for the past 60 years assuming a constant sedimentation rate of this value.

Table 21. *Fallout Radionuclide Concentrations in Powdermill Lake core UKBR2*

Depth		^{210}Pb Total		^{210}Pb Unsupported		^{210}Pb Supported		^{137}Cs	
cm	g cm^{-2}	Bq kg^{-1}	±	Bq kg^{-1}	±	Bq kg^{-1}	±	Bq kg^{-1}	±
0.25	0.05	72.7	8.8	20.8	9.0	51.9	1.8	11.8	1.3
4.25	1.17	57.4	5.3	8.6	5.5	48.8	1.4	15.1	1.0
8.25	2.42	75.3	8.6	24.9	8.9	50.4	2.3	15.3	1.6
12.25	3.88	63.0	6.0	8.6	6.3	54.4	1.8	14.2	1.2
16.25	5.42	49.8	5.1	8.2	5.3	41.6	1.4	14.6	1.2
20.50	7.31	44.2	7.7	2.3	7.8	41.9	1.4	20.0	1.1
24.50	9.42	40.4	4.7	-5.3	4.9	45.7	1.4	25.3	1.3
28.50	11.60	45.8	4.6	6.6	4.8	39.2	1.2	13.9	1.0
32.50	13.90	45.3	5.2	-0.8	5.4	46.0	1.4	25.8	1.1
36.50	16.03	37.8	4.6	-5.4	4.8	43.1	1.4	9.9	0.8
38.50	17.06	42.3	5.2	2.6	5.3	39.7	1.0	2.1	0.6

Figure 32. *Fallout radionuclides in Powdermill Lake core UKBR2 showing (a) total and supported ^{210}Pb, (b) unsupported ^{210}Pb, (c) ^{137}Cs and ^{241}Am concentrations versus depth.*

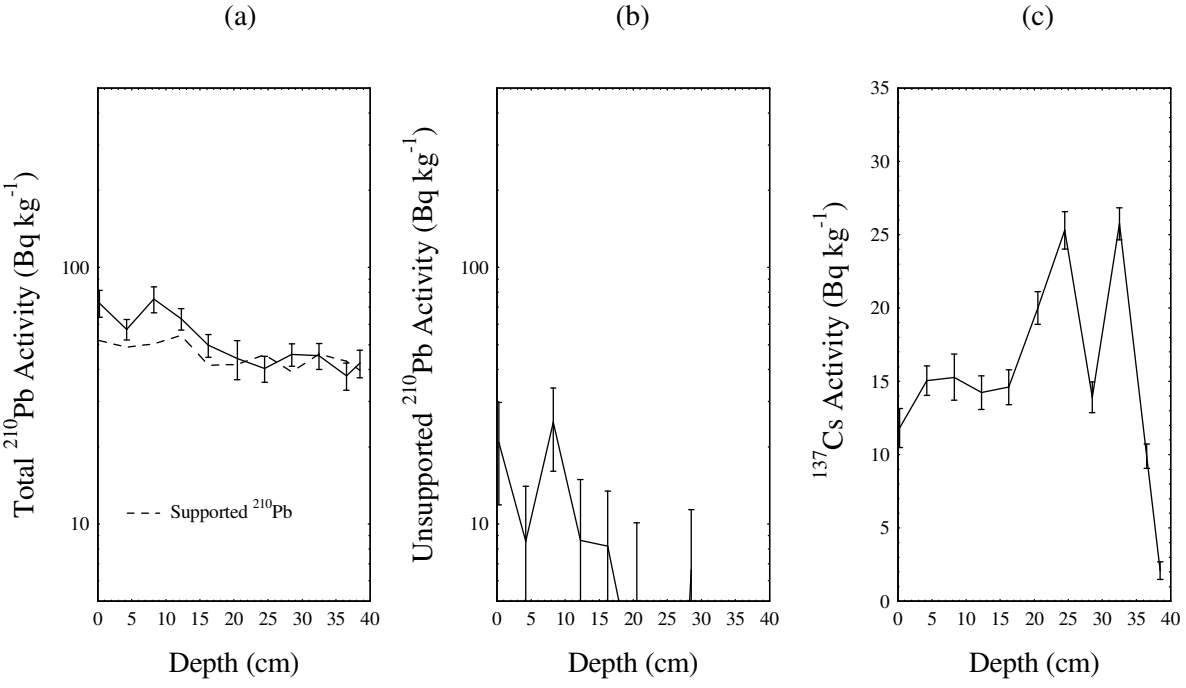

Table 22. *^{210}Pb chronology of Powdermill Lake core UKBR2*

Depth		Chronology			Sedimentation Rate		
		Date	Age				
cm	g cm^{-1}	AD	y	±	g cm^{-2} y^{-1}	cm y^{-1}	± (%)
0.25	0.05	2000	0	0			
4.25	1.17	1996	4	2	0.31	0.97	15.8
8.25	2.42	1992	8	2	0.31	0.92	15.8
12.25	3.88	1988	12	3	0.31	0.83	15.8
16.25	5.42	1983	17	4	0.31	0.73	15.8
20.50	7.31	1977	23	5	0.31	0.66	15.8
24.50	9.42	1970	30	6	0.31	0.60	15.8
28.50	11.60	1963	37	7	0.31	0.58	15.8
32.50	13.90	1956	44	8	0.31	0.57	15.8
36.50	16.03	1949	51	9	0.31	0.57	15.8
38.50	17.06	1946	54	10	0.31	0.57	15.8

Trace metals

Nickel, Zn and Cd concentrations increase from the base of the UKBR2 core to the surface, whilst Cu increases from c. 30 cm to the surface, Hg from 20 cm and Pb from 50 cm (Figure 33). The dry weight, LOI, and wet density profiles of this core (Figure 2) change steadily and gradually indicating a relatively stable lake environment and consistent sediment sources. Extrapolation of the sediment chronology suggests that the core should cover the period since the 1880s. This implies that Ni, Zn and Cd contamination has increased since this time, Pb since the 1920s, Cu from the 1950s and Hg since the 1970s. Only Ni and Cd concentrations in the surface sediments of Powdermill Lake exceed the Probable Effect Level. The other trace metal concentrations exceed the Threshold Effect Level.

The trace metal flux profiles (Figure 34) also show an increase in trace metal inputs to the sediments up to the surface although it is unlikely that the surface Cu peak is a true increase in inputs. Cd, Pb, and Ni show peak fluxes in the 1980s, but there is little sign of recovery in the other trace metal records.

***Figure 33**. The trace metal concentration profiles in core UKBR2.*

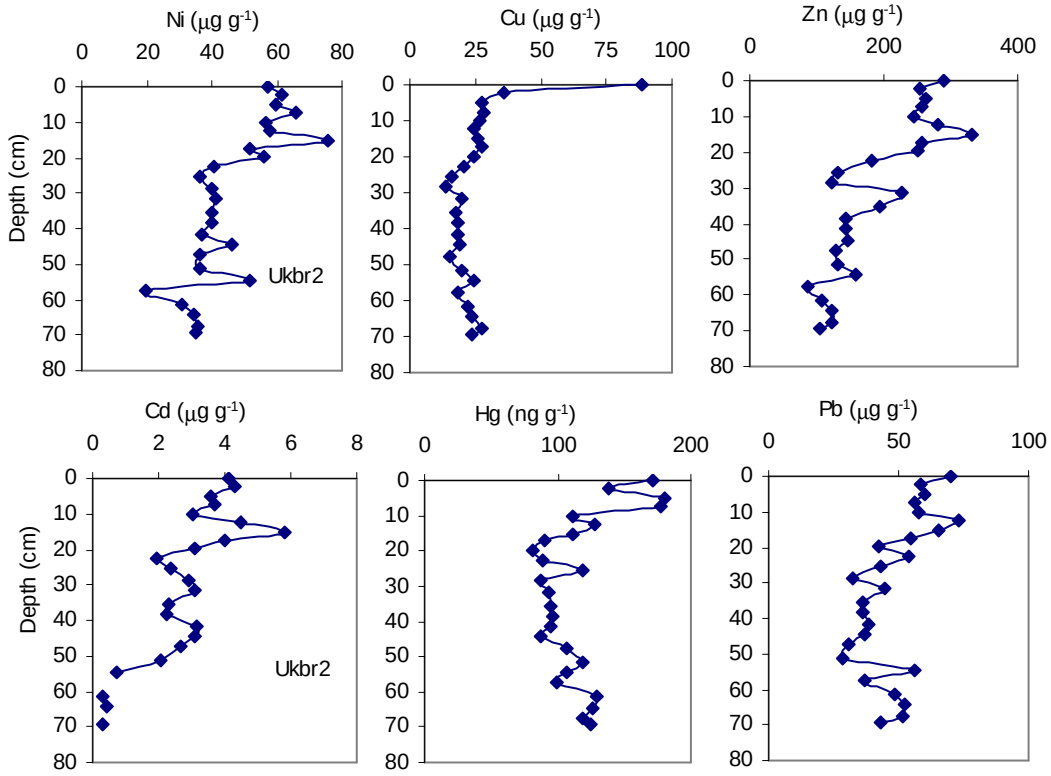

***Figure 34**. The trace metal flux profiles in core UKBR2*

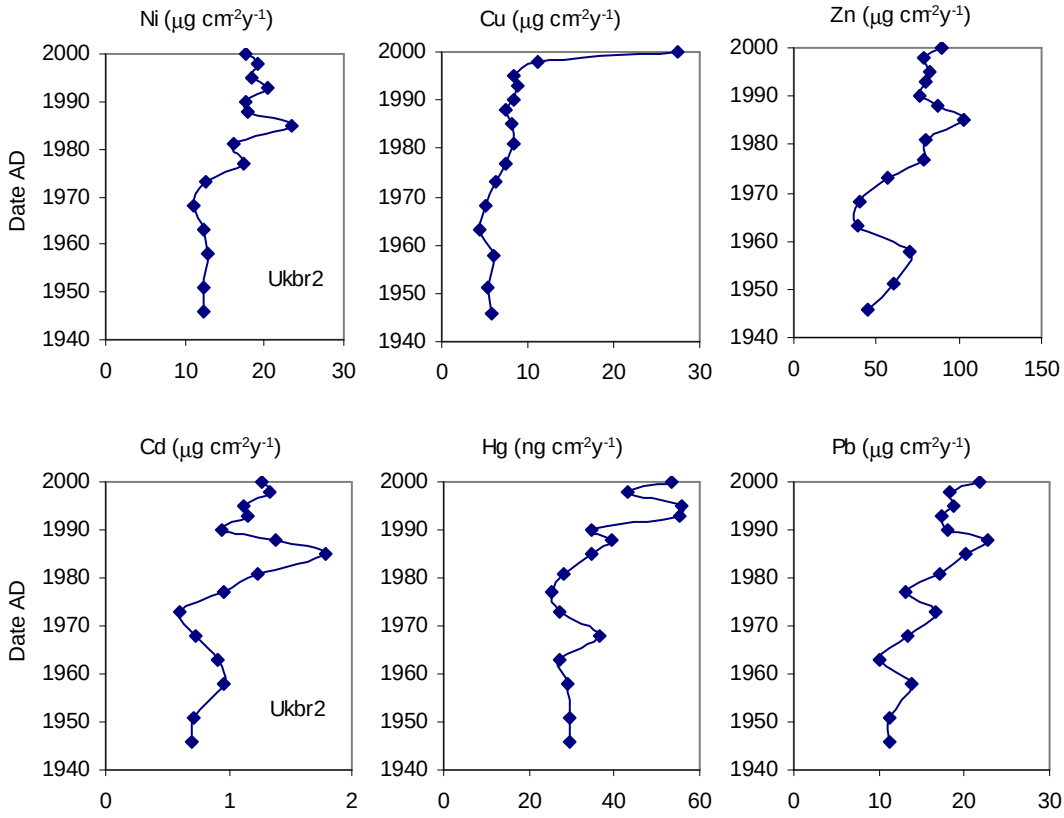

Turton & Entwistle Reservoir

Chronology

Total ^{210}Pb activity in this core reaches equilibrium with the supporting ^{226}Ra at a depth of c.17 cm (Figure 35a). The unsupported ^{210}Pb record (Figure 35b) can be divided into two parts. Above 8.5 cm concentrations are virtually constant with just minor fluctuations about a mean value of 253 Bq kg^{-1}. Beneath this section activity falls rapidly and more or less exponentially with depth. The ^{137}Cs activity versus depth profile (Figure 35c) has a well-resolved peak at 11.25 cm. A small but significant ^{241}Am peak at the same depth shows that this feature records the 1963 fallout maximum from the atmospheric testing of nuclear weapons. Figure 18 plots ^{210}Pb dates calculated using the CRS model, together with the 1963 date suggested by the ^{137}Cs and ^{241}Am records. The irregular ^{210}Pb record precluded use of the CIC model. The results show a significant discrepancy between the ^{210}Pb dates and the 1963 ^{137}Cs date. The ^{210}Pb calculations place 1963 at a depth of 7.6 cm, more than 3 cm above the ^{137}Cs peak. Calculations suggest a 4-fold increase in accumulation rates during the past few decades coupled with an even greater increase in the ^{210}Pb supply rate that may reflect increased top-soil erosion from the catchment. A corrected ^{210}Pb chronology has been constructed using the 1963 ^{137}Cs date as a reference point. The results are shown in Figure 18 and given in detail in Table 24.

Table 23. *Fallout radionuclide concentrations in Turton & Entwistle core TURT1*

Depth		^{210}Pb						^{137}Cs		^{241}Am	
		Total		Unsupported		Supported					
cm	g cm^{-2}	Bq kg^{-1}	±	Bq kg^{-1}	±	Bq kg^{-1}	±	Bq kg^{-1}	±	Bq kg^{-1}	±
0.25	0.02	342.0	49.4	268.2	50.1	73.8	8.6	143.3	9.5	0.0	0.0
2.25	0.25	263.9	25.4	198.5	26.1	65.4	6.0	209.3	7.4	0.0	0.0
4.25	0.59	355.8	27.0	286.2	27.7	69.6	6.2	293.7	9.6	0.0	0.0
6.25	0.93	306.4	20.9	232.3	21.5	74.1	5.0	269.4	7.3	0.0	0.0
8.25	1.21	328.0	21.0	278.4	21.6	49.7	4.9	317.4	7.7	0.0	0.0
9.25	1.36	166.4	19.6	120.4	20.0	46.0	3.9	343.6	7.2	0.0	0.0
10.25	1.53	157.1	14.7	109.8	15.0	47.3	2.8	443.8	5.6	2.7	1.4
11.25	1.72	130.4	13.6	74.3	14.0	56.1	3.4	476.5	6.8	5.5	1.6
12.25	1.90	71.4	10.5	38.0	10.9	33.4	2.8	187.5	4.7	0.0	0.0
13.25	2.11	84.4	7.8	30.4	8.1	54.0	2.3	100.5	2.6	0.0	0.0
14.25	2.39	87.2	8.5	39.1	8.8	48.1	2.3	44.9	2.0	0.0	0.0
15.25	2.76	51.2	6.9	12.8	7.1	38.3	1.4	11.6	1.0	0.0	0.0
16.25	3.20	54.1	5.7	11.6	5.8	42.5	1.4	3.2	0.9	0.0	0.0
18.25	4.32	47.3	6.2	-3.0	6.4	50.3	1.8	1.4	1.0	0.0	0.0
20.50	5.81	48.6	5.8	4.5	6.0	44.1	1.5	0.0	0.0	0.0	0.0

Table 24 *^{210}Pb chronology of Turton & Entwistle core TURT1*

Depth		Chronology			Sedimentation Rate		
		Date	Age				
cm	g cm^{-1}	AD	y	±	g cm^{-2} y^{-1}	cm y^{-1}	± (%)
0.00	0.00	2000	0	0			
0.25	0.02	2000	0	1	0.098	1.13	19.3
1.25	0.13	1999	1	2	0.111	0.90	16.8
2.25	0.25	1998	2	2	0.124	0.67	14.2
3.25	0.42	1996	4	2	0.101	0.58	12.8
4.25	0.59	1994	6	2	0.077	0.50	11.4
5.25	0.76	1992	8	2	0.080	0.50	11.8
6.25	0.93	1990	10	2	0.084	0.50	12.1
7.25	1.07	1988	12	3	0.072	0.45	13.2
8.25	1.21	1986	14	4	0.061	0.40	14.2
9.25	1.36	1983	17	5	0.022	0.17	22.4
10.25	1.53	1974	26	6	0.018	0.11	23.6
11.25	1.72	1964	36	8	0.020	0.12	26.8
12.25	1.90	1957	43	10	0.031	0.14	26.8
13.25	2.11	1950	50	12	0.031	0.11	26.8
14.25	2.39	1938	62	18	0.016	0.07	26.8
15.25	2.76	1921	79	30	0.028	0.06	26.8
16.25	3.20	1902	98	40	0.017	0.05	26.8

Figure 35. *Fallout radionuclides in Turton & Entwistle core TURT1 showing (a) total and supported ^{210}Pb, (b) unsupported ^{210}Pb, (c) ^{137}Cs and ^{241}Am concentrations versus depth.*

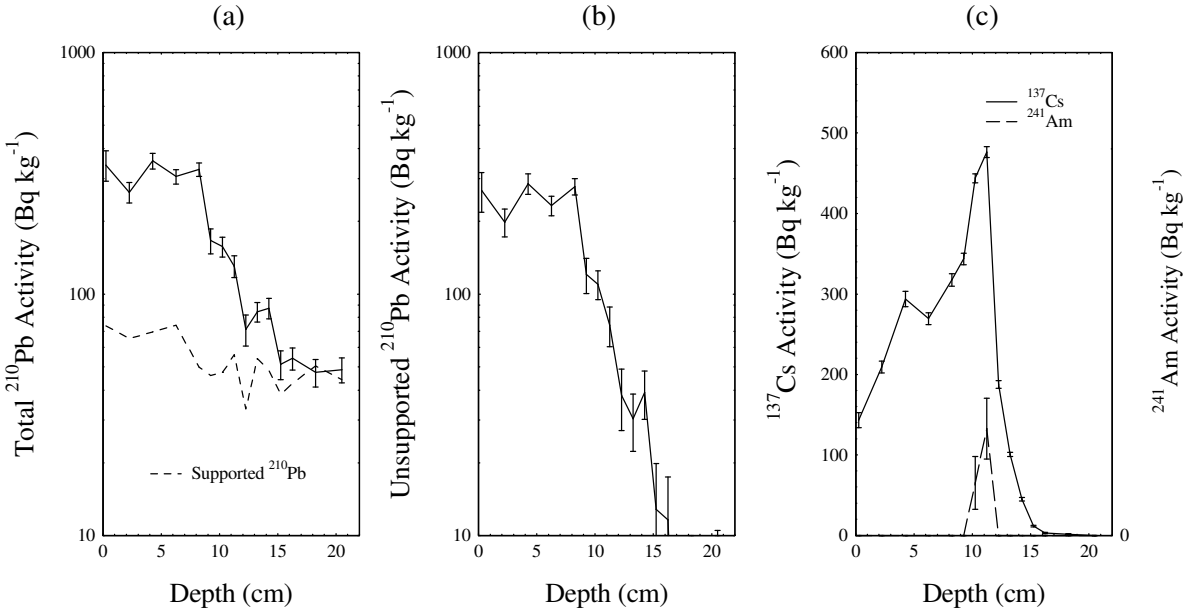

Figure 36. *Radiometric chronology of Turton & Entwistle core TURT1 showing CRS model ^{210}Pb dates together with the 1963 depth estimated from the ^{137}Cs/^{241}Am record. Also shown are the corrected ^{210}Pb dates and sedimentation rates.*

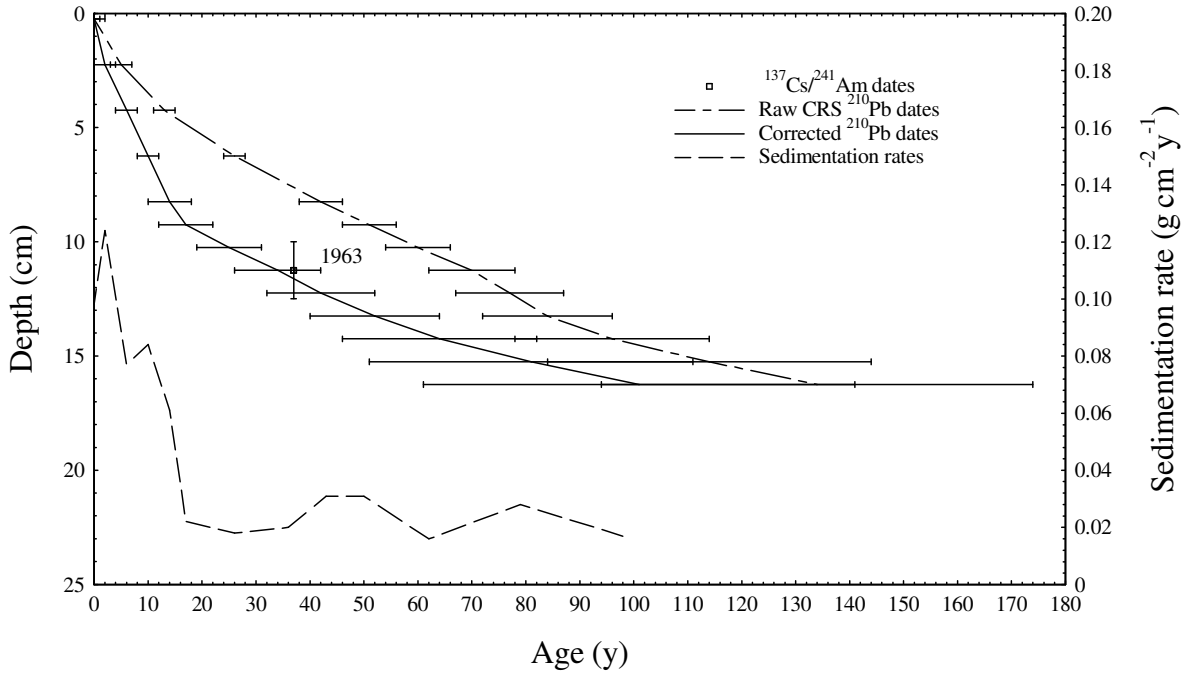

Trace metals

All the trace metal concentration profiles (Figure 37) of TURT1 taken from Turton and Entwistle Reservoir show a slow increase from 30 cm to 20cm followed by a rapid increase to 7 cm, and then a decline in concentrations to the surface. Furthermore, for all metals except Hg there is a peak concentration between 60 – 50 cm. The lithostratigraphy of the core (Figure 2) may explain a great deal of the variation in the trace metal profiles from this site. The 60 – 50cm peak may be due to elevated organic content and the low trace metal concentrations below 30cm may be due to the sandy nature of the sediments. Radiometric data suggests a 4-fold increase in sediment accumulation rate possibly from increased top soil erosion from the catchment. If this is the case, this will affect the trace metal concentrations in the sediments therefore the sediment record could not be used to reveal atmospheric deposition for trace metals. However, high trace metal concentrations in the surface sediments do indicate contamination and Pb, Ni and Zn concentrations in the surface sediments are higher than their Probable Effect Levels. These may be derived from the catchment and soil erosion, in particular, should be monitored.

Although trace metal concentrations have reduced in the upper levels of the core, increased sediment accumulation rate results in no decline in trace metal fluxes to the sediment (Figure 38).

***Figure 37**. The trace metal concentration profiles in core TURT1.*

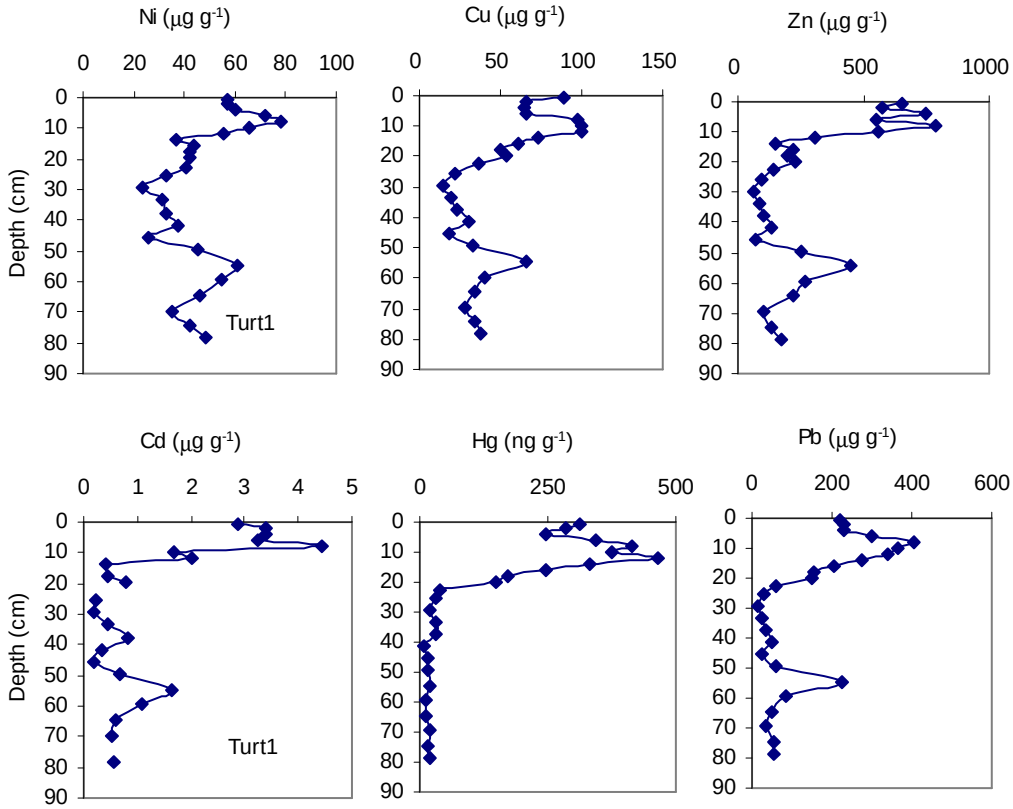

***Figure 38**. The trace metal flux profiles in core TURT1.*

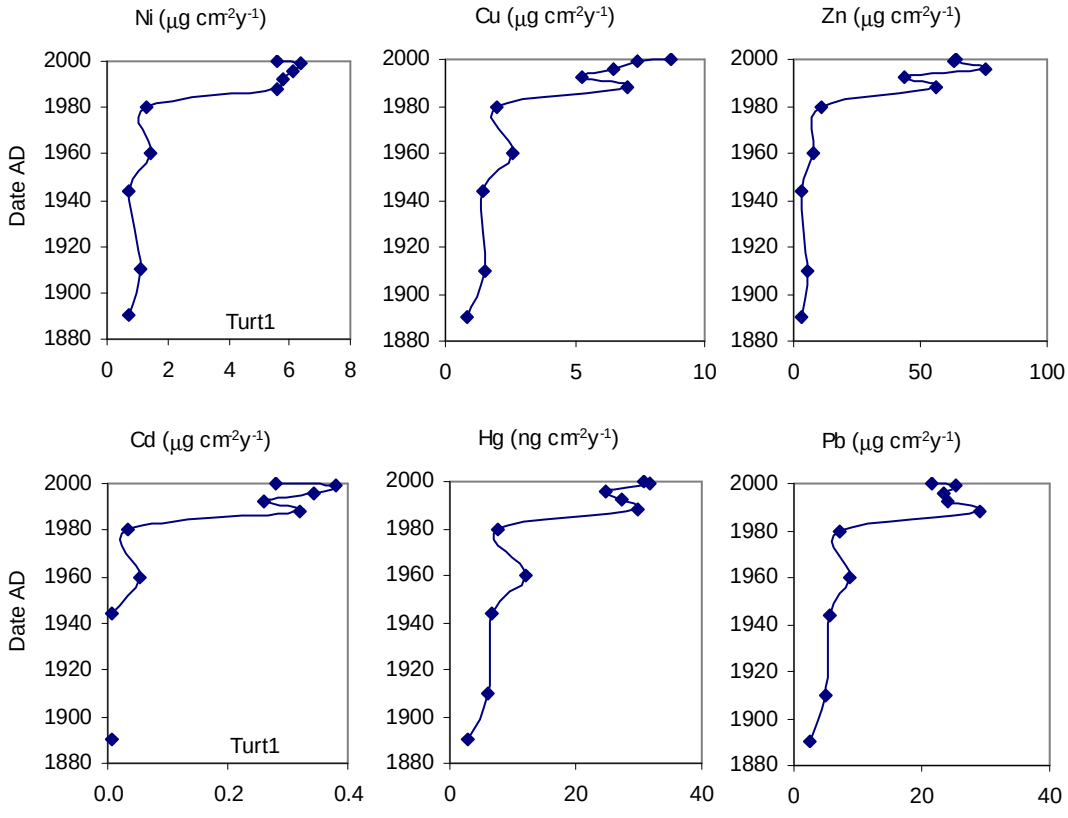

Discussion

Effects of sediment accumulation rate and catchment inputs

Trace metal fluxes, which are used to describe inputs of trace metals into lake sediments, depend upon sedimentation rate and trace metal concentrations. Sedimentation rates, trace metal concentrations and their corresponding trace metal fluxes for 1900, 1950 and 2000 for the ten study sites are summarised in Tables 25 to 30.

In this study, most sites have shown an often considerable increase in sedimentation rate over the last hundred years. Much of the material comprising this elevated sediment load is derived from soils within the catchments whilst a fraction will also be derived from increased productivity as a result of nutrient input. Human activities (e.g. agriculture) are the main factors explaining the elevated sediment load in lowland sites whilst climate change, including the increased frequency of drought and extreme events, will exacerbate this still further and effect more remote sites. Therefore, despite the huge decline in trace metal emissions and deposition, the elevated sediment load to many lakes has compensated for this resulting in no decline in trace metal inputs to lake sediments. Furthermore, given that catchment areas are frequently many times larger than lake areas, the amount of trace metals deposited and stored within the catchment is high compared with metals deposited directly to the lake surface. There is, therefore, a considerable store of deposited contaminants in the catchment areas of many lakes in the UK. Hence, as emissions continue to decline, catchment sources of trace metals become more important, such that metal loads to lake sediments, with the potential for transfer into the food chain via benthic feeders, may remain at current levels or, with increased catchment erosion, continue to increase.

Toxicity levels

Although sedimentation rates effect trace metal fluxes, the concentrations of the metals discussed in this report are also reasonably high such that surface sediments exceed the Probable Effect Levels (PEL) i.e. the concentration of trace metal in the sediment where adverse biological effects are frequently seen. At Diss Mere and Gull Pond, Hg concentrations exceeded the Apparent Effects Threshold, or the concentration above which biological effects have always been observed. It is uncertain whether the locations of these sites, the two most easterly in the dataset, are of consequence to this observation. Table 31 summarises the exceedances for each site and shows that PELs were exceeded at all sites for at least one metal, except Pinkworthy Pond where the TEL only was exceeded for Zn, Hg and Pb. By contrast, Llyn Fach shows PEL exceedance for four metals, whilst Diss Mere and Turton & Entwistle Reservoir are exceeded for three.

However, it is difficult to compare sites and metals by concentration alone and in order to make the comparison more biologically relevant the trace metal concentrations can be scaled to PEL exceedance. Table 32 shows the concentrations of the trace metals in the ten cores normalised to the PEL concentration. Thus, a ratio exceeding 1.0 shows a PEL exceedance. In this way, it is possible to assess which metals are more problematic at which sites and possibly whether any areas are particularly impacted by a metal or metals. Also, it shows the scale of PEL exceedance i.e. whether the surface sediments are slightly exceeded, such that a slight

reduction would reduce the concentration to below the PEL, or many times over the threshold and hence of greater biological significance. The data in Table 32 can then be ranked by metal for each site (Table 33) or by site for each metal (Table 34).

Table 32 shows that most PEL exceedances are relatively small and hence ratios mainly lie between 1.0 and 2.0. However, there are also some major exceedances. At Diss Mere Hg and Pb PELs are exceeded by 5.77 and 6.02 times respectively, whilst at Llyn Fach all exceedances (Ni, Zn, Cd and Pb) are by factors of between 3.07 and 5.6. Other than these two sites the only other exceedances greater than 2 are present at Gormire (Pb), Gull Pond (Pb) and Turton & Entwistle Reservoir (Zn and Pb). Thus Table 33 shows that Pb and Ni show the highest exceedances in all sites except two, whilst Cu, Cd and Hg tend to be exceeded least. Even where Hg concentrations exceed the Apparent Effect Threshold, at Diss Mere and Gull Pond, the scale of the Hg exceedance is exceeded by that of Pb. Table 34 presents these data from the opposite point of view and shows that Pb is exceeded at six of the ten sites, Ni at five, Zn at four, Hg and Cd at two and Cu only at Portmore Loch. It is therefore possible to conclude that the main exceedances across all sites are from Pb, Ni and possibly Zn, whilst although the exceedances of Hg can be high at individual sites, generally, its PEL is not exceeded.

In terms of spatial impacts, it may have been expected that sites in historically industrial areas such as the north of England (Turton & Entwistle Reservoir; 3 exceedances) and south Wales (Llyn Fach; 4) would show exceedances, especially if the role of catchment inputs in releasing previously deposited contaminants is important, and this was seen to be the case. However, it was unexpected that Diss Mere would also show as many exceedances (Pb, Hg and Zn) and, for Pb and Hg in particular, at such high levels. The reason for this remains unclear. At the other end of the scale, Pinkworthy Pond, the site furthest south-west appears to be the least impacted, but it was also unexpected that two sites in the Midlands (Groby Pool and Great Pool Droitwich) would also show low exceedances.

Finally, it is important to consider these data in the light of other UK work, especially to the north and west of the study area. Yang et al. (2002) have undertaken a trace metal study on many ecological compartments including lake sediments within the Lochnagar catchment, a site in the Grampian Mountains to the south-east of the Cairngorms, whilst Rose and Rippey (2002) report lake sediment trace metal concentrations for Loch Coire nan Arr in the north-west of Scotland, an area that could be considered one of the least impacted within the UK. For Lochnagar, a number of sediment cores were reported, but the range of surface sediment concentrations only showed exceedance of the PEL for Pb. For all other trace metals (no Ni data were reported) the range of concentrations spanned the TEL such that some surface sediments showed TEL exceedance but others did not. For Loch Coire nan Arr the concentrations were still lower and no trace metals showed exceedance of even the TEL. The exception was Cd, which exceeded both TEL and PEL (PEL exceedance of 1.27) although the reason for this Cd contamination is unclear. Therefore, although there is little geographical pattern observed from these data, in general, the exceedances of trace metal guideline concentrations at the ten sites in this study are higher than sites to the north and west of Scotland and thus possibly show the potential for greater biological impact than sites in the cleanest areas of the UK.

Table 25. *Comparison for Ni in the studied cores in different times: their sedimentation rates, Ni concentrations and Ni fluxes in 1900, 1950 and 2000.*

Core	1900			1950			2000		
	Sedrate▫	Concen.◦◦	Flux*	Sedrate	Concen.	flux	Sedrate	Concen.	flux
DISS1	0.09	24.8	2.2	0.09	22.4	2.0	0.09	24	2.2
DROI1	0.09	41	3.6	0.09	42	3.8	0.09	42	3.7
FACH1	0.022	120	2.6	0.022	135	3	0.045	145	6.5
GORM3	0.0052	26	0.14	0.012	35	0.42	0.042	27	1.1
GROB1	0.14	36	5.1	0.14	35	4.8	0.14	33	4.6
GULL1	0.015	30.5	0.47	0.035	22.5	0.79	0.048	26.4	1.27
PINK3	0.045	38.6	1.7	0.06	49.6	2.98	0.11	18.9	2.08
PORT1	0.013	62	0.80	0.022	48	1.1	0.036	41	1.5
TURT1	0.021	43	0.90	0.023	45	1.0	0.098	67	5.6
UKBR2	0.31	35	10.9	0.31	40	12.4	0.31	57	17.7

▫: sedrate - sedimentation rate, g cm^{-2} y^{-1}.
◦◦: concen – concentration, µg g^{-1}.
*: flux, µg cm^{-2} y^{-1}.

Table 26. *Comparison for Cu in the studied cores in different times: their sedimentation rates, Cu concentrations and Cu fluxes in 1900, 1950 and 2000.*

Core	1900			1950			2000		
	Sedrate	Concen.	flux	Sedrate	Concen.	flux	Sedrate	Concen.	flux
DISS1	0.09	101	9.0	0.09	92	8.3	0.09	130	11.7
DROI1	0.09	25	2.3	0.09	28	2.5	0.09	86	7.7
FACH1	0.022	100	2.2	0.022	85	1.9	0.045	86	3.8
GORM3	0.0052	68	0.35	0.012	46	0.55	0.042	42	1.77
GROB1	0.14	36	5.0	0.14	55	7.7	0.14	64	9
GULL1	0.015	30	0.45	0.035	30	1.0	0.048	80	3.8
PINK3	0.045	28	1.26	0.06	30	1.8	0.11	33	3.6
PORT1	0.013	133	1.7	0.022	384	8.4	0.036	199	7.2
TURT1	0.021	55	1.2	0.023	82	1.9	0.098	88	8.7
UKBR2	0.31	24	7.3	0.31	17	5.3	0.31	88	27

▫: sedrate - sedimentation rate, g cm^{-2} y^{-1}.
◦◦: concen – concentration, µg g^{-1}.
*: flux, µg cm^{-2} y^{-1}.

Table 27. *Comparison for Zn in the studied cores in different times: their sedimentation rates, Zn concentrations and Zn fluxes in 1900, 1950 and 2000.*

Core	1900			1950			2000		
	Sedrate	Concen.	flux	Sedrate	Concen.	flux	Sedrate	Concen.	flux
DISS1	0.09	423	38	0.09	561	50.5	0.09	629	56.6
DROI1	0.09	129	11.6	0.09	214	19.2	0.09	291	26.2
FACH1	0.022	612	13.2	0.022	861	19	0.045	1124	50.6
GORM3	0.0052	243	1.3	0.012	290	3.5	0.042	380	15.9
GROB1	0.14	158	22	0.14	244	34	0.14	237	33
GULL1	0.015	741	11	0.035	263	9.2	0.048	235	11.3
PINK3	0.045	238	10.7	0.06	297	17.8	0.11	246	27
PORT1	0.013	148	1.9	0.022	174	3.8	0.036	256	9.2
TURT1	0.021	210	4.4	0.023	220	5.1	0.098	653	64
UKBR2	0.31	105	32	0.31	194	60	0.31	289	89

▫: sedrate - sedimentation rate, g cm^{-2} y^{-1}.
◦◦: concen – concentration, μg g^{-1}.
∗: flux, μg cm^{-2} y^{-1}.

Table 28. *Comparison for Cd in the studied cores in different times: their sedimentation rates, Cd concentrations and Cd fluxes in 1900, 1950 and 2000.*

Core	1900			1950			2000		
	Sedrate	Concen.	flux	Sedrate	Concen.	flux	Sedrate	Concen.	flux
DISS1	0.09	0.34	0.41	0.09	1.0	0.48	0.09	1.7	0.60
DROI1	0.09	0.32	0.03	0.09	0.036	0.03	0.09	1.02	0.09
FACH1	0.022	16.3	0.36	0.022	20	0.45	0.045	20	0.89
GORM3	0.0052	0.78	0.004	0.012	1.95	0.023	0.042	1.86	0.078
GROB1	0.14	0.40	0.056	0.14	0.86	0.12	0.14	1.21	0.17
GULL1	0.015	6.8	0.10	0.035	4.2	0.15	0.048	1.4	0.07
PINK3	0.045	1.8	0.08	0.06	2.4	0.15	0.11		
PORT1	0.013	0.46	0.006	0.022	0.5	1.1	0.036		
TURT1	0.021	0.44	0.009	0.023	1.2	0.028	0.098	2.9	0.28
UKBR2	0.31	0.33	0.10	0.31	2.33	0.72	0.31	4.1	1.27

▫: sedrate - sedimentation rate, g cm^{-2} y^{-1}.
◦◦: concen – concentration, μg g^{-1}.
∗: flux, μg cm^{-2} y^{-1}.

Table 29. *Comparison for Hg in the studied cores in different times: their sedimentation rates, Hg concentrations and Hg fluxes in 1900, 1950 and 2000.*

Core	1900			1950			2000		
	Sedrate	Concen.	flux	Sedrate	Concen.	flux	Sedrate	Concen.	flux
DISS1	0.09	4760	428	0.09	850	75	0.09	2809	253
DROI1	0.09	86	7.8	0.09	125	11.3	0.09	153	13.8
FACH1	0.022	247	5.4	0.022	228	5	0.045	264	11.8
GORM3	0.0052	234	1.2	0.012	330	4	0.042	334	14
GROB1	0.14	166	23	0.14	193	27	0.14	193	27
GULL1	0.015	352	5.3	0.035	357	12.5	0.048	550	26.4
PINK3	0.045	133	6	0.06	150	9	0.11	246	27
PORT1	0.013	153	2	0.022	224	4.9	0.036	216	7.8
TURT1	0.021	205	4	0.023	400	8	0.098	313	31
UKBR2	0.31	125	38	0.31	95	29	0.31	172	53

▫: sedrate - sedimentation rate, g cm^{-2} y^{-1}.
▫▫: concen – concentration, ng g^{-1}.
*: flux, ng cm^{-2} y^{-1}.

Table 30. *Comparison for Pb in the studied cores in different times: their sedimentation rates, Pb concentrations and Pb fluxes in 1900, 1950 and 2000.*

Core	1900			1950			2000		
	Sedrate	Concen.	flux	Sedrate	Concen.	flux	Sedrate	Concen.	flux
DISS1	0.09	705	63	0.09	619	56	0.09	551	50
DROI1	0.09	48	4.3	0.09	55	4.9	0.09	66	6.0
FACH1	0.022	269	5.9	0.022	335	7.4	0.045	281	12.6
GORM3	0.0052	209	1.1	0.012	242	2.9	0.042	191	8.0
GROB1	0.14	82	11.4	0.14	97	13.6	0.14	116	16.2
GULL1	0.015	101	1.5	0.035	105	3.7	0.048	258	12.4
PINK3	0.045	87	3.9	0.06	77	4.6	0.11	56	6.2
PORT1	0.013	73	0.95	0.022	75	1.65	0.036	67	2.4
TURT1	0.021	180	3.8	0.023	310	7.1	0.098	219	21.5
UKBR2	0.31	43	13	0.31	37	11	0.31	70	22

▫: sedrate - sedimentation rate, g cm^{-2} y^{-1}.
▫▫: concen – concentration, μg g^{-1}.
*: flux, μg cm^{-2} y^{-1}.

Table 31. *Exceedance of Apparent Effects Threshold (AET) (Hg only), Probable and Threshold Effects Levels (PEL; TEL).*

Site	AET exceedance	PEL exceedance	TEL exceedance
Diss Mere	Hg	Zn, Pb	Ni, Cu, Cd
Llyn Fach		Ni, Cd, Zn, Pb	Hg, Cu
Gormire		Pb, Zn	Ni, Cd, Hg, Cu
Great Pool Droitwich		Ni	Pb, Cu, Zn, Cd
Groby Pool		Pb	Ni, Cd, Zn, Hg, Cu
Gull Pond	Hg	Pb	Ni, Cd, Zn, Hg, Cu
Pinkworthy Pond			Zn, Hg, Pb
Portmore Loch		Ni, Cu	Pb, Cd, Zn, Hg
Powdermill Lake		Ni, Cd	Pb, Cu, Zn, Hg
Turton & Entwistle Res.		Pb, Ni, Zn	Cu, Cd, Hg

Table 32. *Ratio of metal concentration in surface sediments to PEL. (Ratios > 1.0, shown* ***bold*** *and shaded, exceed PEL)*

	Ni	Cu	Zn	Cd	Hg	Pb
Diss Mere	0.66	0.66	**2.00**	0.47	**5.77**	**6.02**
Llyn Fach	**4.00**	0.43	**3.56**	**5.60**	0.54	**3.07**
Gormire	0.74	0.21	**1.20**	0.53	0.69	**2.09**
Great Pool Droitwich	**1.15**	0.44	0.92	0.29	0.31	0.73
Groby Pool	0.91	0.32	0.75	0.34	0.39	**1.25**
Gull Pond	0.73	0.40	0.75	0.39	**1.13**	**2.82**
Pinkworthy Pond	0.52	0.16	0.78	0.15	0.51	0.61
Portmore Loch	**1.15**	**1.01**	0.81	0.25	0.44	0.73
Powdermill Lake	**1.58**	0.45	0.92	**1.15**	0.35	0.76
Turton & Entwistle Res.	**1.58**	0.45	**2.07**	0.81	0.64	**2.40**

Table 33. *PEL exceedance ranking for each site. PEL exceedance shown* ***bold.***

Site	Exceedance rank
Diss Mere	**Pb** > **Hg** > **Zn** > Ni, Cu, Cd
Llyn Fach	**Cd** > **Ni** > **Pb, Zn** > Hg, Cu
Gormire	**Pb** > **Zn** > Ni, Hg > Cd > Cu
Great Pool Droitwich	**Ni** > Zn > Pb > Cu > Cd, Hg
Groby Pool	**Pb** > Ni > Zn > Cu, Cd, Hg
Gull Pond	**Pb** > **Hg** > Zn, Ni > Cu, Cd
Pinkworthy Pond	Zn > Pb > Ni, Hg > Cu, Cd
Portmore Loch	**Ni** > **Cu** > Zn > Pb > Cu > Cd
Powdermill Lake	**Ni** > **Cd** > Zn > Pb > Cu > Hg
Turton & Entwistle Res.	**Pb** > **Zn** > **Ni** > Cd > Hg > Cu

Table 34. *PEL exceedance ranking by trace metal. PEL exceedance shown* ***bold.***

Site	Exceedance rank
Ni	**Fach** > **Powd, Turt** > **Port, Droi** > Grob > Gull, Gorm > Diss, Pink
Cu	**Port** > Diss > Fach, Droi, Gull, Powd, Turt > Grob > Gorm, Pink
Zn	**Fach** > **Turt, Diss** > **Gorm** > Droi, Powd > Gull, Pink, Port, Grob
Cd	**Fach** > **Powd** > Turt > Gorm, Diss > Grob, Gull > Droi, Port > Pink
Hg	**Diss** > **Gull** > Gorm, Turt > Fach, Pink > Grob, Port, Powd, Droi
Pb	**Diss** > **Fach** > **Gull, Turt** > **Gorm** > **Grob** > Powd, Port, Droi > Pink

Conclusions

A suite of toxic trace metals (Hg, Pb, Cd, Ni, Cu, Zn) were analysed from sediment cores taken from ten lakes across southern and eastern UK to complement previous studies in more geologically sensitive, and low deposition, areas in the north and west. The cores, taken for a previous study, were already ^{210}Pb-dated providing, in most cases, a reliable chronology.

The sediment record revealed that all sites have been contaminated with trace metals from atmospheric deposition and also that contamination over background levels occurred as early as the late-18th century. These data therefore have direct significance to the setting of reference conditions for trace metals under the Water Framework Directive and suggest that the setting of an arbitrary mid-19th century level as a

restoration target for trace metals will not restore sites to reference conditions in many UK sites.

Further, it is observed that despite considerable reductions in UK trace metal emissions, surface sediment concentrations in many of these lakes are not declining. This can only be due to increased inputs of trace metals from catchment sources. These catchment metals derive from historical atmospheric deposition and are now being released to water bodies. It is thought that this release is primarily due to catchment disturbance but climate enhanced erosion will also play a role and could significantly increase in the future.

This increased catchment input, and also possibly elevated lake productivity as a result of increased nutrients, has also increased sediment accumulation rates, at some sites by a considerable degree. Sediment accumulation rates combine with trace metal concentrations to produce trace metal fluxes or the rate of metal input to the sediment. Slight, or no, decline in concentration and elevated sediment accumulation rates therefore result in steady or increasing trace metal fluxes to the sediments at many of the sites in this study. Catchment inputs therefore already form an important trace metal source to many lakes. Enhancement of this catchment input, possibly as a result of climate change, will elevate this catchment role still further.

A Probable Effect Level (PEL) has been determined for trace metals in lake sediments at which detrimental biological effects are frequently seen and we have used this level to determine the biological relevance of the trace metal concentrations in this study. The PEL was exceeded for at least one metal at 9 out of the 10 sites, whilst PEL exceedance for four of the six analysed metals at Llyn Fach and three metals at Diss Mere and Turton and Entwistle Reservoir. The PEL for Pb was exceeded at six of the ten sites, Ni at five and Zn at four, whilst that of Cd was exceeded twice and Cu only once. Where the Hg PEL was exceeded, it also exceeded the Apparent Effects Level, the sediment concentration of Hg at which biological effects are always seen. This occurred at Diss Mere and Gull Pond. PEL exceedance of trace metals is therefore widespread across the UK and, in places, greatly exceeded, with several metals exceeding by 5-6 times the PEL concentration.

Comparison with previous studies in cleaner areas of the UK (upland areas in the north and west of Scotland) show that the ten sites in this current study have been more contaminated, over a longer period, and that PEL is exceeded by more metals and to a higher degree. However, the full geographical extent of these exceedances is currently unknown as are the biological consequences of trace metal contamination in UK freshwaters.

Recommendations for further work

The conclusions of this study show that trace metal concentrations in 9 out of the 10 study sites exceeded a defined threshold for biological effects for at least one trace metal. This is in agreement with a previous DEFRA-funded study (Rose et al., 2003) which showed evidence for toxicity to benthic invertebrates at a number of UK sites, mainly in the uplands and to the north and west of the UK. This former study also showed that the main component of the toxicity was derived from trace metals rather

than persistent organic pollutants (POPs) due to their presence in far higher concentrations. Our current study confirms the widespread nature of exceedance over this biological threshold level across southern Scotland, England and Wales.

There is, therefore considerable potential for trace metals to enter the freshwater food chain via benthic feeders and the data suggest that these trace metal levels could be detrimental to biota. However, the full extent of these exceedances is unknown, both spatially and by degree of exceedance, as the datasets are still small and comparable data separated by some years.

Given the increasing evidence for biological impact from trace metals in freshwaters and the likelihood of continued and possibly increasing trace metal inputs from catchment sources, despite emissions reductions, there is now an urgent need to fully assess the distribution and extent of trace metal concentrations and exceedance across the whole of the UK, and determine the impacts across the freshwater food chain. Furthermore, given the potential for increased inputs there is a need to monitor metals in freshwaters in order to identify directions and rates of change. In summary the following is required:

1. A UK-wide survey of trace metals in freshwater bodies, including waters, sediments and biota
2. Further work on the biological impact of trace metals across the aquatic food chain
3. The establishment of a UK-wide trace metals monitoring network for freshwaters, to include a range of lake and stream types.

Acknowledgements

This project was funded by the Department for Environment, Food and Rural Affairs as an extension to Contract No. EPG 1/3/160. The fieldwork and dating of the sediment cores was undertaken as part of a project funded by the Natural Environment Research Council (GR9/04557). We wish to thank Peter Appleby for the use of his sediment chronology data.

References

Appleby, P.G, 2001. Chronostratigraphic techniques in recent sediments. In: Last, W.M. & Smol, J.P. (eds.) Tracking Environmental Change Using Lake Sediments Volume 1: Basin Analysis, Coring, and Chronological Techniques, Kluwer Academic, pp 171-203.

Appleby, P.G., Nolan, P.J., Gifford, D.W., Godfrey, M.J., Oldfield, F., Anderson, N.J. & Battarbee, R.W. 1986. ^{210}Pb dating by low background gamma counting. Hydrobiologia 141:21-27.

Appleby, P.G. & Oldfield, F. 1978. The calculation of ^{210}Pb dates assuming a constant rate of supply of unsupported ^{210}Pb to the sediment. Catena, 5:1-8

Appleby, P.G. & Oldfield, F. 1983. The assessment of ^{210}Pb data from sites with varying sediment accumulation rates. Hydrobiologia. 103:29-35.

Appleby, P.G., Richardson, N. & Nolan, P.J. 1991. ^{241}Am dating of lake sediments. Hydrobiologia, 214:35-42.

Avocet Consulting, 2003. Development of Freshwater Sediment Quality Values for Use in Washington State – Phase II Report: Development and Recommendations of SQVs for Freshwater Sediments in Washington State. Prepared for the Washington State Department of Ecology under contract to SAIC. Publication No. 03-09-088.

Baker, S.J. 2001. Trace and major elements in the atmosphere at rural locations in the UK: Summary of data for 1999. A report produced for the Department of the Environment, Transport and the Regions; the Scottish Executive; the National Assembly for Wales and the Department of the Environment in Northern Ireland. National Environmental Technology Centre Report AEAT/R/ENV/0264. 80pp.

Dean, W.E. Jr. 1974. Determination of carbonate and organic matter in calcareous sediments and sedimentary rocks by loss-on-ignition: comparison with other methods. Journal of Sedimentary Petrology. 44: 242-248.

Engstrom, D.R. & Swain, E.B., 1997. Recent declines in atmospheric mercury deposition in the Upper Midwest. Environmental Science & Technology 31: 960 – 967.

Rose, N.L. & Appleby, P.G. (2005). Regional applications of lake sediment dating by spheroidal carbonaceous particle analysis I: United Kingdom. Journal of Paleolimnology.

Lee, D.S., Nemitz, E., Fowler, D., Hill, P., Clegg, S. & Kingdon, R.D. 2000. Sources, sinks and levels of atmospheric mercury in the UK. Defence Evaluation and Research Agency Report for the Department of the Environment, Transport and the Regions. 133pp.

MacDonald, D. D., Ingersoll, C. G., Berger, T. A.. 2000. Development and evaluation of consensus-based sediment quality guidelines for freshwater ecosystems. Archives of Environmental Contamination and Toxicology 39: 20-31.

Markert, B., 1994. The biological system of the element (BSE) for terrestrial plant (glycophytes). Science of the Total Environment.155: 221-228.

Rose, N.L. and Rippey, B. 2002. The historical record of PAH, PCB, trace metal and fly-ash particle deposition at a remote lake in north-west Scotland. Environmental Pollution. 117: 121 – 132.

Rose, N.L., Rippey, B., Yang, H. and Harrad, S. Lake sediment toxicity in the UK: The role of trace metals and persistent organic pollutants. Environmental Change Research Centre, University College London. Research Report No 88. 48pp.

Stevenson A.C., Patrick S.T., Kreiser A. and Battarbee R.W. 1987. Palaeoecological evaluation of the recent acidification of susceptible lakes: Methods utilised under Department of the Environment contract PECD 7/7/139 and the Royal Society Surface Water Acidification Project. Palaeoecology Research Unit, University College London Research Papers No. 26. 36pp.

Yang, H., Rose,N.L., and Berry, A. (2001). Trace element measurements within London and across the UK with particular emphasis on mercury. Final Report to the Department of the Environment, Transport and the Regions, Department of the Environment Northern Ireland, National Assembly for Wales and the Scottish Executive. (Contract No. EPG 1/3/159). Environmental Change Research Centre, University College London. Research Report No. 75.

Yang, H., Rose, N., Battarbee, R. W., and Boyle, J. F., 2002a. Mercury and lead budgets for Lochnagar, a Scottish mountain lake and its catchment. Environmental Science & Technology 36: 1383 – 1388.

Yang, H., Rose, N.L. and Battarbee, R.W. 2002b. Distribution of some trace metals in Lochnagar, a Scottish mountain lake ecosystem and its catchment. Science of the Total Environment 285: 197 – 208.
Yang, H., and Rose, N. L., 2003. Distribution of mercury in six lake sediment cores across the UK. Science of the Total Environment. 304: 391 – 404.
Yang, H., and Rose, N., 2005. Trace element pollution records in some UK lake sediments, their history, influence factors and regional differences. Environment International.31: 63 – 75.

Appendix. Trace metal concentrations in the sediment cores

(Ni, Cu, Zn and Pb in μg g^{-1}, Hg in ng g^{-1}).

DISS1

Depth (cm)	Ni	Cu	Zn	Cd	Hg	Pb
0-1	23.97	130.51	629.16	1.66	2808.75	550.69
2-2.5	24.35	116.99	666.42	1.85	2975.09	547.18
5-5.5	25.68	116.72	587.16	2.14	2514.27	623.60
7-7.5	26.98	114.98	578.41	1.41	2740.30	621.54
10-10.5	29.81	117.55	601.40	1.46	1972.53	696.33
12-12.5	29.18	109.84	619.15	1.52	1937.69	703.43
15-15.5	23.24	106.74	650.74	2.42	1755.16	630.82
17-17.5	25.08	107.79	537.76	1.96	1273.84	671.92
19.5-20	25.96	94.16	663.89	2.50	973.38	650.34
22-23	28.40	112.96	615.09	3.70	1475.59	844.46
25-26	25.15	102.90	569.31	2.79	1205.28	761.80
28-29	22.45	92.04	561.35	1.00	801.92	618.63
31-32	20.88	107.67	590.20	2.68	1254.68	665.34
35-36	19.55	90.74	570.34	0.68	2546.17	577.33
38-39	23.64	86.80	636.56	0.76	2614.43	654.74
41-42	24.73	93.69	670.90		2834.08	686.07
45-46	18.54	90.04	442.54	0.70	3793.20	645.45
48-49	24.83	100.65	423.01	0.34	4759.93	704.82
51-52	23.08	94.41	430.77		6346.15	654.95
55-56	18.16	79.12	170.76	0.63	3263.75	421.65
59-60	21.52	192.79	262.46	0.69	4241.38	610.05
63-64	21.89	207.30	185.80	0.76	6669.96	516.01
67-68	21.79	219.08	139.70		14145	617.89
71-72	22.58	213.87	121.99		18232	505.47
74-75	21.01	179.04	125.68		18987	461.70

FACH1

Depth (cm)	Ni	Cu	Zn	Cd	Hg	Pb
0-0.5	144.94	85.56	1123.98	19.80	263.97	280.88
1.5-2	145.54	72.26	827.75	21.68	289.06	300.69
3.5-4	185.13	73.90	612.60	24.07	243.10	315.05
5.5-6	192.77	77.28	715.99	27.28	215.93	350.69
7.5-8	192.84	75.61	835.65	24.87	198.97	358.14
9.5-10	155.06	73.20	708.95	22.12	240.36	328.70
11.5-12	151.55	76.91	767.84	21.30	248.49	334.70
13.5-14	144.23	82.18	751.04	22.57	271.99	342.26
15.5-16	135.22	84.64	861.33	20.51	227.86	334.82
17.5-18	117.57	73.99	764.19	14.56	242.60	246.41
19.5-20	129.86	84.76	875.36	20.32	270.95	300.13
22-23	120.22	99.85	601.72	16.28	247.46	294.72
25-26	114.81	117.83	549.88	13.75	218.21	269.33
29-30	84.70	100.10	630.63	8.76	194.64	160.16
32-33	85.47	89.79	608.08	8.42	207.63	144.30
35-36	111.02	81.73	645.25	12.41	186.22	159.62
39-40	78.03	73.78	458.35	4.23	204.94	108.03
42-43	60.36	68.83	162.14	2.06	284.51	101.48
45-46	52.50	50.56	98.30	0.63	269.63	45.50
49-50	79.68	55.45	118.57	0.78	219.71	48.43
54-55	44.10	47.39	93.43	0.19	86.63	36.69
59-60	69.45	60.19	203.97	2.26	110.34	74.80
65-66	64.30	79.37	446.81	4.12	101.32	95.53
71-72	55.94	62.09	407.25	2.87	85.06	65.61
77-78	55.54	72.20	454.87	2.63	90.25	79.94

GORM3

Depth(cm)	Ni	Cu	Zn	Cd	Hg	Pb
1.0-2.0	26.75	42.10	379.73	1.86	334.32	191.04
2.0-3.0	21.24	38.35	403.15		305.31	227.56
4.5-5	36.65	39.16	281.95	2.35	317.20	225.56
7-7.5	39.38	38.28	278.01	2.05	323.01	246.10
9.5-10	37.88	46.04	298.17	1.97	340.37	246.93
12-12.5	31.89	45.56	286.85	1.90	313.21	234.30
14.5-15	26.25	67.71	243.06	0.78	234.38	208.93
17-17.5	32.77	33.61	326.80		236.34	201.68
19.5-20	43.03	76.50	219.93	0.72	150.60	147.53
22-23	28.23	20.30	104.56		93.41	80.66
25-26	28.25	22.83	111.78	1.07	96.32	73.39
28-29	26.84	24.40	94.89	0.51	99.13	69.71
31-32	31.68	22.00	87.99		131.98	75.42
34-35	31.10	22.68	89.98		72.89	52.76
37-38	28.41	20.72	72.34		77.69	48.20
40-41	27.90	21.96	77.49	0.48	94.44	49.81
43-44	29.13	20.88	80.04	0.39	70.47	44.29
46-47	28.40	20.42	74.26		88.76	42.96
49-50	31.54	23.78	75.10		98.57	41.84
54-55	20.26	22.51	66.71		77.39	41.81
59-60	19.38	19.57	65.24		71.56	45.30
65-66	24.73	18.32	68.70		77.29	44.17
69-70	31.51	33.06	152.34		109.39	47.51
74-75	36.10	27.08	83.57		78.97	46.42
79-80	31.80	23.85	97.16		69.55	45.42

DROI1

Depth (cm)	Ni	Cu	Zn	Cd	Hg	Pb
0-0.5	41.633	86	290.8	1.0204	153	66.47
2-2.5	43.36	30	211	1.5056	158	64.52
4.5-5	37.641	28	208.6	0.3921	165	180.1
7-7.5	43.359	30	220.7	0.4301	161	67.84
9.5-10	45.402	29	207.4	0.7276	120	49.89
12-12.5	42.793	30	208.2	0.3715	111	66.23
14.5-15	41.107	31	208.3	0.3426	139	63.42
17-17.5	43.179	28	196.9	0.3911	141	61.68
19.5-20	41.848	28	214	0.3633	125	54.8
22-23	37.937	28	162.7	0.416	131	54.2
25-26	45.642	26	162	0.7924	101	51.62
28-29	43.188	27	148.5	0.3213	106	55.09
31-32	40.606	25	129.3		86.3	47.57
34-35	45.405	25	136.1	0.4505	101	58.69
37-38	36.024	19	92.65		50	31.45
40-41	41.667	18	87.22		45.3	24.59
43-44	40.37	20	84.1		42.1	21.63
46-47	40.655	18	78.42		31.8	16.94
49-50	36.912	18	78.61		34.6	17.14
52-53	38.63	19	74.79		27.4	17.56
55-56	30.244	17	71.56		21	9.601
59-60	33.074	17	68.45		24.3	15.29
62-63	34.436	17	82.53		22.8	8.681
65-66	35.789	17	69.59		11.2	7.669
68-69	32.456	16	72.12		16.2	9.273

GROB1

Depth (cm)	Ni	Cu	Zn	Cd	Hg	Pb
0-1	32.83	64.37	236.96	1.21	193.11	115.87
2-2.5	31.48	67.62	257.52	1.75	170.51	119.92
5-5.5	29.17	58.51	221.27	1.01	172.16	115.74
7-7.5	28.50	59.36	225.59	1.48	161.40	101.77
10-10.5	31.58	66.67	258.33	0.88	151.32	129.32
12-12.5	32.92	65.84	260.61	0.91	198.88	122.27
15-15.5	33.55	67.89	322.48	1.00	179.71	133.50
17-17.5	34.40	63.37	250.83	0.75	147.10	134.49
19.5-20	34.45	62.21	231.84	0.36	172.27	115.66
23-24	27.73	57.51	234.13	0.39	150.18	108.27
27-28	34.91	54.76	243.84	0.86	192.51	96.80
31-32	34.09	47.91	234.17	0.84	156.67	80.21
35-36	35.89	39.88	217.06	0.83	155.78	65.52
39-40	34.91	38.78	195.74	0.40	193.92	74.80
43-44	36.66	38.97	186.14	0.33	149.44	72.87
47-48	38.42	35.89	161.69		141.88	77.33
51-52	36.13	35.92	158.48	0.40	166.40	81.50
55-56	41.17	33.81	135.91	0.37	145.44	69.04
60-61	37.85	32.04	126.83	0.75	129.54	66.94
65-66	36.42	29.13	107.90	0.61	122.91	56.19
70-71	34.57	23.57	87.31		127.68	29.19
75-76	38.03	23.88	101.04	0.34	98.17	28.34
80-81	36.21	23.13	93.88	0.38	96.18	31.04
84-85	44.51	23.02	96.64		95.93	24.12
87-88	44.40	23.84	101.41	0.31	83.25	25.37

GULL1

Depth(cm)	Ni	Cu	Zn	Cd	Hg	Pb
0-0.5	26.42	79.51	235.32	1.38	550.46	257.93
1.5-2	27.55	42.10	259.04	1.91	531.00	154.17
3.5-4	30.98	41.55	241.05	1.34	534.19	164.84
5.5-6	20.77	43.02	216.79	0.79	531.16	167.27
7.5-8	24.99	41.65	201.39	1.86	490.93	168.32
9.5-10	25.84	40.20	204.57	2.15	492.57	166.11
11.5-12	19.54	35.82	216.54	1.63	402.96	120.02
13.5-14	22.46	29.50	262.72	4.25	357.39	105.03
15.5-16	22.27	28.28	595.71	5.97	342.99	97.71
17.5-18	30.53	30.01	741.37	6.85	352.25	100.64
19.5-20	24.43	21.33	610.82	5.09	239.97	82.27
22-23	14.22	14.92	481.17	2.30	197.52	45.15
24-25	15.25	14.12	509.88	2.47	222.33	45.98
27-28	34.50	15.33	571.48	2.87	251.53	52.57
29-30	16.41	18.24	590.86	2.44	300.41	53.59
32-33	12.71	12.10	197.62	2.27	221.26	44.09
35-36	20.98	11.66	190.37	1.75	196.68	77.92
37-38	12.69	11.75	172.39	0.88	211.57	90.67
40-41	8.67	12.04	144.51		203.22	80.51
42-43	9.62	8.02	117.56	1.20	234.45	87.94
45-46	3.80	7.39	49.26	0.79	83.12	48.86
47-48	13.59	6.47	25.16	0.40	97.06	41.60
50-51	18.79	7.31	10.44	0.39	70.44	5.37
53-54	6.29	5.24	8.73	0.33	49.11	2.25
56-57	2.86	2.39	1.99		26.84	2.04

PINK3

Depth (cm)	Ni	Cu	Zn	Cd	Hg	Pb
0.5-1	18.92	32.79	245.90		245.90	56.21
2.5-3	32.19	21.26	177.14	0.50	166.07	78.57
4.5-5	30.60	19.89	180.46	0.83	176.78	62.50
7-7.5	40.27	21.97	202.49	0.97	135.71	53.18
9.5-10	41.92	25.32	243.15	0.83	154.12	59.45
12-12.5	37.67	26.60	323.04	1.81	193.45	55.96
14.5-15	34.91	22.19	280.26	3.03	181.54	80.40
17-17.5	40.63	35.21	292.69	3.20	170.72	82.31
19.5-20	49.64	29.98	297.22	2.44	149.92	77.10
22-23	46.05	31.04	389.69	4.99	221.73	133.04
26-27	43.83	32.23	291.13	3.45	184.16	115.43
30-31	37.79	27.90	237.67	1.82	133.43	87.34
33-34	38.58	27.86	230.27	1.67	167.17	88.84
37-38	32.27	30.63	230.83	2.00	159.81	89.04
41-42	44.36	31.03	264.32	3.04	161.88	97.13
45-46	37.33	29.12	234.35	1.62	134.80	99.83
50-51	43.76	29.07	265.69	2.84	126.41	97.51
54-55	31.91	28.58	236.45	2.42	152.10	94.82
59-60	34.69	22.55	245.44	1.88	169.11	93.41
63-64	38.98	27.64	177.45	0.77	127.97	73.71
67-68	39.02	25.93	195.39	1.27	140.91	72.47
71-72	32.20	27.91	206.72	2.33	124.03	75.75
75-76	32.88	26.30	194.85	1.10	87.68	60.12
79-80	32.35	24.54	190.83	0.88	110.99	60.09
82-83	24.46	29.45	235.57	0.88	153.12	78.75

PORT1

Depth (cm)	Ni	Cu	Zn	Cd	Hg	Pb
0-0.5	41.40	199.33	255.55		215.62	67.03
1.5-2	46.33	211.64	162.07		209.14	62.51
3.5-4	43.89	237.75	160.53	0.91	233.17	65.84
5.5-6	49.60	261.31	155.20	0.71	224.49	75.75
7.5-8	50.95	299.23	170.73	0.51	227.46	79.72
9.5-10	52.66	342.84	152.37	0.69	226.28	75.23
11.5-12	47.73	384.51	174.58	0.50	223.75	75.01
13.5-14	57.25	427.35	157.36	0.75	245.97	76.67
15.5-16	68.85	360.66	163.93		190.57	78.69
17.5-18	62.27	133.43	148.26	0.46	152.89	73.07
19.5-20	59.52	68.68	131.42		114.46	65.41
21-22	49.88	50.99	118.24		106.00	62.71
24-25	43.92	48.80	93.84	0.35	95.02	36.20
27-28	43.33	35.11	96.97		107.21	49.01
30-31	25.97	31.56	51.09		81.15	11.59
33-34	33.09	50.25	65.36		124.08	9.45
37-38	35.90	46.93	70.40		132.00	9.05
42-43	33.91	47.10	69.77		111.85	5.38
46-47	43.53	46.35	73.89		119.03	7.77
51-52	37.89	50.29	97.47		131.58	6.02
56-57	49.22	48.74	79.25		120.36	6.11
62-63	38.94	54.81	84.14		149.29	11.13
68-69	36.18	48.81	76.56		153.42	11.07
74-75	36.16	57.40	90.88		150.13	7.38
83-84	44.46	58.38	108.53		138.94	7.22

UKRB2

Depth (cm)	Ni ug/g	Cu ug/g	Zn (ug)	Cd ug/g	Hg ng	Pb (ug)
0-0.5	57.05	88.30	288.52	4.10	172.13	70.26
2-2.5	61.59	35.97	254.85	4.28	139.01	58.66
5-5.5	59.50	27.26	263.92	3.60	179.94	60.32
7-7.5	65.91	28.34	257.20	3.71	178.15	55.99
10-10.5	56.91	26.79	245.93	3.05	111.79	58.07
12-12.5	57.82	24.33	279.71	4.46	127.14	73.42
15-15.5	75.45	25.95	332.15	5.79	111.68	65.24
17-17.5	51.92	27.32	255.61	4.01	90.14	54.95
19.5-20	55.87	24.34	251.78	3.10	81.47	42.56
22-23	40.68	20.45	182.86	1.96	88.01	53.64
25-26	36.03	16.16	129.93	2.37	118.52	43.34
28-29	40.20	13.90	122.99	2.91	87.39	32.46
31-32	41.33	19.73	227.34	3.10	93.00	44.88
35-36	39.94	17.25	194.02	2.33	94.85	36.51
38-39	39.71	18.46	143.74	2.26	95.89	36.10
41-42	36.86	18.09	142.73	3.14	94.25	38.30
44-45	46.13	18.87	146.92	3.08	86.49	36.90
47-48	36.21	15.43	127.41	2.64	107.50	31.04
51-52	36.39	19.74	131.73	2.07	118.90	28.36
54-55	51.43	24.35	158.73	0.71	107.14	56.33
57-58	19.78	17.98	87.92		98.91	36.74
61-62	30.83	21.90	108.48	0.32	130.07	48.45
64-65	34.58	24.02	120.97	0.40	126.08	52.15
67-68	35.93	27.22	123.83		118.51	51.33
69-70	35.07	23.55	104.79	0.33	124.54	43.27

TURT1

Depth (cm)	Ni	Cu	Zn	Cd	Hg	Pb
0-1	56.99	88.44	653.46	2.87	313.22	218.99
1.5-2	57.35	66.45	573.46	3.41	286.73	229.38
3.5-4	60.37	64.50	747.68	3.39	246.71	232.20
5.5-6	72.08	66.16	548.45	3.26	342.78	302.20
7.5-8	77.89	97.04	784.82	4.43	413.06	404.63
9.5-10	65.76	99.63	557.95	1.66	373.63	364.38
11.5-12	55.11	99.84	303.51	2.00	464.26	342.31
13.5-14	36.74	73.05	150.39	0.40	332.34	276.23
15.5-16	43.68	60.67	218.42		245.72	202.82
17.5-18	42.00	50.17	194.45	0.44	170.63	156.01
19.5-20	42.33	53.17	227.66	0.77	149.54	152.50
22-23	40.73	36.20	138.78		40.73	58.18
25-26	32.83	21.89	93.23	0.23	30.78	28.14
29-30	23.75	14.13	64.39	0.18	21.20	13.33
33-34	30.98	18.99	83.08	0.45	30.04	24.42
37-38	32.76	22.61	104.13	0.83	31.02	35.45
41-42	37.55	30.63	135.62	0.33	7.49	49.65
45-46	25.90	18.85	71.12	0.19	16.75	22.97
49-50	45.43	33.35	249.86	0.68	15.21	57.95
54-55	60.79	66.08	448.68	1.65	20.65	224.67
59-60	55.04	40.63	269.16	1.10	11.78	84.01
64-65	45.76	33.89	223.70	0.61	11.35	49.80
69-70	35.14	27.89	99.93	0.52	19.61	35.86
74-75	41.80	34.33	136.68		14.20	54.52
78-79	48.56	37.47	176.20	0.56	21.08	53.96